Diss. ETH No. 15857

Modeling phosphorus runoff at the catchment scale

A dissertation submitted to the

Swiss Federal Institute of Technology Zürich

for the degree of

Doctor of Natural Sciences

presented by

Patrick Lazzarotto

Dipl. Natw. ETH

born on 21 January 1974

citizen of Oberriet SG

accepted on the recommendation of

Prof. Dr. H. Flühler, examiner

Dr. C. Stamm, co-examiner

Dr. V. Prasuhn, co-examiner

2004

Contents

List of Figures

List of Tables

Preface

This thesis was carried out in the context of a project entitled "Modeling phosphorus runoff at the catchment scale" within the scope of the COST action 832 "Methodologies for estimating the agricultural contribution to eutrophication". The project was initially sponsored by Agroscope FAL Reckenholz while the major financial support arised from the Swiss Federal Office for Education and Sciences within the scope of the COST action 832 and by the Soil Physics group of the Institute of Terrestrial Ecology, ETH Zurich. This project was initiated as a result of the evaluation projects to test the efficiency of ecological measures to reduce the phosphorus losses from grassland areas. It was a joint project of Agroscope FAL Reckenholz, the Soil Physics group of the Institute of Terrestrial Ecology, ETH Zurich, the Swiss Federal Institute for Environmental Science and Technology (EAWAG) and the Environmental Protection Agency of the Cantone Lucerne.

I am very much indebted to all the following persons and institutions who contributed to the success of this study:

Prof. Dr. Hannes Flühler enabled me to carry out my studies with a maximum of scope and with all the support I needed. Dr. Christian Stamm strongly supported me with his excellent ideas and knowledge to understand the interactions between the soil physics, the nutrient dynamics and agriculture, thereby working out the main concept to simulate diffuse P-loss at the catchment scale. Dr. Volker Prasuhn gave me full support with his large experience in the field of water protection and agriculture and helped me to analyse the agricultural data. These three persons were my major advisors during my study and I very much appreciated to work in such an uncomplicated and friendly environment. Dr. Felix Herzog, as the head of the evaluation projects, also navigated this project and gave me valuable stimulations. Without these four persons this project would have been never initiated.

This project would not have been possible without the substantial support of the Environmental Protection Agency of the Cantone Lucerne. Ernst Butscher and Cornelia Crespi

took a huge effort to support the online-monitoring station and the routine sampling monitoring at the outlet of the Lippenrütibach catchment. They provided me full access to their data and gave me full support anytime.

I am very grateful to Dr. Armin Keller who collected additional soil-P data in a comprehensive campaign in the Lippenrütibach, to Dr. Michael Schärer and Tobias Vollmer who collected P-runoff data on grassland plots in the Lake Greifen region. All gave me full access to their data and important advices to use these data for modelling. Dr. Josef Blum, Bernhard Koch and Otto Barmettler (FÖK Sursee) as agricultural consultants for the farmers in the Lake Sempach region always supported our study and us with detailed management data.

Without the good collaboration with the farmers in the Lippenrütibach who provided me with detailed data for manure this project would have not been possible. Adrian Weidmann processed these data and transformed their manure data into P-equivalents.

Valuable comments arised in interesting discussions with R. Flisch, H.-J. Bachmann, E. Spiess, W. Richner, P. Stadelmann, P. Herzog, B. Müller, K. Stoob, N. Aschwanden, C. Wüthrich-Steiner, K. Beven, J. Freer, T. Page, P. Haygarth, F. Näf and P. Schmocker-Fackel.

A special thank goes also to those who contributed to the success of this study in the one or the other way: Dr. D. Bänninger, Dr. M. Schwank, M. Nussberger, C. Hofer, M. Decrem, Y. Moosmann, M. Gugerli, K. Zangger and R. Stierlin.

Last but not least, my best supporter was and still is Monika Zuberbühler especially at less pleasant times during this study. Thank you a lot! And many thanks also to my family and my friends for their support during all the years.

Summary

Diffuse losses of phosphorus (P) from intensively managed grassland catchments with high live stock densities and excessive P-fertilization may reach surface waters and can cause eutrophication problems in lakes. While the P accumulated in the topsoils due to excessive P-fertilization over decades is a long-term source for P-mobilization the manure applications are temporarily important in generating additional P-losses. However, the relevance of P-loss from the soil or from fresh manure/fertilizer applications (called incidental P losses, IPL) is still under debate. This question, however, is relevant in the context of developing efficient measures to reduce diffuse P-loss and many studies quantified the efficiency of such measures by field experiments at the plot-scale. At the catchment scale, however, it is more difficult to quantify their effects.

Before measures are implemented the risk areas for P-loss should be identified. These are sites with a large pool of available P as well as a high probability for the occurrence of fast flow (surface runoff and preferential flow) transporting P into surface waters. The main goal of this thesis was to identify such risk areas and to quantify the diffuse P-loss from soils and from IPL at the event time-scale by numerical simulations. Therefore, the grassland catchment Lippenrütibach (3.3 km^2) in the region of Lake Sempach (Kt. Luzern) was selected with an extensive data-set for manure application, soil-P and measurements of the P-export dynamic. To account for all this data a parsimonious dynamic rainfall-runoff model and a P-model at the catchment scale were developed. The findings and results of this study contributed to the project "Evaluation of ecological measures in agriculture".

Since the rainfall-runoff model has to include the dominant transport processes the P-export dynamic from two neighbouring small grassland catchments (Lippenrütibach and Kleine Aa) in the Lake Sempach region was analyzed. In the Kleine Aa catchment, the typical pattern for fast P-transport was found: Strong increases of the dissolved reactive P (DRP)-concentrations up to values >1000 mg m^{-3} with rising discharge while DRP remained low (<100 mg m^{-3}) during baseflow. This pattern also occurred in the Lippenrütibach catchment from 1998 to 1999 but was partially replaced by a new one during the following years: In the growth period DRP reached only 200 to 400 mg m^{-3} during peak flows but did not rise at all or increased only very slowly reaching its maximum only days after the runoff event. During baseflow, however, DRP was high (200 to 300 mg m^{-3}) and strong daily oscillations in DRP up to 300 mg m^{-3} occurred in parallel with the change from the typical to the new pattern. The reason for this change is not clear but may be related to influences of biogeochemical processes in the saturated zone or in the brook-sediments while leaks from manure tanks could be ruled out. Independent of this drastic change in the P-export dynamic no statistically significant reduction was observed in the annual DRP-load over the last 10 years.

The discharge dynamics in catchments of Lake Sempach were strongly influenced by

the areal fractions of well and poorly drained soils. Smoother hydrographs exhibited in catchments with high areal fractions of well drained soils while the hydrographs became peakier in catchments with increasing areal fractions of poorly drained soils. Based on the typical pattern of the P-export dynamic a slow and a fast flow component were assigned to each well and poorly drained soils, considered as hydrological response units. These flow components were quantified with the rainfall-runoff model by simultaneously fitting the simulated catchment response in four catchments (Lippenrütibach, Rotbach, Meienbach and Greuelbach) with different areal fractions of well and poorly drained soils. Despite a short 11-day period for calibration the discharge dynamic for intermediate and high runoff events was generally well reproduced for two short periods in all four catchments and also during the growth period from 1999 to 2002 in the Lippenrütibach. The simulations suggested that poorly drained soils produced the most fast flow per unit area but during large stormflows the well drained soils substantially contributed to fast flow as soon as the well drained soils were wet enough. Maps were created for distinct runoff events indicating the probability of fields contributing to fast flow. Based on these probability maps the major part of these four catchments had a low risk for contributing to fast flow for small and large runoff events as well. Even during a major flood less than 20% of the Lippenrütibach catchment had a very high risk for fast flow generation. This suggested that it is only a small part of the catchment area where fast flow and associated P-loss was commonly produced.

The fast flow components were separated into new water, which is relevant for fast P-transport, and into old water. The P-model calculated diffuse P-loss by linking the high DRP-concentrations from topsoils and those from IPL with the new water flow components while the low DRP-concentrations during baseflow were assigned to the old water flow components. Several scenarios were applied to describe the P-mobilization from topsoils and IPL based on field data and all model parameters for P could be derived from plot/field experiments. The hourly observed DRP-load was well reproduced for some stormflows in the Lippenrütibach in the growth period in 1999 using 500 Monte-Carlo simulations. However, the very high DRP-peaks were partly underestimated. Despite the fact that a detailed data-set for manure application and soil-P status was used, which was unique in Switzerland, the prediction bands for the DRP-loads varied largely. The model results indicated that most of the DRP-loss during the growth period 1999 originated from topsoils with 23 to 110 kg DRP loss (depending on the applied scenarios) while the loss from manure was less relevant (5 to 7 kg DRP). For single runoff events, IPL contributed up to 30% to the total DRP-loss. The reason for this dominance of the DRP-loss from soils over IPL was that a large number of fields had a high soil-P status. Therefore, the mobilized DRP-concentrations from soils often overran those from manure during most of the growing season. This suggested that measures are primarily needed to reduce the high soil-P status in this catchment.

Zusammenfassung

Diffuse Phosphor (P)-Verluste aus landwirtschaftlich intensiv genutzten Graslandgebieten mit hohen Tierzahlen und übermässiger Düngung können in die Gewässer gelangen und zur Eutrophierung von Seen führen. Während die durch jahrzehntelange übermässige Düngung mit P angereicherten Oberböden eine langzeitige Quelle für die Mobilisierung von bodenbürtigem P darstellen, sind auch P-Verluste durch direkte Gülleabschwemmung eine kurzzeitige zusätzliche Belastungsquelle. Der Beitrag dieser beiden Pfade zur Gesamtbelastung ist jedoch noch nicht geklärt. Diese Frage ist jedoch wichtig für die Auswahl und Effizienz von Massnahmen, um diffuse P-Verluste zu reduzieren. Viele Studien haben die Wirkung von Massnahmen auf der Testparzellen/Feld-Skala bereits untersucht, auf Einzugsgebiets-Skala ist eine entsprechende Quantifizierung jedoch schwieriger.

Bevor Massnahmen im Einzugsgebiet eingesetzt werden, sollten die Risikoflächen für P-Verluste bekannt sein. Dies sind Flächen mit Bildung von schnellem Abfluss, einer hohen P-Anreicherung im Oberboden und/oder frischer Applikation von Gülle oder Mineraldünger. Das Hauptziel dieser Dissertation war, mit numerischen Simulationen diese Risikoflächen zu identifizieren und die Beiträge der diffusen P-Verluste aus bodenbürtigem P und direkter Gülleabschwemmung für einzelne Abflussereignisse zu berechnen. Dazu wurde das Graslandgebiet Lippenrütibach (3.3 km^2) in der Region des Sempachersees (Kt. Luzern) mit sehr detaillierten Daten über Güllegaben, P-Verfügbarkeit im Oberboden und Messungen von Nährstoffen im Abfluss ausgewählt. Um diese Daten bestmöglichst zu berücksichtigen, wurde ein dynamisches Niederschlag-Abfluss-Modell (NAM) und ein P-Modell auf Einzugsgebiets-Skala entwickelt. Die Ergebnisse dieser Studie liefern einen Beitrag zum Projekt "Evaluation der Ökomassnahmen in der Landwirtschaft".

Da das NAM die dominanten Prozesse für Wasserfluss und schnellen P-Transport abbilden muss, wurde zuerst die Dynamik der gelösten reaktiven P (DRP)-Konzentrationen und des Abflusses von zwei Graslandgebieten (Lippenrütibach und Kleine Aa) in der Region des Sempachersees analysiert. Dabei wurde das klassische Muster für schnellen P-Transport in der Kleinen Aa gefunden: Eine schnelle Zunahme von DRP - oftmals > 1000 mg m^{-3} - im steigenden Abfluss während DRP bei Basisabfluss tief blieb (20 bis 100 mg m^{-3}). Im Lippenrütibach trat dieses Muster zwischen 1998 und 1999 ebenfalls auf. Ab 1999 fand sich während der Vegetationsperiode jedoch ein neues Muster: Mit steigendem Abfluss variierte DRP nur zwischen 200 bis 400 mg m^{-3}, stieg aber nicht weiter an oder nahm nur sehr langsam zu, bis Maximalkonzentrationen einige Tage nach dem Abflussereignis erreicht wurden. Bei Basisabfluss blieben die Konzentrationen jedoch hoch (200 bis 300 mg DRP m^{-3}). Zudem traten bei Basisabfluss, fast gleichzeitig mit dem Wechsel vom alten zum neuen Muster, starke Tagesschwankungen von DRP bis zu 300 mg m^{-3} auf. Die Ursache für diesen Wechsel ist unklar. Bio-geochemische Prozesse in der gesättigten Zone oder in Bachbettsedimenten könnten jedoch eine Rolle spielen, Sickerverluste aus

Gülletanks konnten ausgeschlossen werden. Unabhängig von diesem Wechsel im Muster der P-Dynamik war kein statistisch signifikanter Rückgang der jährlichen DRP-Frachten innerhalb der letzten 10 Jahre zu beobachten.

Die Abflussdynamik in diesen Gebieten ist stark von den Flächenanteilen von gut und schlecht durchlässigen Böden beeinflusst. Der Verlauf der Abflussganglinien war ausgeglichener in Gebieten mit einem hohen Anteil an gut durchlässigen Böden währenddem die Abflussganglinien in Gebieten mit einem hohen Anteil an schlecht durchlässigen Böden stärker zu- und abnahmen. Aufgrund des klassischen Musters für schnellen P-Transport wurde den gut und schlecht durchlässigen Böden, welche im NAM als Hydrotope behandelt wurden, je eine langsame und eine schnelle Abflusskomponente zugewiesen. Diese Abflusskomponenten wurden mit dem NAM durch eine simultane Anpassung des Gesamtabflusses in vier Gebieten (Lippenrütibach, Rotbach, Meienbach und Greuelbach) mit unterschiedlichen Flächenanteilen von gut und schlecht durchlässigen Böden kalibriert. Trotz einer kurzen Kalibrierungsperiode von nur 11 Tagen wurde die Abflussdynamik bei mittleren und grossen Ereignissen in den vier Gebieten als auch über die Vegetationsperiode der Jahre 1999 bis 2002 im Lippenrütibach gut nachgebildet. Die Resultate zeigten, dass die schlecht durchlässigen Böden am meisten schnellen Abfluss pro Einheitsfläche bilden. Bei grösseren Ereignissen tragen jedoch auch die gut durchlässigen Böden stark zum schnellen Abfluss bei, sobald deren Bodenwasserspeicher einen bestimmten Grenzwert überschritten hat. Zudem wurde für verschiedene Abflussereignisse die Wahrscheinlichkeiten, dass einzelne Felder zu schnellem Abfluss beitragen, berechnet. Diese Karten zeigen, dass das Risiko für schnellen Abfluss im grössten Teil der vier Gebiete bei kleineren als auch bei grösseren Ereignissen klein ist. Im Lippenrütibach wiesen sogar während einer langen Hochwasserperiode weniger als 20% der Gebietsfläche ein sehr grosses Risiko auf. Das bedeutet, dass schneller Abfluss und damit verbundener P-Verlust nur auf relativ wenige Flächen im Gebiet begrenzt ist.

Da neues Wasser den schnellen P-Transport bestimmt, wurden die schnellen Abflusskomponenten in neues und altes Wasser unterteilt. Im P-Modell wurden die hohen DRP-Konzentrationen (Mobilisierung von bodenbürtigem P und direkter Gülleabschwemmung) mit der Komponente aus neuem Wasser verrechnet und die tiefen DRP-Konzentrationen mit der Komponente aus altem Wasser. Mehrere Szenarien zur Mobilisierung von bodenbürtigem P und dem P aus der direkten Gülleabschwemmung wurden aufgrund von verfügbaren Daten aus Feldexperimenten gerechnet und die Modell-Parameter für P aus diesen Daten abgeleitet. Für einige Abflussereignisse während der Vegetationsperiode 1999 wurden die stündlichen DRP-Frachten im Lippenrütibach mit 500 Monte-Carlo Simulationen gut nachgebildet, die höchsten Spitzenfrachten jedoch unterschätzt. Obwohl ein in der Schweiz einzigartiger, detaillierter Datensatz zu Güllegaben und P-Gehalte der Böden zur Verfügung stand, trat eine grosse Streuung in den Vorhersagebändern der DRP-Frachten auf. Gemäss den Modellrechnungen stammte mit 23 - 110 kg DRP (je nach Szenarien) während der Vegetationsperiode 1999 der grösste Teil der DRP-Frachten vom bodenbürtigen P. Die DRP-Frachten aus direkter Gülleabschwemmung betrug viel weniger (5 - 7 kg DRP), machten jedoch bei Einzelereignissen bis zu 30% der gesamten DRP-Fracht aus. Ursache für die hohen DRP-Verluste aus dem Boden sind die vielen Parzellen mit einem hohen P-Gehalt im Oberboden. Die dabei mobilisierten DRP-Konzentrationen sind während der Vegetationsperiode meist grösser als diejenigen aus der direkten Gülleabschwemmung. In solchen Gebieten sind deshalb Massnahmen zum Abbau der hohen P-Gehalte der Böden prioritär.

Chapter 1

Introduction

Phosphorus (P) is growth-limiting in many freshwater systems and excessive P-input into surface waters enhances their eutrophication and leads to blooms of algae and aquatic plants. After dying, bacteria decompose algae and deplete the oxygen storage in the water. Dissolved oxygen concentrations substantially decline and are too low to allow fish to breathe, leading to fish kills (*Foy and Withers*, 1995). The further depletion of oxygen in the bottom water-layers may cause the release of P previously bound to sediments. This increases the P-concentration in water amplifying the effects of external P-input.

In Switzerland, the P-loss from non-point sources (agriculture) and point sources (households, sewage water treatment plants) into surface waters markedly increased during the middle of the last century (*Bundesamt für Landwirtschaft*, 2001). This situation caused eutrophication problems in Swiss lakes. After most point sources had been eliminated by the mid eighties by measures such as the ban of P-containing detergents and the connection of all households to waste water treatment plants, P-losses into the lake did not decrease as predicted. The total P (TP) concentrations reached 165 mg m^{-3} in 1984, dramatically exceeding the water quality goal of 30 mg TP m^{-3} and leading to a massive fish kill in Lake Sempach (*Stadelmann*, 1988). This suggested that diffuse P-losses from agriculture had increased and actually counterbalanced the reduced losses from waste water.

A first package of ecological measures was introduced in 1993 to reduce agricultural diffuse P-loss, such as buffer strips or balanced P-budgets (*Forni et al.*, 1999). In regions of concern stricter measures were implemented at the end of the 1990s within the scope of Art. 62a of the Swiss law for water protection (*Bundesversammlung der Schweizerischen Eidgenossenschaft*, 1991). Such additional measures encompass, among others, reduced P-inputs to 80% of plant needs, reduced livestock density or the installation of nutrient

retention ponds. Apart from measures aiming at a reduction of the P-load entering water bodies lake-internal measures were applied in the past as well to improve the water quality of Lake Sempach. Although lake-internal measures do not eliminate the source of the problem they limited their impacts by artificially injecting oxygen or circulating the water. This should prevent P-resolubilization from sediments into water by maintaining aerobic conditions at the sediment-lake interface. Since 1986, the average P-concentration in the lake water steadily dropped and reached the water quality goal of 30 mg total P m^{-3} in 2002.

Several ecological measures related to agriculture have been implemented in catchments to reduce the diffuse P-loss into surface waters and the efficiency of such measures must be evaluated. This evaluation can be carried out with field experiments or by using simulation models. One advantage of field experiments is that one can measure the effect of distinct treatments on P-loss (*Schärer*, 2003) under relatively well defined initial and boundary conditions. Although causal relationships between management practices and the measured P-loss can be established it takes many years before impacts of treatments on the P-loss are obtained (*McIsaac et al.*, 1991). Furthermore, plot-scale studies indicate rates of P-mobilization but they do not describe how P was transferred from hillslope sites to surface waters (*Heathwaite et al.*, 1998).

At the catchment scale, however, the derivation of causal relationships is more difficult. The P-export dynamic is discharge-driven since wet and dry periods yield strongly varying P-loads. Furthermore, the P-dynamic is commonly measured at the outlet of a catchment and interpreted as a superposition of several P-subdynamics from various spatial origins. During P-transport from the source to surface waters P is stored and released depending on flow pathways and its soil chemistry. Since the original P-input signal from a single field is getting naturally perturbed during transport the P-response from single fields can generally not be reconstructed from the observed P-signal at the catchment outlet.

For these reasons, modeling is one alternative to assess the effects of ecological measures on the P-loss in catchments. Modeling can account for various hydrological conditions such as initial and boundary conditions and allows for scenario calculations of distinct management practices. There are drawbacks as well since a model only allows for a simplified reproduction of the ecological system and the quality of model results depends on the quality of input data. At the catchment scale, for example, detailed data as required by models is often not available and observations obtained from the point-scale have often to

be up-scaled to the scale of the spatial model resolution. A further problem is to pose assumptions about the spatial heterogeneity of soil properties or how the mechanisms of an ecological system can be described at the catchment scale. Generally, there is substantial uncertainty associated with the model results as uncertainty arises from measurement errors in the data and from the model structure itself. It is therefore important to identify the dominant processes in a system which must be incorporated in the model (section 1.3). These relevant processes for diffuse P-loss will be discussed in the following.

1.1 Phosphorus cycle in soils

The P-cycle in soils is complex with multiple interactions between distinct soil reservoirs for P and can be grouped, according to their kinetic reaction rates, into slow inorganic-P, slow organic-P and rapid cycling of organic and inorganic-P (Fig. 1.1). A comprehensive overview of P in soils is given in *Frossard et al.* (1995) and *Frossard et al.* (2004).

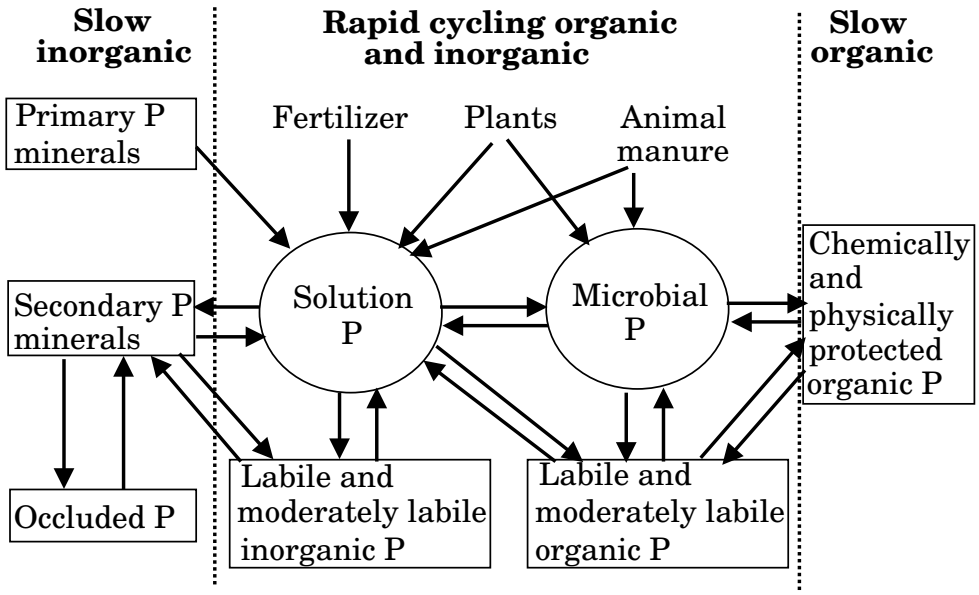

Figure 1.1: *The P-cycle in soils according to Sharpley and Rekolainen (1997)*

Soils contain 100 to 3000 mg P kg^{-1} soil mostly as stable organic and anorganic P-compounds while most of the P required by plants is taken up as orthophosphate from the soil solution (*Frossard et al.*, 2004). Most of the anorganic P exists as plant-unavailable strongly bound apatite (primary P-minerals). Since the natural background of plant-available P is not sufficient for intensive plant production P-amendments in organic or

inorganic form are used to maintain adequate P-availability in soils for plant uptake. Once applied, P is taken up by plants and incorporated into organic P or may be weakly or strongly adsorbed to Al, Fe and Ca-surfaces to become partly unavailable for plants (*Ryden et al.*, 1973). Processes related to inorganic P include physico-chemical reactions, such as precipitation/dissolution and sorption/desorption. Another important P-form contained in the soil is the organic P which varies, depending on the soil-types, between 30 to 65% of the total P (*Harrison*, 1987). Since organic P compounds are not directly available for plants organic P is hydrolyzed by enzymes to release orthophosphate which can be taken up by plants. Organic P-compounds may also become resistant to hydrolysis through complexation with Al and Fe. Plants and microorganisms take up P which was released during the weathering of primary and secondary minerals including solubilisation of soil P-minerals. Inorganic P is also recycled via complex food chains through a series of mineralisation and immobilisation reactions. Factors controlling the immobilization of inorganic into organic P and the mineralization of organic into inorganic P are the microbial activity, the vegetation, soil properties, climate and land use as well. Labile and moderately labile inorganic and organic P-pools also interact with the solution-P pool.

1.2 Sources, mobilization and transport mechanisms for P

Haygarth and Jarvis (1999) suggested the classification of distinct mechanisms for P-transfer from the source into water bodies. They distinguished dissolution/solubilization, physical detachment and incidental/event based mechanisms. Solubilization represents mobilization of different forms of dissolved P such as anorganic or organic P-compounds that become solubilized during rainfall. Detachment summarizes soil erosion and associated removal of P. Incidental P-loss occurs when P from freshly applied manure or mineral fertilizer is mobilized by the onset of rainfall (*Withers et al.*, 2003).

The P-forms are separated into particulate and dissolved P. Particulate P (PP) was defined as P associated with particles >0.45 μm and dissolved P (DP) as the fraction below this threshold. Dissolved P is often the dominant form in surface runoff or preferential flow from grassland (*Braun et al.* (1993) and *Gaston et al.* (2003)), is directly available for algae and therefore of special concern for the eutrophication of surface waters. The dissolved reactive P (DRP)-concentrations in runoff from grassland, commonly determined by colorimetric methods (*Murphy and Riley*, 1962), often exceed levels between 100 and >1000 mg DRP m^{-3}. This is one or two orders of magnitude above the concentrations of

an oligotrophic lake (*Vollenweider and Kerekes*, 1980).

1.2.1 Sources

In intensively managed agroecosystems with high stock densities as in the Lake Sempach region (> 2 dairy-cow-equivalents ha^{-1}) the manure production is the main source for P-inputs for grassland. Since the average P-application rates (35 to 40 kg P ha^{-1} y^{-1}) exceed the P-demand of plants the resulting P-surplus is stored in the topsoils. This excessive fertilization over decades has led to a situation where most soils are P-overloaded (*Keller and van der Zee*, 2004). Although the difference between P-input and P-output in the farm-specific nutrient balances substantially dropped from 21 kg P ha^{-1} y^{-1} in 1996 close to zero in 2001 (*FÖK*, 2002) a significant degradation of the P stored in topsoils to environmentally tolerable levels will probably take more than 10 years. This suggests that the P stored in soils is a long-term source for dissolved P-loss.

1.2.2 Mobilization

Only a small part of the soil-P is mobilised by solubilization and detachment. The term solubilisation refers to the P released from the soil matrix and soil biota into the soil water for potential transfer due to dissolution of precipitated P, desorption from secondary P-minerals or due to mineralization of organic material. The potential for solubilization reflects the long-term management history and increases with rising soil-P status (*Sibbesen and Sharpley* (1997); *Schoumans and Groenendijk* (2000); *McDowell and Sharpley* (2001)). It is known that soils, having a soil-P status above a certain level of P-saturation (change point), loose proportionately more dissolved P in runoff than soils below these levels (*Heckrath et al.* (1995); *Hesketh and Brookes* (2000); *McDowell and Sharpley* (2001)).

The P-mobility is generally low due to the low solubility of P-compounds, the high P-binding capacity of soil material (*Sharpley and Rekolainen*, 1997) and is controlled by the chemical soil conditions such as pH, redox potential, ionic strength, temperature and organic acids. Basically, the surface charges of Fe-Al-hydroxides are the main sorption sites for anionic-P. Mobilization of inorganic-P is enhanced with increasing pH-values (*Hartikainen and Yli-Halla*, 1996) and decreasing ionic strength (*Chardon et al.*, 1997). At elevated temperature more P is released due to the faster mineralization of organic matter coupled with a decreasing P-adsorption (*Barrow*, 1992). The P-mobilization is promoted if sorption sites are covered by organic acids from manure or plant roots (*Gerke*, 1992)

or under reduced conditions in the anoxic zone of saturation of soils where Fe-compounds are reduced. Soluble organic P from soil biomass can also be released during wetting and drying cycles (*Turner and Haygarth*, 2001).

Physical detachment is related to soil erosion when water flow carries non-dissolved P associated with soil particles (*Kronvang* (1990) and *Quinton et al.* (2001)). However, this P-export mechanism is less important in grassland-dominated catchments.

1.2.3 Transport

Phosphorus is transported along surface and subsurface flow pathways. On grassland sites, DP-loss in runoff predominantly arises from the P mobilized from P-enriched topsoils and from incidental P-losses (IPL, see *Withers et al.* (2003)). However, areas with a high soil-P status and recent manure additions are not necessarily those areas susceptible to P-transfer (*Preedy et al.*, 2001). The reason is that without runoff occurring on such sites there is no P-loss irrespective of the soil-P status (*Gburek and Sharpley* (1998) and *Gburek et al.* (2000)). Hence, transport of DP requires (i) a high soil-P status and/or recent manure applications, (ii) the occurrence of fast flow and (iii) an existing hydrological connectivity from the field to the brook enabling fast P-transport. Such constellations are thought to be limited to a few fields - hot spots - that contribute above-average to P-loss. In catchments of humid conditions, discharge is mostly controlled by the occurrence of saturated overland flow. Simultaneous surface and subsurface flow processes at different locations or successive flow processes at the same location are initiated by rainfall and influenced by topography, vegetation, structural soil properties and the soil moisture. This influences how hydrological contributing areas for P-loss expand and contract over time during dry and wet periods.

Surface and subsurface transport pathways

The generation of surface runoff such as Hortonian overland flow is determined by the infiltration capacity of the upper soil layer according to *Horton* (1933). A temporally limited infiltration capacity can also lead to “temporary Hortonian overland flow” under certain conditions, e.g. for a dry hydrophobic layer (*Burch et al.*, 1989). However, this flow process disappears after wetting of the water repellent upper soil layer. Saturated overland flow is more frequent in humid catchments and occurs when the infiltration capacity of a soil is exceeded and the surface depressional storage is filled to its capacity. It generally emerges in flat areas or nearby stream channels where surface and subsurface flow accumulate. The

amount of P mobilized and transported in surface runoff varies with the storm duration, rainfall intensity, soil-P status, vegetation roughness, slope, antecedent moisture and infiltration capacity (*Heathwaite*, 1997). Surface runoff is a fast flow process and the runoff volume may increase due to soil compaction through trampling (*Heathwaite and Johnes*, 1996) or due to the sealing of the soil surface by manure (*Withers et al.* (2000); *Smith et al.* (2001); *Burkhardt et al.* (accepted)).

Subsurface flow processes can be distinguished into processes within the unsaturated (throughflow, interflow) and in the saturated zone (groundwater flow, deep subsurface flow). For soils with a permeable upper layer most of the precipitation infiltrates into the soil matrix. Commonly, the DRP-concentration in water percolating through the soil profile is small due to strong P-sorption (*Haygarth et al.*, 1998). Exceptions occur in peaty, sandy, or acid organic soils with low P-sorption capacity due to the mostly negatively charged surfaces and complexing of Al- and Fe-oxides by organic ligands (*Sharpley and Rekolainen*, 1997). Subsurface lateral matrix flow is induced in the unsaturated soil layers when the hydraulic conductivity is larger in the lateral than in the vertical direction, e.g. when more permeable upper soil layers overlay less permeable subsoil layers. Lateral subsurface matrix flow is commonly parallel to the impermeable layers but it can be diverted by lateral or vertical macro- and mesopores and reach the saturated zone of the groundwater. Fast flow through such networks of macropores, cracks or fissures is known as preferential flow when large amounts of water rapidly bypass the soil matrix and high P-loads are transported within a short time from the surface through the soil with little sorption to the matrix (*Hesketh and Brookes*, 2000). Evidence for preferential flow was found in many soils (*Gächter et al.* (1998); *Stamm et al.* (1998); *Dils and Heathwaite* (1999); *Turner and Haygarth* (1999)) and has also been discussed in detail by *Hoffmann-Riem* (2003). Preferential flow is caused by local differences in the hydraulic conductivity which is low at locations of low porosity (clayey material) or of water-repellent surfaces of the solids (*Ritsema and Dekker*, 2000). This forces the water to flow through soil regions with higher hydraulic conductivity (e.g. macropores, cracks, earthworm burrows, root channels, etc.) collecting water from the surrounding soil. This way, P rapidly moves through macropores to tile drains and poses a large potential for P to be laterally transported into surface waters (*Stamm et al.*, 1998).

P-loss from grassland fields

Numerous studies have shown that DRP-concentrations in surface runoff, released from the P stored in topsoils, are well correlated with the soil-P status (*McDowell and Sharpley* (2001); *Torbert et al.* (2002); *Quinton et al.* (2003)). However, the P-loss may strongly increase as soon as a threshold level of P-saturation, which is also known as the change point, is exceeded (*Heckrath et al.* (1995) and *McDowell and Sharpley* (2001)). Runoff experiments on intensively grassland sites often exhibited DRP-concentrations from 0.2 to 2 mg l^{-1} depending on the soil-P status (*McDowell and Trudgill* (2000); *Heathwaite and Dils* (2000); *Vollmer et al.* (in prep.)). However, with increasing flowpath-length during overland flow these concentrations may also drop as a result of dilution (*Haygarth and Jarvis*, 2002).

When rainfall coincides with recently applied manure, known as incidental P-loss (IPL), substantial P-loss may emerge. In that case, total-P concentrations may increase to 26 mg l^{-1} and DRP-concentrations above 5 mg l^{-1} (*Braun et al.* (1993); *Stamm et al.* (1998); *Withers et al.* (2003)). Such circumstances which favor IPL are not uncommon in the Lake Sempach region since the period of heavy manure application overlaps with the period of highest rainfall amounts. In this region, manure is commonly applied shortly after the last grass cut (4 to 5 times per year) and such a tight schedule makes it difficult for farmers to spread manure always under suitable conditions. Several studies showed that the timing of the application substantially influences the DRP-concentrations in surface runoff which markedly decline with increasing duration between manure application and the onset of surface runoff (*von Albertini et al.* (1993); *Braun et al.* (1993); *Edwards and Daniel* (1993b); *Sharpley* (1997); *Withers et al.* (2003); *Tabbara* (2004)). This behaviour can be explained with the increasing contact time of added P with the soil matrix. These concentrations may still be high after a few weeks without substantial rainfall.

In the drainage effluent from grassland soils *Stamm et al.* (1998) observed extremely high DRP-concentrations >4 mg l^{-1} when liquid manure was applied one or two days before. *Simard et al.* (2000) noted that P-transport by preferential flow may be important during storm events that rapidly follow periods of manure applications and drought periods creating fissures in the surface soil. However, the dominant P-forms in tile drains strongly vary with different site-conditions (*Heckrath et al.* (1995); *Beauchemin et al.* (1998); *Haygarth et al.* (1998)).

Despite considerable research effort in the past there are still open questions. One

important question is how relevant the contribution of P-loss from soils or from IPL in catchments is or whether there are causal relationships between manure application and the observed P-loss from a catchment? Which are the risk areas or "hot spots" in a catchment and how large is the P-loss from such "hot spots" compared with the total P-loss from the whole catchment? Such questions can be tackled by modeling if adequate data is available for a catchment.

1.3 Possibilities and limitations in catchment modeling

Despite the fact that many models are available to simulate diffuse P-loss at the catchment scale the prediction of diffue P-loss still faces many fundamental scientific problems. This section gives an overview of the wide-spread model types and the problems related to modeling diffuse P-loss at the catchment scale.

1.3.1 Spatial discretization and parameterization

Models can be distinguished into lumped, semi-distributed or distributed types in terms of their spatial discretization and parameterization of landscape units. While lumped models do not account for the spatial variability of processes, input, boundary conditions or geometric landscape characteristics (*Singh*, 1995) semi-distributed models use the same parameters for the same landscape units irrespective of their location in the catchments. Distributed models apply distinct parameters for the same landscape units depending on their location in the catchment.

1.3.2 Empirical models

The simplest structures encompass empirical models. They focus on identifying a relationship between input and output without worrying explicitly about the physical, chemical and biological mechanisms converting input into output. Catchments or subcatchments are treated as single units using average parameters. These parameters have little physical or chemical meaning and the results represent cumulated nutrient losses for such units. For example, *Lek et al.* (1996) linked catchment features with observed P-concentrations and P-loads by using neural networks. A more experimental approach is the export coefficient method that up-scales the exported nutrient loads measured from distinct units by field experimental studies to large catchment sizes (*Johnes* (1996) and *Johnes and Heathwaite* (1997)) thereby accounting for complex land-use systems. This approach has also been

combined with the HOST classification (Hydrology of Soil Types, *Boorman et al.* (1995)) by *Heathwaite et al.* (2003) to derive hydrologically effective rainfall to predict mean annual P-export and to estimate the impact of land-use and management change. Other approaches such as the index method for P (*Gburek et al.* (2000) and *Braun et al.* (2001)) assign site-specific risk values based on various factors such as the land-use, method of manure application, chemical and hydrological site conditions which govern P-loss. For each field, the risk-values of all factors are weighted to yield a total risk for P-loss and export coefficients are assigned to these total risk-values to estimate the site-specific P-loss. This approach strongly relies on the subjective assignment of risk-values based on expert-knowledge and on their weighting procedure. Although this concept is widely used to estimate mean-annual P-loss, it is a static approach and not suitable for event-based predictions.

1.3.3 Conceptual models

Conceptual models describe the physical, chemical and biological P-processes by using conceptual reservoirs for different P-pools. The temporal change of these P-reservoirs is determined by simple flux rates between P-pools to account for sorption, mineralization, uptake by plants, etc. They offer a practical compromise between physically-based and empirical models and do not request a vast amount of distributed parameters and catchment data (*Viney et al.*, 2000). However, the parameters must be derived from observations and the transfer of parameters obtained from catchments used for calibration into others is limited. Examples for such models are CREAMS (*Knisel*, 1980), GLEAMS (*Leonard et al.*, 1987), EPIC (*Sharpley and Williams*, 1990), SWAT (*Arnold et al.*, 1998) or ICECREAM (*Tattari et al.*, 2001). These models apply similar formulations for the P-cycle and mainly differ in their hydrological description and purposes. Some are designed for event-based simulations (AGNPS (*Young et al.*, 1995)), others neglect preferential flow (HSPF (*Donigian et al.*, 1995)) and some are only applicable to field-sized applications in domains they were calibrated for (CREAMS, ICECREAM, EPIC). More often, widespread conceptual rainfall-runoff models such as TOPMODEL (*Beven and Kirkby*, 1979) or HBV (*Lindström et al.*, 1997) are extended with components for agricultural drain-flow (*Kim and Delleur*, 1997) or diffuse P loss.

1.3.4 Physically-based models

Physically-based models start from our understanding of the underlying physics of hydrological processes that govern the catchment response. They describe the physical, chemical and biological processes by partial differential equations for mass, momentum and energy, e.g. the Richards equation (*Richards*, 1931) is applied to calculate water flow and the convective-dispersion-equation to simulate mass transport. Examples for such models are the hydrological model SHE (*Abbott et al.*, 1986) or the diffuse P-model ANIMO (*Groenendijk and Kroes*, 1999). Although these models might benefit from physically meaningful parameters they are confronted with several problems: They are extremely data-demanding although such detailed data is often not available at the catchment scale and classic transport approaches such as the convective-dispersion equation can not reproduce fast transport mechanisms such as preferential flow.

A major problem is the scale issue which addresses the variation in results that can be obtained when data acquired from small areal units are progressively aggregated into fewer, larger units. Generally, the scale of measurement does not correspond to the scale of the model. Such models rely on descriptions of point-scale processes which are derived from small-scale physics of relatively homogeneous systems while the scale (commonly the grid scale) of real applications of such models is much larger. Hence, the model parameters are scale-dependent as a result from the heterogeneity of soil properties below the scale of application. Parameters representative at a small scale substantially change when upscaling to the larger model grid scale (*Wood et al.* (1988); *Beven* (1989); *Grayson et al.* (1992); *Blöschl and Sivapalan* (1995); *Western et al.* (2001)). This rises the question what the physical meaning of parameters is at larger scales, for example, what is the saturated hydraulic conductivity or the water retention curve of a pixel?

Such models have also been critized for loosing their physical basis because a few effective parameters are used to account for the heterogeneous soil properties on a wrong conceptual basis (*Beven*, 1989). In fact, these effective parameters degrade to lumped parameters since the calibration is mostly performed via adjusting these parameters. Since physically-based models are complex they require a large number of parameters. Compared with the available data, however, the system is highly underdetermined. This adds to the uncertainty arising from data and from the model structure and substantially amplifies the number of possible parameter combinations yielding reasonable model results.

1.3.5 Equifinality in parameters

Since all models of ecological systems are drastic simplifications of reality there is no obvious justification for the selection of a single model as the true description of an ecological system (*Reichert and Omlin*, 1997). As one option to account for uncertainty *Beven* (1993) proposed the concept of equifinality instead of seeking the optimum set of parameter values during calibration. Equifinality means that multiple parameter combinations yield similar acceptable model predictions (*Beven* (1996) and *Beven* (1997)). This concept suggests to accept all parameter sets yielding satisfying results. However, a good agreement between observations and simulations does not imply that the model-internal state-variables and the distributed predictions are correctly estimated (*Grayson and Blöschl* (2001a) and *Seibert and McDonnell* (2002)).

1.3.6 Implications for modeling

Hillel (1986) proposed the basic principles for model design: (i) The parameters should relate to observable and available field data and their number be kept to a minimum, (ii) the scope and applicability of a model should not be overstated, (iii) the accuracy of prediction cannot be better than the accuracy of the measurements, and (iv) the limits of a model must be testable for its validity. In addition, the observations from an ecological system must be first analyzed for its dominant pattern and influencing variables. It is therefore crucial in the context of this project to account in the model for the dominant processes for runoff generation, mobilization and transport of P.

1.4 Objectives and contents of this thesis

The Swiss Federal Office for Agriculture (FOAG) initiated packages of ecological measures in 1993 and 1999 to reduce the agricultural P-losses into surface waters by 50% until 2005 relative to the reference period from 1990 until 1992 (*Forni et al.*, 1999). Agroscope FAL Reckenholz was mandated by the FOAG to evaluate the effect of these measures on the water quality (*Prasuhn and Lazzarotto*, in press) by selecting a small grassland catchment in the Lake Sempach region. Our project, being part of a bundle of other evaluation projects, is called "Modeling phosphorus runoff at the catchment scale". The main objective of this PhD-thesis was to develop a dynamic parsimonious P-export model at the catchment scale which accounts for the dominant hydrological and P-transport processes. This tool is

meant as a support for policy-makers to identify risk areas for P-loss before implementing ecological measures in a catchment. Within this scope we tested several hypotheses:

- What are the dominant variables that influence the observed P-dynamic? Can we detect significant trends in the P-dynamic before and after the introduction of the ecological measures?
- Is the hydrological catchment response of several agricultural catchments in the Lake Sempach region mainly influenced by the areal fractions of two major soil types?
- Is the model capable to reproduce the observed P-loads using only the dominant hydrological and P-relevant factors? Is P lost mostly from the P stored in topsoils or is it lost mostly from recently applied manure?

In Chapter 2, we analyzed the temporally highly resolved data of discharge and nutrient concentrations of two grassland-dominated catchments to determine the dominant patterns and the main characteristics of the DRP-export dynamic in those catchments. This allowed to identify the factors which must be included in the model.

Since P-transport is governed by hydrology we developed a conceptual rainfall-runoff model to quantify the hydrological response of two major soil-types in four catchments in this region. Chapter 3 describes the model and the joint calibration in four catchments in the Lake Sempach region. Further, we report on how the model was used to test if the catchment response was strongly influenced by the areal fractions of these soil-types.

Chapter 4 focussed on (i) the quantification of the flow response from well and poorly drained soil-types, (ii) the variation in parameter estimates, (iii) the identification of hydrologically contributing areas relevant for diffuse P-loss in a catchment and (iv) the further classification of these areas into risk areas according to assigned probabilities.

Chapter 5 combined the rainfall-runoff model with the simple P-model which was exclusively calibrated with experimental field data. This model was driven by an extensive data-set for manure-management and soil-P status for all fields in the test catchment. We investigated, among others, if most P-loss occurred from soils or from incidental P-loss.

Chapter 6 draws the conclusions condensing the knowledge gained from all the preceding chapters.

Chapter 2

Phosphorus export dynamics from two Swiss grassland catchments

P. Lazzarotto, V. Prasuhn, E. Butscher, C. Crespi, H. Flühler and C. Stamm

Published in Journal of Hydrology 304 (2005), 139-150.

2.1 Abstract

Phosphorus (P) export from agricultural catchments is often event-driven and variable in time. Accordingly, a proper monitoring requires high-temporal resolution sampling during flow events. We report on a comparative study on the P-export dynamics from two grassland catchments in Switzerland, where concentrations of dissolved reactive phosphorus (DRP) have been monitored at a high temporal resolution for periods of 1.2 and 5 y, respectively. The data set is complemented by measurements on total P (TP), total dissolved P (TDP) and particulate P (PP) obtained from routine sampling ongoing since 1984 in both catchments. In one area, the high-temporal resolution monitoring revealed a pattern of the P-export dynamic as expected from other studies. During flow events DRP-concentrations usually increased significantly exceeding 1000 mg DRP m^{-3} during peak flow, while the values remained low between 20 and 100 mg DRP m^{-3} at baseflow. This pattern was partially confirmed in the second catchment. The expected pattern was observed in 1998 and 1999 but was partially replaced by a new one for the following years. In the growing season, DRP only weakly increased with flow rate or remained almost constant. During flow events values larger than 300 to 400 mg DRP m^{-3} were rare. In contrast to these relatively low peak flow concentrations, high values (200 to 300 mg m^{-3}) were recorded at baseflow during

the years 2000 to 2002. During the same period, DRP-concentrations exhibited strong daily oscillations. Independent sampling and analytical control measurements verified the findings. Point sources like leaks from manure tanks could be ruled out based on the ammonia measurements. We suggest that biogeochemical processes within the brook are responsible for this change in the P-export dynamics. Despite these changes in the pattern of the P-export dynamic and ecological measures implemented on the farms no significant effect on the annual P-loads could be observed during the last 10 years.

2.2 Introduction

Research during the last decades has shown that in a country like Switzerland where grassland is one of the dominating agricultural land uses, the diffuse runoff of Phosphorus (P) from grassland soils is a major source for eutrophication of surface waters. Lake Sempach is one of the Swiss lakes having this problem since the seventies. After most point sources had been eliminated by the mid eighties, P-losses into the lake did not decrease as predicted but reached total P (TP) concentrations of 165 mg m^{-3} in 1984, dramatically exceeding the water quality goal of 30 mg TP m^{-3} (*Stadelmann*, 1988). This indicated that diffuse P-losses from agriculture had increased and actually counterbalanced the reduced losses from waste water. Based on calculated P balances for Lake Sempach, the diffuse P-losses should not exceed 0.5-0.9 kg DRP ha^{-1} y^{-1} to reach the goal of 30 mg P m^{-3} in the lake water (*Gächter and Stadelmann*, 1993). Some catchments are still far from reaching this environmental standard since their annual load ranges between 0.3 to 1.3 kg DRP ha^{-1} y^{-1} for the period 1998 to 2002.

In most grassland soils, the sources of the diffuse P-losses are the P accumulated in the topsoil and the P contained in manure that has been recently applied. Phosphorus gets mobilized from these surface layers and is transported to surface waters mainly by surface runoff and preferential transport into subsurface drainage systems (*Sims et al.* (1998) and *Dils and Heathwaite* (1999)). The relevance of both processes has been clearly demonstrated in the catchment of Lake Sempach (*von Albertini et al.* (1993); *Braun et al.* (1993); *Stamm et al.* (1998); *Stamm et al.* (2002)). During fast transport, P-sorption to soil material is also limited due to the short contact time, the small soil-water ratio in those flow paths and possibly to colloid-facilitated transport. Therefore, the P-dynamic in a brook draining small agricultural catchments is expected to be strongly influenced by storm events with P-concentrations increasing during high flow periods. Several studies in tributaries of the

Lake Sempach confirmed this expectation.

These studies were based on discrete sampling on a predefined schedule and flow-proportional sampling under high flow conditions. This procedure yields a relationship between discharge and P-concentration that can be used to calculate the P-loads based on continuous discharge measurements. Such relationships however, show large scatter (*Gächter et al.*, 1996) demonstrating that much of the observed variability of P-concentrations can not be explained by discharge alone. Continuous measurements can improve the understanding of P-export dynamics. A first monitoring campaign of this type was carried out in 1993 and 1994 in one of the Lake Sempach catchments ("Kleine Aa", *Gächter et al.* (1996)) measuring dissolved reactive P (DRP), nitrate and ammonia. The study confirmed the expected P-dynamics. In a further study the transport of particulate P (PP) was measured during a few selected events (*Pacini and Gächter*, 1999).

Overall, these studies demonstrated that high-temporal resolution monitoring is a useful tool to investigate in detail the P-export from such small agricultural catchments. Therefore, we adopted the same monitoring strategy for testing the effectiveness of ecological measures implemented in Swiss agriculture. A first set of ecological measures was introduced in 1993 in Switzerland such as balanced P budgets of 100±10% and ecological compensation areas. Since this set seemed not to be sufficient to reach the water quality goal a second, regional project started in 1999. This second set based on stricter directives such as to apply manure according to soil conditions, 5m wide buffer strips, P-balances<100%, infrastructural measures on the farm and manure export. The Lippenrütibach catchment adjacent to that of the Kleine Aa was chosen as a test area.

In this paper, we first compare the P-export dynamic in those two catchments which are very similar with respect to land use, soil types, topography and climate. Second, we investigate whether the P-export and its dynamics changed over periods of several years. For this purpose, we combine the data from the intense online measurements with those from the conventional sampling that provides further information on the P- forms.

2.3 Material and Methods

2.3.1 Site description

Lake Sempach in central Switzerland has a surface area of 14 km^2 and its watershed covers 60 km^2 (Fig. 2.1). It consists of several catchments that drain separately into the lake. Av-

erage precipitation varies from 1100 to 1200 mm y^{-1} and highest monthly rainfall typically occurs in May and June. Soils developed from glacial till (Würm glaciation) and Molasse. Agriculture dominates the land use (75% of the area) primarily as intensive livestock production (2.4 dairy-cow equivalents ha^{-1} for the period 1996 to 2001, *FÖK* (2002)). From 2001 onwards, many farms have balanced P-budgets of 100% (*FÖK*, 2002).

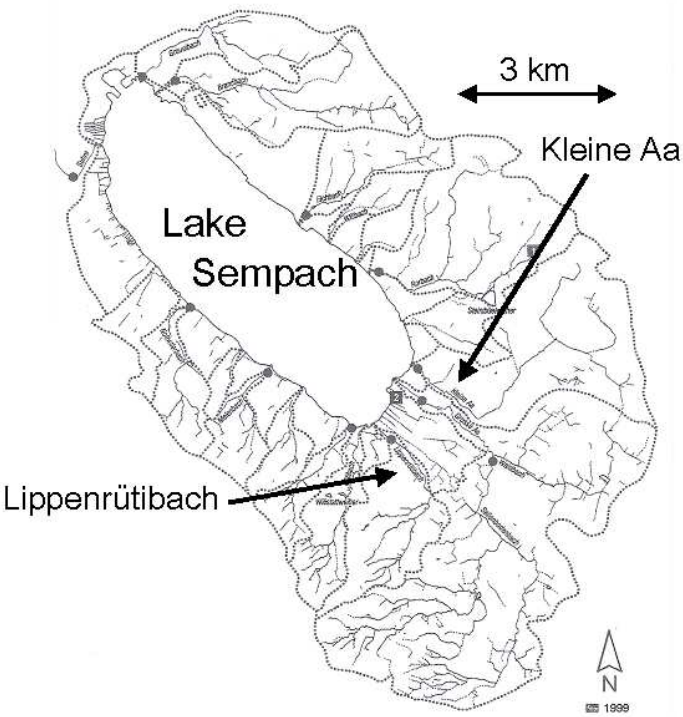

Figure 2.1: *The Lake Sempach region and its catchments. Filled squares represent sewage treatment plants and filled circles limnigraph stations. Map: Environmental protection agency of the Kt. Luzern.*

The studied catchments Kleine Aa (7 km^2) and Lippenrütibach (3.3 km^2) are quite similar. The altitude varies from 505 to 670 and 505 to 820 m a.s.l., respectively. The land use is intensely managed grassland (60 to 65%), arable land (10 to 15%), forest (15 to 20%) and urban areas (5 to 10%). The main soil types are eutric and dystric Cambisols and eutric Gley soils. About 44 to 48% of the soils are poorly drained (*AGBA*, 1993) and a similar proportion of the catchment area is artificially drained with tiles. Manure applications are frequent (4 to 5 y^{-1}) and amount in the average to about 40 kg P ha^{-1} y^{-1} (*Pacini and Gächter*, 1999). Accordingly, soils are enriched with P: A detailed investigation (*Keller and van der Zee*, 2004) carried out in the Lippenrütibach catchment in 2002 revealed that

half of all topsoils had a P-saturation index of 25% or more. This level was shown to be critical for eutrophication (*Schoumans and Groenendijk*, 2000). In absence of significant point sources the diffuse losses dominate the P-input into the brooks (*Pacini and Gächter*, 1999).

2.3.2 Sampling and analysis

Water quality was measured at a high time resolution in the Lippenrütibach and Kleine Aa catchment for two periods (Kleine Aa: every 30 min from January 1993 until March 1994; Lippenrütibach: every 60 min since January 1998). Automated samples were taken, simultaneously with the pH and temperature measurements. The samples were filtered and analyzed for DRP. The P-analyses were conducted with a flow-injection analyser (Procon-Online-Analyzer, Procon AG, 3401 Burgdorf, Switzerland) to photometrically determine DRP as the ammonium-molybdenum reactive P (*Murphy and Riley*, 1962). Hydrazine and Sn(II)-chloride were used to reduce phosphate for the molybdenum-blue reaction. Two-point calibrations were carried out automatically every six hours. Discharge was determined at the same temporal resolution based on the level measured by a pressure transducer and the gauged level-discharge relationship.

The routine sampling monitoring is an independent procedure. Samples are taken at low flow conditions every 22 d for 24 h using a sampler (Techema AG, 4012 Basel, Switzerland) yielding mixed daily samples. Additionally, this bottle starts to fill as soon as a critical level is reached yielding a composite sample under high-flow condition. Depending on the water pressure at the sampler inlet, the duration of high flow sampling varied from 12 to 24 h. This sampling procedure is proportional to the water level above the probe and approximately flow proportional. All samples were analyzed for TP, TDP (total dissolved P) and DRP. Samples of TP (unfiltered) and TDP (filtered) were determined according to *Murphy and Riley* (1962) after potassium persulfate digestion. Particulate P (PP) was calculated as the difference between TP and TDP.

In order to compare the annual P-loads one has to remove the influence of the different hydrological conditions each year. We did so by calculating loads combining the discharge data of 1994 with the discharge-concentration relationships for the year of interest. The latter were based on the routine sampling data analyzed as a kind of moving average for each year. E.g. for the year 1992, pooled data pairs from 1991, 1992 and 1993 were considered and at least 70 data points were included for each year. The 95% confidence

intervals were calculated according to the common method of error propagation.

2.4 Results

The online monitoring between January 1993 and March 1994 in the Kleine Aa catchment exhibited a consistent pattern for the P-export dynamic. DRP-concentrations increased with rising discharge. This is a pattern expected for fast P-transport from the fields to the brook via macropores to tile drains and/or surface runoff. Nevertheless, discharge and DRP-concentrations were generally not perfectly synchronized: DRP often peaked with a little delay to the maximum flow (Fig. 2.2).

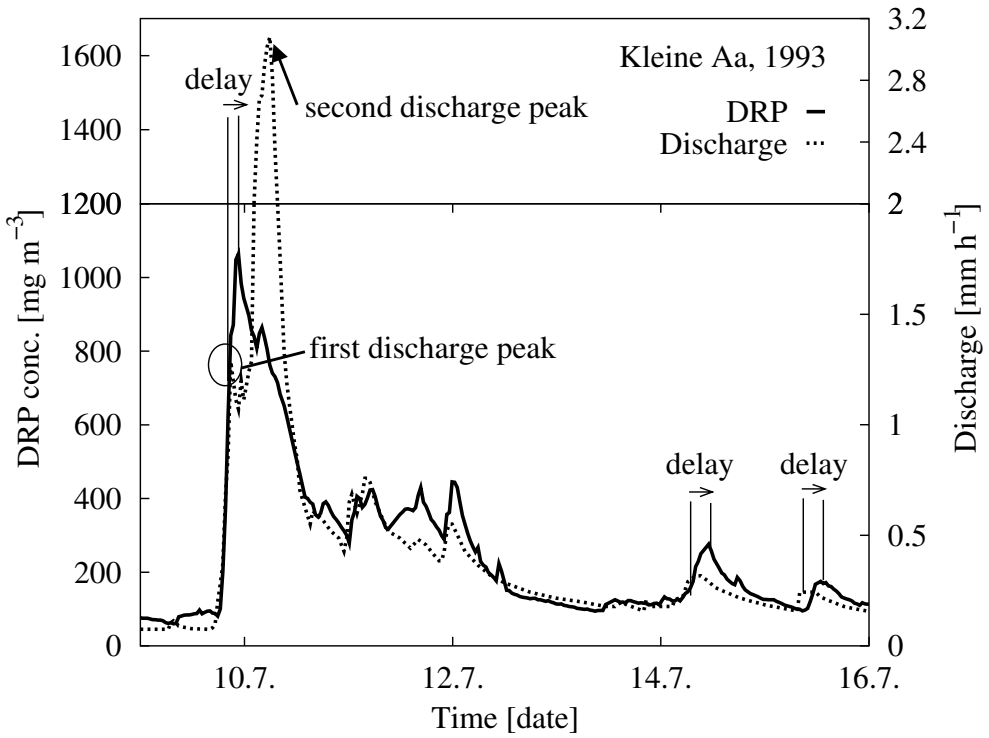

Figure 2.2: *Discharge (dotted line) and DRP-concentrations (solid line) measured online in the Kleine Aa catchment for a 1-week period in July 1993.*

A possible explanation could be sorption to suspended sediments during the initial stage of the events. Pacini et al. (1999) found in the Kleine Aa that suspended sediments and particulate P commonly reached the maximum before the peak in discharge while DRP was mostly delayed. For larger stormflow events (Q > 0.1 mm h^{-1}), the peak DRP-concentrations varied from 300 to 2000 mg m^{-3}. Smaller events (0.05-0.1 mm h^{-1}) resulted in concentrations up to 300 mg DRP m^{-3}. The flow rate, however, was not the only factor controlling DRP-concentrations. There were also indications that the P-availability in the

soil for transport influenced the concentration level in the brook. An example is depicted in Fig. 2.2. The first discharge peak caused the highest DRP-values, the very large discharge peak following shortly after, caused lower P-concentrations indicating a depletion of the P-pool. Under baseflow conditions, the DRP-concentrations were relatively low, ranging from 20 to 100 mg DRP m^{-3}. A seasonality effect could not be detected (Fig. 2.3, left).

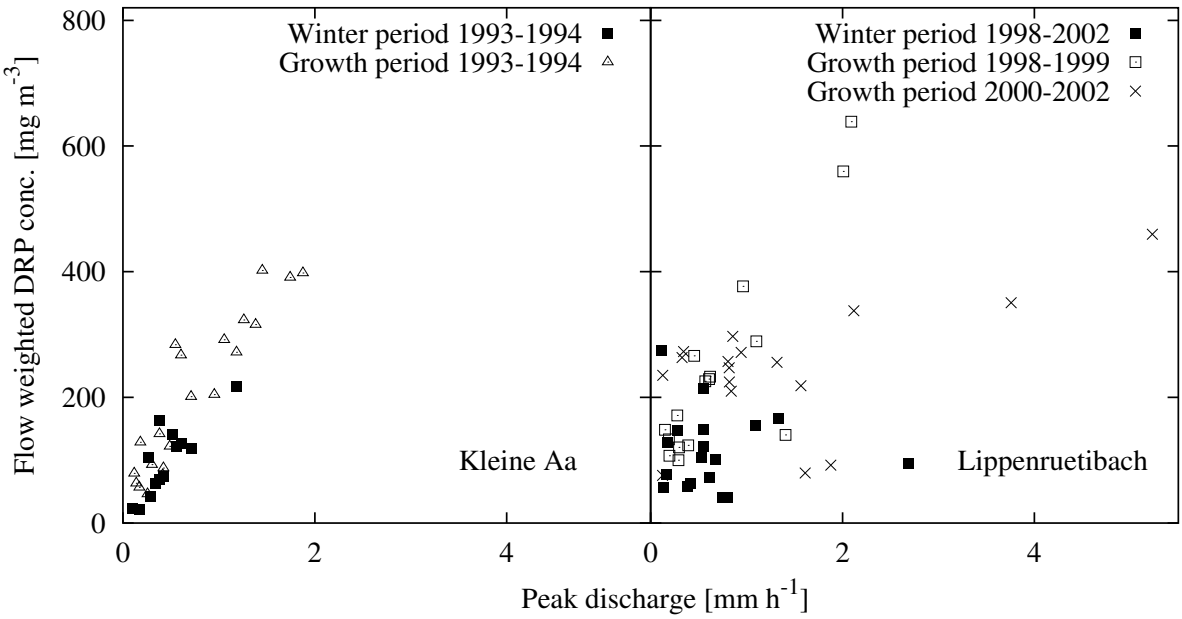

Figure 2.3: *Flow-weighted DRP-concentrations of single flow events derived from online monitoring as a function of peak discharge in the two catchments Kleine Aa (left) and Lippenrütibach (right). Filled black symbols indicate events in the period from November to March, open symbols depict events during the growth period (April to October).*

Based on the similarity of both catchments, we expected a similar P dynamic in the Lippenrütibach catchment. This expectation was only partially confirmed during the monitoring period 1998 to 2002. In the beginning of this period, we observed the pattern described above with low DRP-concentration under baseflow conditions and very pronounced increases during flow events (Fig. 2.4 and 2.5).

This "typical" pattern was observed in 1998 and during most of the year 1999. Thereafter, it only occurred in the winter. During the vegetation period, a new pattern emerged

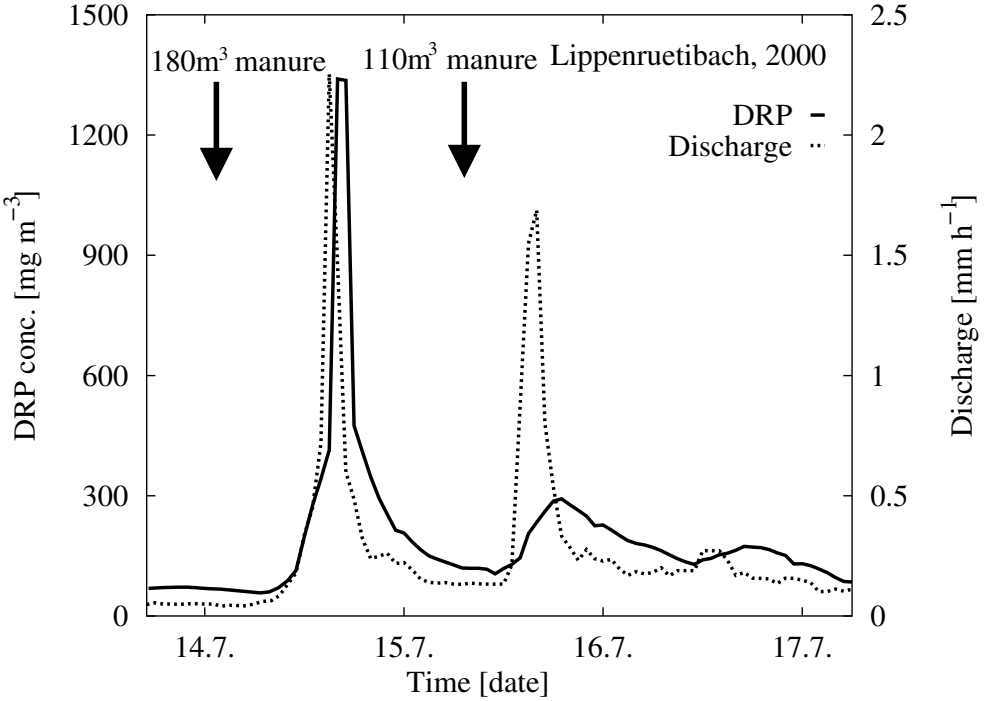

Figure 2.4: *Discharge (dotted line) and DRP-concentrations (solid line) measured online in the Lippenrütibach catchment for a 3 day period in July 2000.*

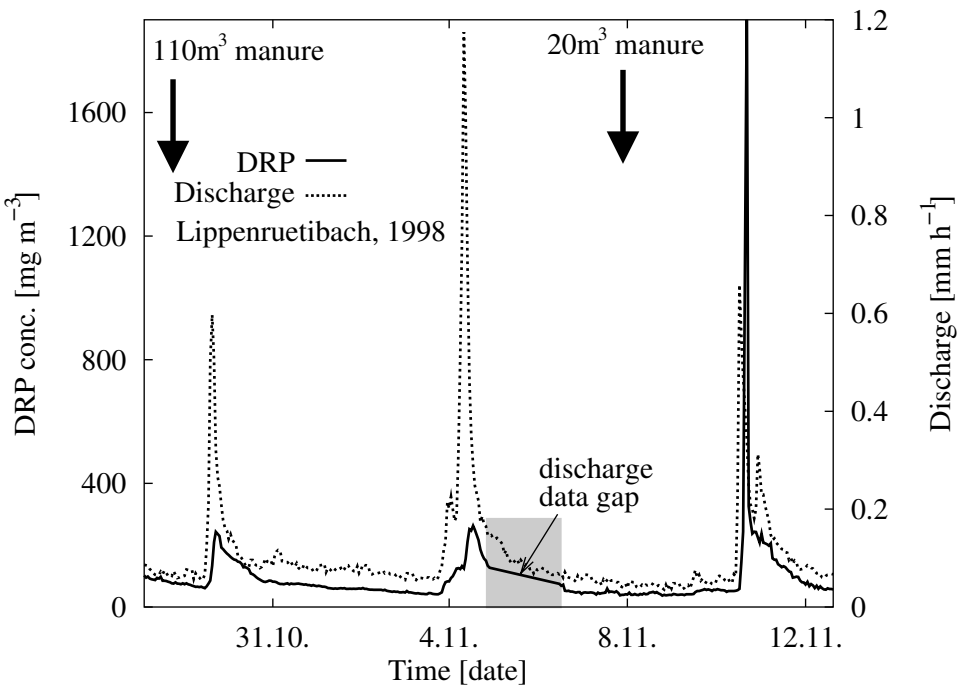

Figure 2.5: *Discharge (dotted line) and DRP-concentrations (solid line) measured online in the Lippenrütibach catchment for a 2-week period in November 1998.*

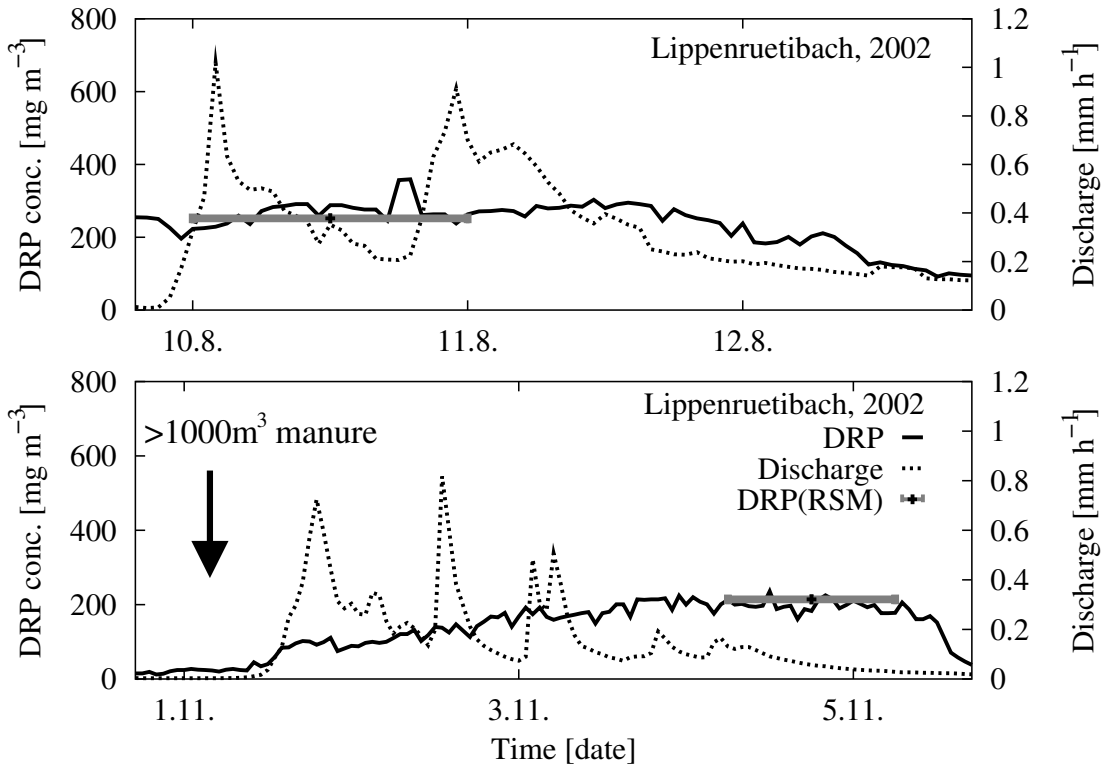

Figure 2.6: *Modified P-export pattern in 2002. Discharge (dotted line) and DRP-concentrations (solid line) measured online in the Lippenrütibach catchment for a 4 day period in November 2002 (bottom) and for a 3 day period in August 2002 (top), respectively. The horizontal grey lines indicate the DRP-concentration obtained from the independent routine sampling (RSM) at the corresponding period.*

(Fig. 2.3, right). This was shortly observed also in spring 1999 and dominated the P-export between May and October of the subsequent years (with exceptions, like that in July 2000, see Fig. 2.4). With the new pattern, the close relationship between discharge and DRP-concentration was lost (Fig. 2.3, right). Instead, we observed that either DRP increased only very slowly reaching its maximum only days after the runoff event (Fig. 2.6, bottom) or it did not rise at all (Fig. 2.6, top).

As mentioned before, DRP-concentrations cannot be explained by discharge alone even with the "old" export pattern. The availability of P seemed to control DRP-concentrations as well (see above; Fig. 2.2). Therefore, one may argue that these concentrations could be strongly influenced by the amount of manure that was applied in the catchment prior to a given event. Since we have access to this kind of data for the Lippenrütibach area we can test this idea for certain series of discharge events.

For the example depicted in Fig. 2.4, we know that during the week just before the first event on July 14 180 m^3 manure were applied on four fields. This event caused very

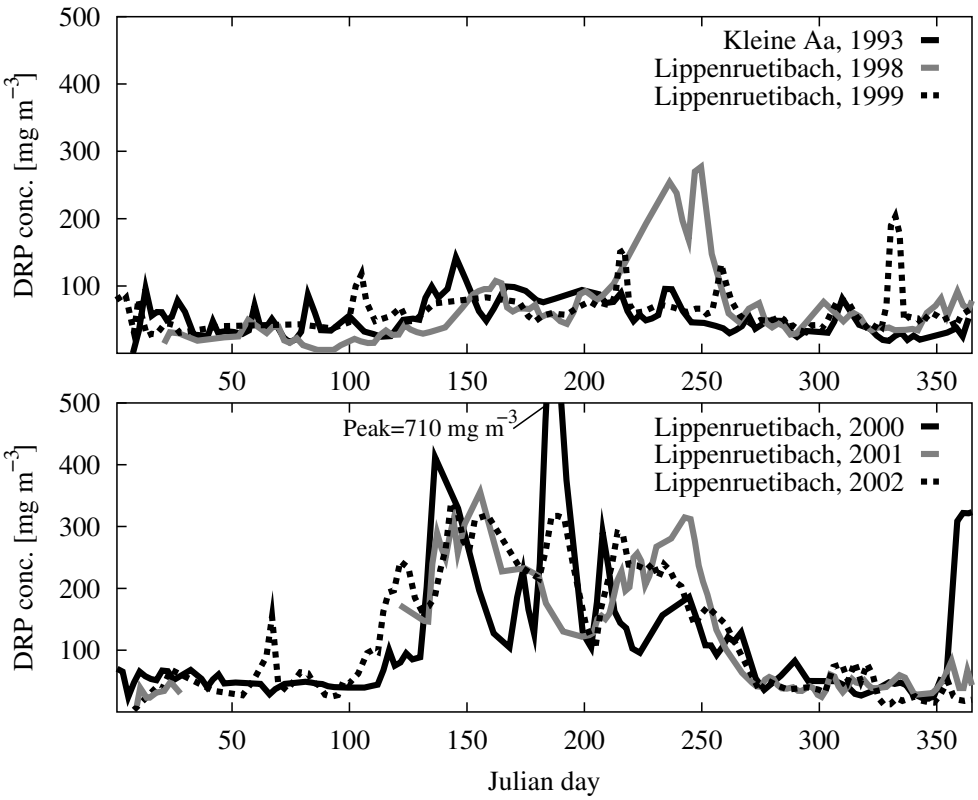

Figure 2.7: *DRP-concentrations during baseflow (Q<0.1 mm h^{-1}) in the two catchments Kleine Aa and Lippenrütibach for several years.*

high DRP-concentrations (>1200 mg m^{-3} for peak discharge > 2 mm h^{-1}) that may be due to incidental losses after these manure applications. One day after the first flow peak, additional 110 m^3 manure were spread by one farmer on three other fields. Despite the wet soil conditions, the subsequent discharge event of similar magnitude caused much lower DRP-concentrations.

A second example how manure applications influenced the DRP-concentrations in the brook is depicted in Fig. 2.5. Although maximum flow rates were of the same magnitude for these three events in autumn 1998, the maximum DRP-concentrations differed substantially. Shortly before the first event, 110 m^3 slurry was applied on five fields. In contrast, only 20 m^3 were spread between the second and third event but very high concentrations were observed thereafter.

The new DRP-pattern makes an analysis even more complex. Prior to the series of flow peaks depicted in Fig. 2.6 (top and bottom) more than 1000 m^3 slurry were spread during the two weeks before the first respective runoff event. Despite these massive manure applications onto 15 fields in the catchment, the flow peaks did not cause peaks of high DRP-concentrations, as expected from the system's response from previous observations.

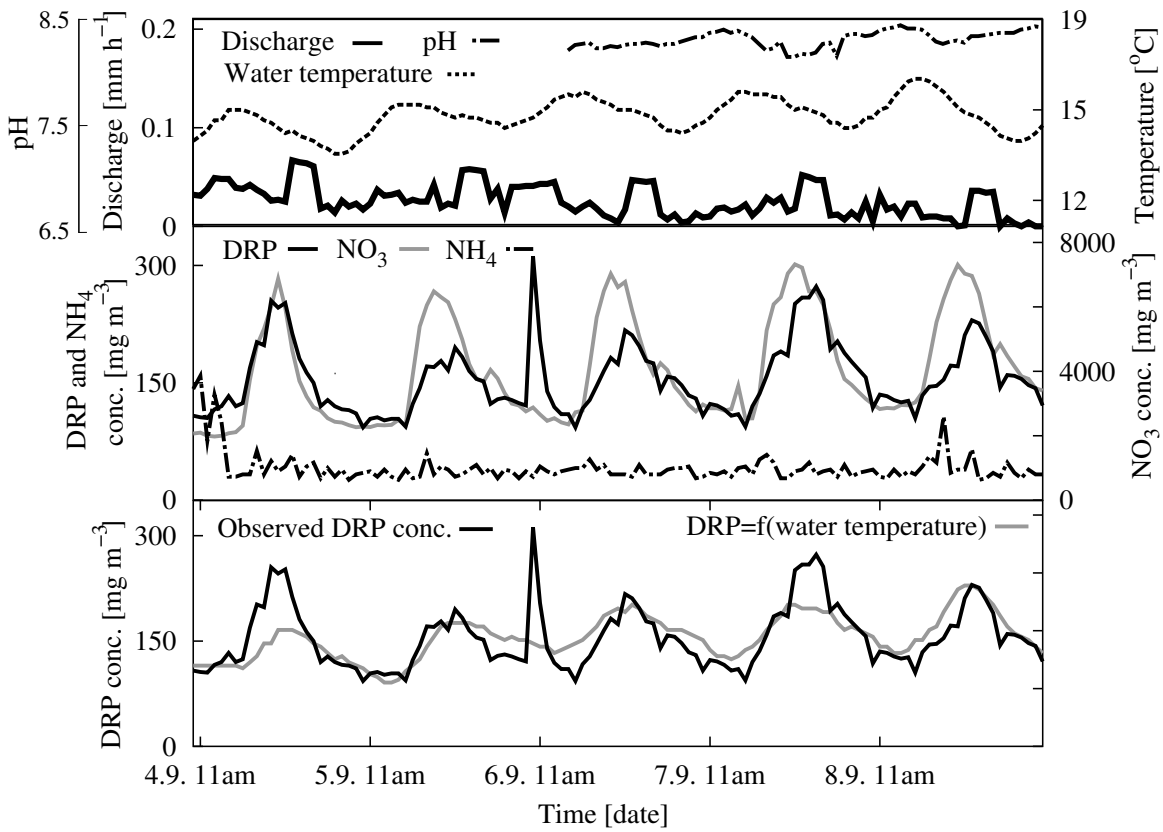

Figure 2.8: *Daily oscillations of DRP (solid black line), nitrate (solid grey line) and ammonia (dotted black line) concentrations under baseflow conditions (Q<0.1 mm h^{-1}) observed with the online monitoring for a 5 day period in September 2002 in the Lippenrütibach (middle). Discharge (solid line), pH (dotted-solid line) and water temperature (dotted line) are in the top figure. The bottom figure shows the observed (black line) and the calculated DRP-concentration (DRP, grey line) based on the water temperature T by DRP=a+b*T(t-6h)+c*T^2(t-6h) with t as the time in hours and the fitted parameters and standard errors a=115.51±13.14, b=-42.61±5.55 and c=2.96±0.35.*

These three examples indicate that the amount of manure applied in a catchment is a poor predictor for DRP-concentrations in the brook at the outlet of the catchment. The results highlight the importance to understand the spatial variability of the susceptibility of individual fields to export P.

In the year 2000, a dramatic change of the P-dynamic started to appear under baseflow conditions (Q<0.1 mm h^{-1}). Very consistently, the DRP-concentrations remained on a high level from May to October (200 to 400 mg m^{-3}; Fig. 2.7 bottom; lines smoothed). During these periods of high DRP baseflow concentrations, we also noticed pronounced daily DRP- and NO_3-oscillations (Fig. 2.8, middle). For DRP, the amplitudes tended to rise with average concentrations and often reached magnitudes of 100% (50 to 300 mg DRP m^{-3}). The maximum DRP-concentrations were always observed during the night

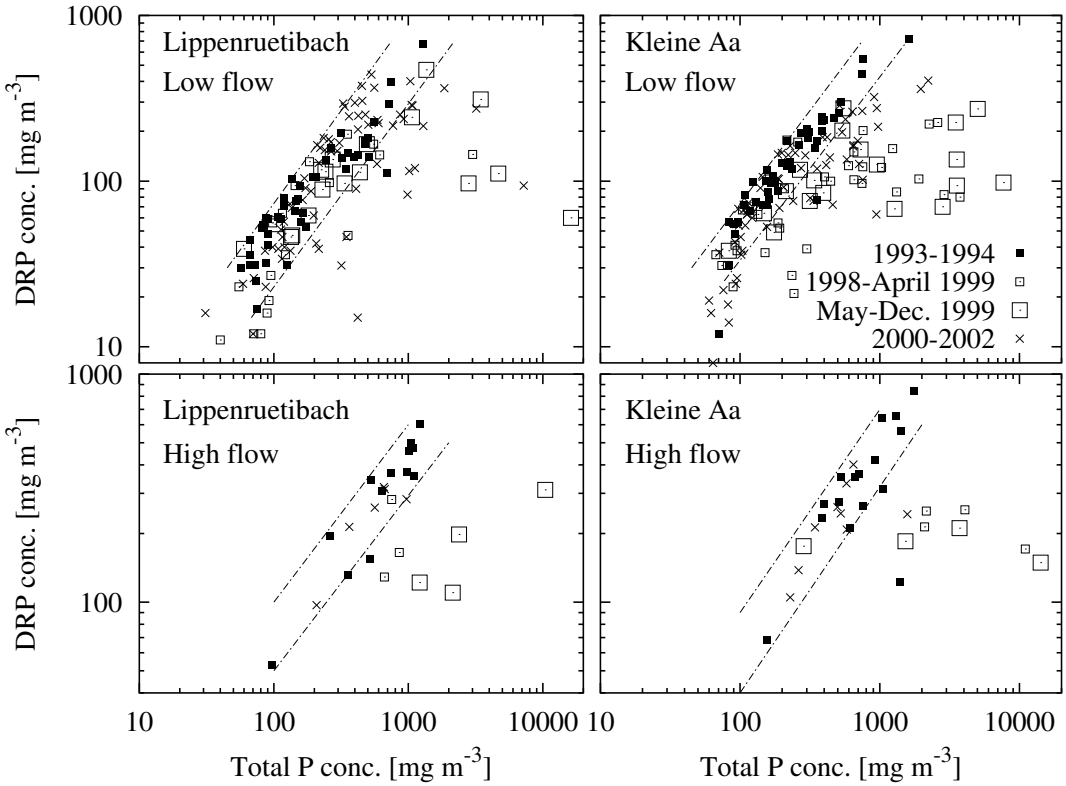

Figure 2.9: *Relationships between total P (TP) and DRP-concentrations in the Lippenrütibach (left) and Kleine Aa (right) under low (top) and high flow conditions (bottom), respectively for the routine sampling monitoring. Dashed lines represent upper and lower ranges of most water samples taken between 1993 and 1994. Large squares are water samples taken between May and December 1999.*

(9pm-2am) and minima during day time (11am-5pm).

The fact that oscillations of DRP were strongly correlated with those of nitrate (Fig. 2.8, middle) suggests that the underlying processes influenced P and N simultaneously. In contrast, ammonia didn't show these daily oscillations. This excludes the possibility that the high DRP-concentrations during baseflow were due to some leakage from manure tanks. However, the phase of the DRP and nitrate oscillations was closely related to the temperature of the brook. The two nutrients followed temperature with a constant delay of six hours (Fig. 2.8, bottom).

We checked the online measurements with composite samples from the routine monitoring program. This yielded a completely independent data set based on a different sampling procedure and an offline verification of the same analytical procedure. The comparison revealed that the new pattern - relatively low DRP-concentrations under storm flow, relatively high DRP-concentrations under baseflow conditions - was real. In Fig. 2.6,

Table 2.1: *Mean and standard deviation for DRP and PP expressed as percentages of TP in water samples during low and high flow rates in the Kleine Aa and Lippenrütibach catchments for the years 1993-1994, 1998-1999 and 2000-2002 obtained with the routine sampling monitoring.*

	Lippenrüti				Kleine Aa			
	Low flow		High flow		Low flow		High flow	
	%DRP	%PP	%DRP	%PP	%DRP	%PP	%DRP	%PP
1993-1994	47±13	43±15	47±12	48±12	57±13	34±10	47±15	45±12
1998-1999	33±18	60±19	15±12	83±13	26±20	70±22	14±20 ‡	84±23
2000-2002	42±23	51±22	46±10	50±9	42±18	47±18	48±15	46±15

‡non-gaussian distributed due to outliers

we included the mean DRP-concentrations measured in the composite sample showing an excellent match. The general comparison of DRP-concentrations obtained by the two monitoring programs revealed a reasonable correlation (R^2=0.63, no bias) for all water samples for the period 1998-2002. Low flow samples of the two sampling programs agreed better (R^2=0.71) than high flow samples (R^2=0.38). The poor correlation obtained for high flow periods is partially due to three events in 1999 and one in summer 2002. Excluding these from the analysis improved the match (R^2=0.79 and 0.82 for all data and high flow data, respectively). Nevertheless, the comparison demonstrates that for single events one or both methods may yield results of considerable uncertainty. This highlights the importance of regular independent quality controls in monitoring studies.

Apart from giving an independent quality control of the online measurements, the routine sampling provided data on various P-forms and made it possible to analyse long-term trends of P-concentrations. In this study, routine samples at low and high flow rates were split into three groups (1993-1994, 1998-1999 and 2000-2002). The first two-year period refers roughly to the online monitoring period in the Kleine Aa catchment. The others correspond to the monitoring period in the Lippenrütibach catchment, split into two groups according to the pattern of the P-export dynamic (Fig. 2.9).

The composition of TP varied considerably over time. From 1993 to 1994, the samples contained 50% DRP and 50% PP on average for all flow regimes in both catchments (Tab. 2.1) with only a few exceptions. The years 1998-1999 revealed a strong shift in the P-fractions towards a PP dominance (60 to 84%) over DRP (14 to 33%) independent of flow rate (Fig. 2.9). This was the case in both catchments but was less pronounced in the

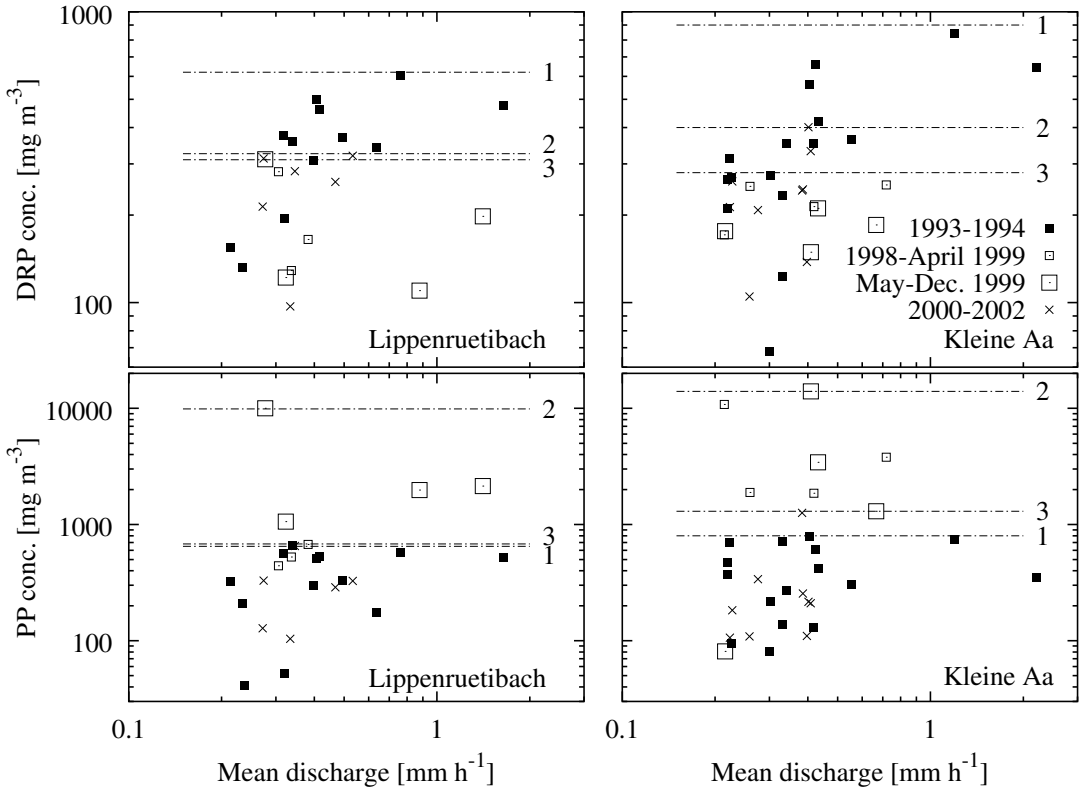

Figure 2.10: *Relationship between the mean discharge and P-fractions for the Lippenrütibach (left) and the Kleine Aa (right) for DRP- (top) and PP-concentrations (bottom), respectively for the routine sampling monitoring. The dashed lines and numbers represent the highest P-concentrations observed during stormflows for each period of 1993-1994 (1), 1998-1999 (2) and 2000-2002 (3). Large squares denote water samples taken between May and December 1999.*

Lippenrütibach for low flow rates (only 60% PP). This shift however was only temporary. From 2000 to 2002, P-fractions in water samples tended to retrograde towards the ratios observed from 1993 to 1994. This holds for both catchments and is very clear at high flow rates (Fig. 2.9 bottom).

Most samples with elevated PP-fractions in 1998-1999 occurred between May and December 1999 (large squares in Fig. 2.9 bottom). This seven month period started with a six day major stormflow in May 1999 (>100 mm rainfall) when discharge peaks exceeded 2 mm h^{-1} and enhanced streambank erosion yielded high PP-fractions. The coincidence of this major flood event and the temporal shift in the P fractionation indicates that a single extraordinary event may affect the P-export dynamic of a catchment over several months.

Comparing the relationships between mean discharge of flow events and P concentrations revealed some interesting trends over time (Fig. 2.10). For both catchments and similar flow rates, the highest DRP-concentrations dropped markedly from 1993-1994 (dashed

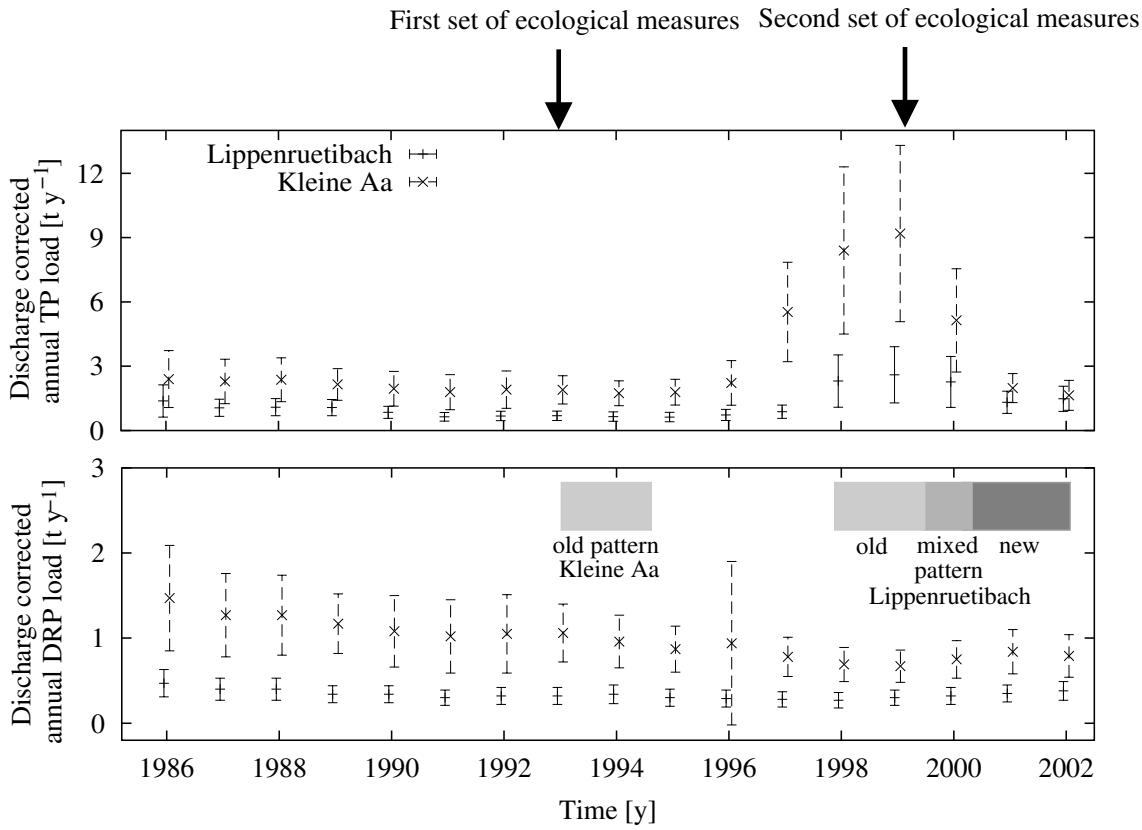

Figure 2.11: *Discharge-corrected annual TP- (top) and DRP-loads (bottom) calculated with the year 1994 as the reference period for daily discharge and various concentration-discharge relationships for each year. Error bars indicate the 95% confidence intervals for the annual P-loads and the grey shaded bars represent the period of the online monitoring campaign with the various patterns of P-export dynamic.*

lines denoted as 1) to 2000-2002 (dashed lines denoted as 2). In the early 1990s, mean DRP-concentrations reached values up to 900 mg m^{-3}. In the later periods, these values were below 400 mg m^{-3} for similar flow rates. Again, the years 1998 and 1999 were extraordinary with extremely high PP-values. Most of them were observed during and after the major flood of May 6, 1999. Obviously, this event made much sediment available for transport. Afterwards, it seems that a new, stabilized state was reached.

These high PP-concentrations were also reflected in the discharge-corrected annual P-loads from 1986 to 2002 (Fig. 2.11). In both catchments, very large TP-loads were observed. Apart from these two years, there were non-significant declines from 1986 until 1990/91 followed by constant loads until 1995. An immediate effect of ecological measures, implemented in 1993, is not seen. After 1999, the TP-losses significantly retrograded but were still higher in the Lippenrütibach relative to the levels before 1997 but similar to the TP-loads before 1997 in the Kleine Aa.

For DRP in the Lippenrütibach, there is a slight but non-significant trend from 1986 to 2002 for declining annual loads (Fig. 2.11, bottom). This tendency was slightly more pronounced in the Kleine Aa catchment. The introduction of the ecological measures did not cause a significant reduction in any of the two catchments. It seems that the high DRP-concentrations during baseflow in the growing season with the new pattern counterbalanced the lower loads during high flow as known from the old pattern.

2.5 Discussion

Our measurements demonstrate a strong change in the P-export dynamics in the Lippenrütibach catchment since 2000. First, the relationship between discharge and DRP-concentration during flow events as it had been observed before was almost lost. Instead, high DRP-concentrations were measured during baseflow conditions in the growing season. Additionally, they exhibited strong daily oscillations during these periods. Overall, this shows a dramatic change in the sources and possibly the retention processes within the catchment.

Independent verifications of the online-system confirmed that these changes were real and not due to some basic problem with sampling or analytics. The routine samples analyzed offline in the laboratory verified high concentrations during baseflow (see the DRP-concentration denoted as RSM in Fig. 2.6). In May 2004, hourly sampling by an independent device and subsequent analysis in the laboratory confirmed the strong daily DRP oscillations and high baseflow concentration levels. These measurements further indicated that the oscillations were more pronounced in a tile drain outflow compared to the brook itself.

Hence we conclude that there was a P-source delivering DRP at high concentrations under baseflow conditions. An obvious explanation would be the existence of a point source like a corrupt manure tank or a feedlot wherefrom P was leaking into the brook. However, the low ammonia concentrations lacking any daily oscillations contradict this hypothesis. A further argument against an anthropogenic source is the limitation to the growing season. We do not know of any anthropogenic operation limited to that period of the year that could explain the observed P-input. One could also argue that the change was due to the implementation of the ecological measures in agriculture because the P retention was increased during discharge events. However, this cannot explain the high P-concentrations during baseflow conditions.

Interestingly, *Müller et al.* (2003) observed similar daily nitrate oscillations at the outlet of a subsurface drainage system in the Kleine Aa catchment . They explained the effect by variable nitrate uptake by plant roots during the day. We doubt that root uptake can explain daily nutrient changes in the saturated zone. It seems more plausible that biogeochemical processes in the saturated zone itself, possibly in the brook sediments, caused the release of DRP and nitrate. This would agree with the delay compared to the temperature oscillations because the sediment temperature probably lags behind that of the flowing water. Similar oscillations have been clearly shown for some metals in rivers (*Nimick et al.*, 2003). For arsenate, daily oscillations followed the pH cycle with an analogous lag as we have observed with the temperature cycles. Sorption kinetics was put forward to explain this observation (*Fuller and Davis*, 1989). They conclude that continual disturbances of equilibrium could affect the bioavailability of other substances like P as well. Hence, phenomenologically our observations fit well into a picture of biogeochemical processes in streams that are only poorly understood so far.

A possible hypothesis for the observed changes starts with substantial changes of the river bed due to the large flood in 1999 and the exposure of bare subsoil after a heavy storm ("Lothar") in 1999, which caused a lot of damage in the forests of the region. Both events could have exposed subsoil that may get mobilized during flow events and acts as P sinks preventing a strong DRP increase. Furthermore, it may be speculated that organic material was buried by brook sediments causing oxygen depletion when microorganisms degrade it during the warm growing season. These could cause the sediments to release DRP.

Whatever the explanation will be, our results show that the P-export dynamics in the Lippenrütibach catchment can not be explained by the two sources commonly considered relevant to understand the P-status of brooks: point source of manure and the diffuse losses during rain events. Obviously, other processes may be relevant as well. It might be that even for small agricultural catchments processes within the brook and its sediments are of crucial importance for the nutrient dynamics.

The observed change of the P-export dynamics makes it more difficult to assess the effects of the ecological measures introduced in 1993 and 1999. Assuming that the major part of DRP originated from the soil a noticeable reduction in the DRP-loads could be expected only after many years due to the large P pool in the topsoil. Therefore the second set of measures aimed at avoiding incidental P-losses. If incidental P- losses (see

Withers et al. (2001) and *Withers et al.* (2003)) were dominating P-export, one would expect immediate results. However, the overall evolution of the P-loads doesn't indicate any effects at all. This is not surprising since the agricultural P-input did not significantly change from 1998 to 2002 as detailed data from farmers in the Lippenrütibach catchment reveal: We observed a decrease of 10% in beef but an increase of 5% in pig numbers, about steady rates of manure being exported out of the catchment, more farms disposing less P-containing feed (20 farms in 1998 and 23 farms in 2002) and smaller grassland area (-8%) compared to an increment of arable land (+6%) and buffer belts (+2%). Combining these data, the average amount of P applied in manure for 1998 was 36 kg P ha^{-1} and remained at a similar level with 34 kg P ha^{-1} in 2002 despite these measures. One reason for this non-significant reduction of P applied in manure in the Lippenrütibach catchment may be that not all farmers participated in this project which started in 1999 but the number of farmers is continuously increasing from 20% in 2000 to 50% in 2002. If all farmers in this catchment joined this project one could expect stronger reductions in the P-inputs. However, one must be aware that the evaluation of possible effects of the ecological measures is difficult because possible effects of the measures could have been counterbalanced by larger P-losses during baseflow. In addition, Moosmann et al. (2003) concluded that a significant reduction of the P-losses into Lake Sempach may not be seen before six years at the earliest.

2.6 Conclusions

Without a proper mechanistic understanding of the dominant processes in a catchment monitoring programs are not sufficient to allow for a reasonable evaluation of effects of changed land use practices. Actually, one reason to choose the Lippenrütibach catchment to carry out the evaluation of the ecological measures was that one thought to understand the P-export sufficiently well. The observed change in the P-export pattern, however, demonstrates the opposite. The monitoring program itself yielded results demonstrating the limitations of this understanding. These changes would have gone unnoticed without continuous measurements at high temporal resolution. According to the previous understanding of how the system works the high temporal resolution would not have been necessary at baseflow. This points to necessity to complement monitoring strategies with additional measurements wherefrom one can check the validity of crucial underlying assumptions of these strategies.

For P studies it follows that a proper understanding of the P-export from a catchment

may need long-term monitoring with high temporal resolution for all flow conditions. This requires substantial resources. Hence, the development of reliable and affordable probes for measuring P online might substantially help to improve monitoring programs.

Acknowledgments We are grateful for the financial support of the COST action 832 "Methodologies for estimating the agricultural contribution to eutrophication". R. Gächter initiated the online monitoring in the Lake Sempach region and carried out the online measurements in the Kleine Aa catchment together with A. Mares. They kindly gave full access to their data. We further acknowledge F. Herzog for giving useful comments to this paper; Beat Müller, Ruth Stierlin and Krispin Stoob helped with the field measurements in May 2004.

Chapter 3

A parsimonious soil-type based rainfall-runoff model simultaneously tested in four small agricultural catchments

P. Lazzarotto, V. Prasuhn, H. Flühler and C. Stamm

Submitted to Journal of Hydrology

3.1 Abstract

Discharge data from seven small agricultural catchments in the humid low-land region of Switzerland indicate that the hydrologic response is strongly influenced by the areal fractions of well and poorly drained soils. We report on a method to quantify the average flow contributions from well and poorly drained soil types during single runoff events. This study is based on data from four catchments with different areal fractions of well and poorly drained soils and with rainfall and discharge measured every hour. Each catchment was divided into four lumped hydrological response units (HRU) such as two soil types, one urban and one forested HRU. A slow and a fast flow component was assigned to each of the well and poorly drained HRUs. We calculate these flow components with a dynamic time-series model assuming that the areal fraction producing fast discharge depends on the soil water storage and the topographic index. The model is calibrated by simultaneously fitting the modeled catchment response in all four catchments with the restriction that equal HRU-types have

equal parameter values in all catchments. We used a single 11-day observation period for calibration. This period was chosen because it covers much of the discharge variability observed in the entire observation periods. The calibrated model was validated with two 10- and 11-day periods in four catchments and with four 6-months periods in one catchment only. Generally, the discharge dynamic in different catchments was reasonably well simulated for intermediate to high discharge peaks even for validation periods that are 15 times longer than the calibration record. The model showed limitations in periods with low antecedent soil moisture and for small peaks. In those cases, the model efficiency parameters were low possibly indicating that the concept of the topographic index is less applicable under such conditions. However, to distinguish well and poorly drained pedological units as HRUs appears to be a sufficient parameterization that is necessary to reproduce the discharge dynamics in periods of intermediate and high discharge.

3.2 Introduction

Rainfall-runoff models at the catchment scale are often applied for assessing the impact of land use practices and for testing hypotheses about the hydrological functioning of watersheds. The catchment response is a superposition of various flow contributions from different spatial origins and is a mixture of mobile waters from groundwater stored in the riparian zone and that from hillslope (*McGlynn et al.*, 1999). The pre-event component often dominates stream flow during stormflow (*Slash et al.* (1986) and *Burns et al.* (2001)). The hydrological response is influenced by processes occurring on different scales, by the topography, and is modified by anthropogenic features such as roads, tile drains, culvert systems and land use. Soil heterogeneity causes a vertically and laterally non-uniform distribution of soil moisture. Fast subsurface flow through preferential flow paths (*Flury et al.*, 1994) often exceeds the contribution of matrix flow in terms of response rapidity and spatial heterogeneity. This violates the uniform-flow assumptions on which many models are based (*Grayson and Blöschl*, 2001b). Hence, the question of how to derive a mechanistically acceptable model that captures the dominant flow responses from subareas of the catchment with a minimal number of fitting parameters is still one of the basic issues in catchment hydrology.

Catchment scale modeling requires variables that capture the relevant catchment features. *Hillel* (1986) proposed the basic principles for model design: (i) The parameters should relate to observable and available field data and their number be kept to a mini-

mum (ii) the scope and applicability of a model should not be overstated, (iii) the accuracy of prediction cannot be better than the accuracy of the measurements, and (iv) the limits of a model must be testable for its validity. Discharge alone is a weak constraint for testing the process hypotheses and a good fit does not imply that the observed and predicted internal state variables actually correspond (*Beven* (1996) and *Western et al.* (1999)). The model output is uncertain partly because parameters are derived from a generally incomplete data set. Errors in the data and in the model structure, the process complexity, temporal and spatial variability of runoff processes lead to equifinality in the model parameters, a constellation when equally good model runs can be obtained with multiple parameter sets (*Beven*, 1993). Commonly, a close fit between calculated and observed variables is possible for models with a high number of parameters even if the model assumptions are false (*Beven* (1997) and *Grayson et al.* (1992)).

Although relevant hydrological processes span about eight orders of magnitude in space and time (*Blöschl and Sivapalan*, 1995) the spatial data used for modeling is often aggregated from the scale of measurement to the scale of model resolution. Data aggregation might eliminate the information relevant on the particular model scale and the accuracy of parameterizing the small-scale variablility is partially lost when physiographic information is aggregated or generalized. One option to include spatial information is to structure the catchment in subunits of similar discharge dynamics, commonly refered to as hydrological response units (HRU). The hydrological similarity is often associated with soil types (*Leavesley and Stannard*, 1995) and topographic indices (*Beven and Kirkby* (1979); *Ambroise et al.* (1996); *Beven and Freer* (2001b)). One possibility to characterize the flow dynamic from the HRUs is the comparison of the response of several catchments. *Andréassian et al.* (2004) combined a series of catchment pairs (5 to 3900 km^2 area size) to compose a series of virtual catchments for which two semi-lumped models with the same global parameters were run. They concluded that the greatest improvement in model reliability was due to accounting for spatial rainfall variability. *Lilly et al.* (1998) defined and quantified river flow indices at the catchment scale based on the Hydrology-Of-Soil-Types (HOST-) classification (*Boorman et al.*, 1995). Soil attributes were derived from soil morphology used as surrogates for the hydraulic parameters to determine the prevalent flow pathways. These authors characterized the soil-type hydrology based on the areal fractions of soil types in the catchment. This approach captures the average long term flow behaviour but not the discharge dynamic. *Dunn et al.* (1998) used the HOST-classification for dynamic

modeling for two Scottish catchments with generally well drained soils. They derived non-metric soil parameter values from the HOST-classification and assigned metric values to describe the discharge dynamic with a distributed model. The variability of the absolute parameters across both catchments was consistent and showed the potential usefulness of the HOST-classification for dynamic modeling.

This approach may also be useful for assessing the hydrological impact of land use management. It has been observed that losses of herbicides may vary strongly between fields even within small catchments (*Leu et al.*, 2004). Knowing the risk areas would help to restrict the use of such compounds to those areas and to protect surface waters from getting contaminated. For the same reason, it has been proposed to determine contributing areas in order to identify the risk areas for phosphorus (P) (*Gburek et al.*, 2000). In this context, conventional soil maps may allow to pin down the hydrological response and P-export potential of areas. The main problem to use this soil information is to attribute quantitative hydrological characteristics to given pedologically defined soil units especially for event-based predictions.

In this paper we test the hypothesis that soil types largely control the hydrology in four adjacent small agricultural catchments in the Lake Sempach region. Based on our hydrological understanding from long-term discharge and P-export monitoring in those catchments we derive an event-based model that accounts for soil moisture and distinguishes a slow and a fast flow component for each of the well and poorly drained HRUs. The dynamic time-series model uses the areal fractions of different HRUs in four catchments by simultaneously comparing the catchment response. In this way we derive global parameter sets for equal HRUs of the four catchments to describe the average flow from those HRUs.

3.3 Material and Methods

3.3.1 Study area

The four agricultural catchments drain into Lake Sempach, Switzerland (Fig. 3.1), where agriculture dominates the land use (Tab. 3.1). These catchments markedly differ in their soil properties: Well drained soils cover 42 to 78% of the total catchment area and poorly drained soils 16 to 40%. Based on conventional soil maps (*AGBA*, 1993) we delineated just these two soil types. The vertically permeable soils such as the eutric and dystric Cambisols and the eutric Regosols are categorized as well drained. Poorly drained soils

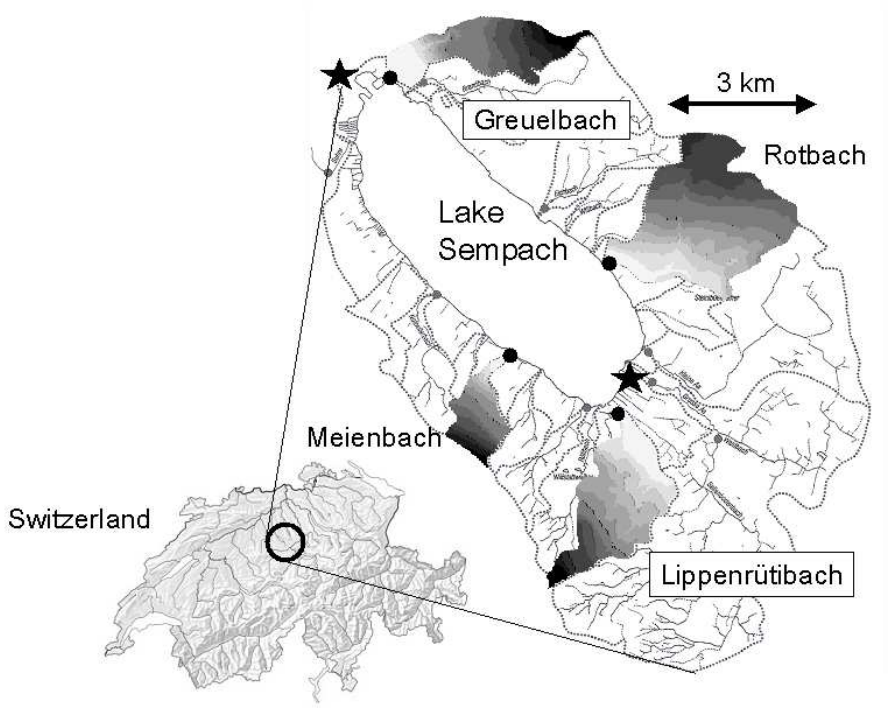

Figure 3.1: *Catchments of the Lake Sempach region based on a modified map of the Environmental Protection Agency, Cantone Lucerne, Switzerland. The four selected catchments are shaded and their topography is defined by digital elevation models. The catchment outlets are denoted as black dots. The two rainfall gauges are indicated as black stars.*

comprise water-logged gleyic Cambisols and eutric Gleysols. Soils have developed from glacial till (Würm glaciation deposits on molasse). The topography in these catchments is fairly similar, natural terrasses alternate with hillslopes. The hydrographs reflect the rainfall distribution since snow melt at 500-820 m a.s.l. is less important. Precipitation varies from 1100 to 1200 mm y^{-1} and highest monthly rainfall occurs normally in May and June. In catchments dominated by poorly drained soils, roughly 30% of agricultural fields are artificially drained, mostly with tiles. The urban area is small (2 to 4%) with some small villages and farm houses.

Rainfall and discharge measurements Rainfall was measured with two tipping bucket gauges; one close to the Lippenrütibach and the other, installed since the year 2000, close to the Greuelbach (Fig. 3.1). Discharge was recorded with limnigraphs at the catchment outlets. In addition, a pressure transducer was used to measure the water level in the Lip-

Table 3.1: *Areal structure of the four selected Lake Sempach catchments: The areal fractions of different hydrological response units* $HRU_{\mathrm{i}}^{\mathrm{k}}$ *as expressed relative to the total area of the individual catchment* k*. The label* i *refers to the individual* $HRU_{\mathrm{i}}^{\mathrm{k}}$ *and* k *to the index of the catchment.*

	HRU	Lippenrütibach	Rotbach	Meienbach	Greuelbach
	i	k=1	k=2	k=3	k=4
Agricultural land:					
- Well drained soils [%]	1	42	60	78	64
- Poorly drained soils [%]	2	40	24	16	19
Urban area [%]	3	3	3	2	4
Forested area [%]	4	15	13	4	13
Total area [km^2]		3.3	6.2	1.2	2.6

penrütibach since 1998 every hour. For three periods in 1999 and 2000, the limnigraphs were digitized and the recorded levels transformed into discharge using level-discharge curves (LDC). The available LDC are based on flow measurements (dilution method) taken mostly under low discharge conditions. This discharge range of the LDC was calibrated well but the method was unclear how the LDC were extrapolated to high discharge ranges. Thus, we recalculated the LDC with the Darcy-Weisbach equation (*Bathurst*, 2002) to approximate the laminar flow, Q, through a known cross-section A_{profile} at a given level,

$$Q = A_{\mathrm{profile}}\overline{v} = A_{\mathrm{profile}}\sqrt{8gR_{\mathrm{h}}\frac{\gamma}{f_d}} = A_{\mathrm{profile}}\sqrt{8gR_{\mathrm{h}}K} \tag{3.1}$$

where A_{profile} is the area of the water-filled cross-section, $\overline{v}$ is the laminar mean flow velocity, g is gravity, R_{h} is the hydraulic radius, γ is the channel slope and f_d a dimensionless Darcy friction coefficient. For a given water level, R_{h} was calculated and the ratio γf_d^{-1} replaced by a constant parameter K. The Darcy-Weisbach equation was fitted via K to the available discharge measurements in the calibrated range of low discharge and then extrapolated to high discharge levels.

3.3.2 Conceptual model

The hydrologic catchment response is the sum of all flow components from distinct types of hydrological response units (HRU) in the catchment. These HRUs significantly differ in their flow dynamics and parameters. We assign a global parameter vector $\mathbf{P}_{\mathrm{i}}$ to the same

Table 3.2: *Global parameters in the vector $\boldsymbol{P}_i$ and their value ranges within which they were calibrated using Uniform Monte Carlo simulations. These global parameters are defined for a particular type of $HRU_{\mathrm{i}}^{\mathrm{k}}$ and apply to all catchments k.*

Global parameter	Minimum value	Maximum value	Property	Used in $\mathrm{HRU}_{\mathrm{i}}^{\mathrm{k}}$
$S_{\mathrm{i,max}}$ [mm]	50	500	Maximum soil water storage capacity	$i = 1, 2$
a_{i} [-] ‡	0	1	Fast flow decline rate	$i = 1, 2, 3$
b_{i} [-] ‡	0	1	Proportion of rainfall converted into fast flow on the contributing areas	$i = 1, 2, 3$
c_{i} [mm]	0	1	Factor relating the scaled soil water storage to the slow flow components	$i = 1, 2$
n_{i} [-]	1	10	Expansion control of areas contributing to fast flow	$i = 1, 2$

‡a_3 and b_3 for the urban $\mathrm{HRU}_3^{\mathrm{k}}$ were independently pre-calibrated for eight small runoff events during summer at low antecedent moisture

type of HRU in all catchments and weight the flow from these HRUs with their respective areal fraction of their respective catchments. The global parameters in $\mathbf{P}_{\mathrm{i}}$ are then jointly calibrated by simultaneously comparing the catchment response in the four catchments. After the calibration the average flow rates from the soil-type HRUs are quantified.

3.3.3 Catchment characteristics

Hydrological response units To simultaneously compare the discharge in catchments with different areal fractions of the HRUs we selected four catchments, $k = 1, \cdots, 4$, with four different types of HRUs, $i = 1, \cdots, 4$ (Fig. 3.2a). The main HRU-types are well (i=1) and poorly drained soils (i=2), urban (i=3) and forested areas (i=4). In the following, we use the subscript i to refer to the HRU-types and k as the catchment index. This yields the notation $\mathrm{HRU}_{\mathrm{i}}^{\mathrm{k}}$. We aggregate all grid cells in the various subareas of a given $\mathrm{HRU}_{\mathrm{i}}^{\mathrm{k}}$ in catchment k to a single lumped $\mathrm{HRU}_{\mathrm{i}}^{\mathrm{k}}$ irrespective of their location in the catchment (Fig. 3.2b). The $A_{\mathrm{i}}^{\mathrm{k}}$ are the areal fractions of the respective lumped $\mathrm{HRU}_{\mathrm{i}}^{\mathrm{k}}$ expressed relative to the total area in catchment k.

Since the same type i of $\mathrm{HRU}_{\mathrm{i}}^{\mathrm{k}}$ behaves hydrologically similar in all catchments k we apply a vector $\mathbf{P}_{\mathrm{i}} = \{S_{\mathrm{i,max}}, a_{\mathrm{i}}, b_{\mathrm{i}}, c_{\mathrm{i}}, n_{\mathrm{i}}\}$ (see Tab. 3.2) containing constant global parameter

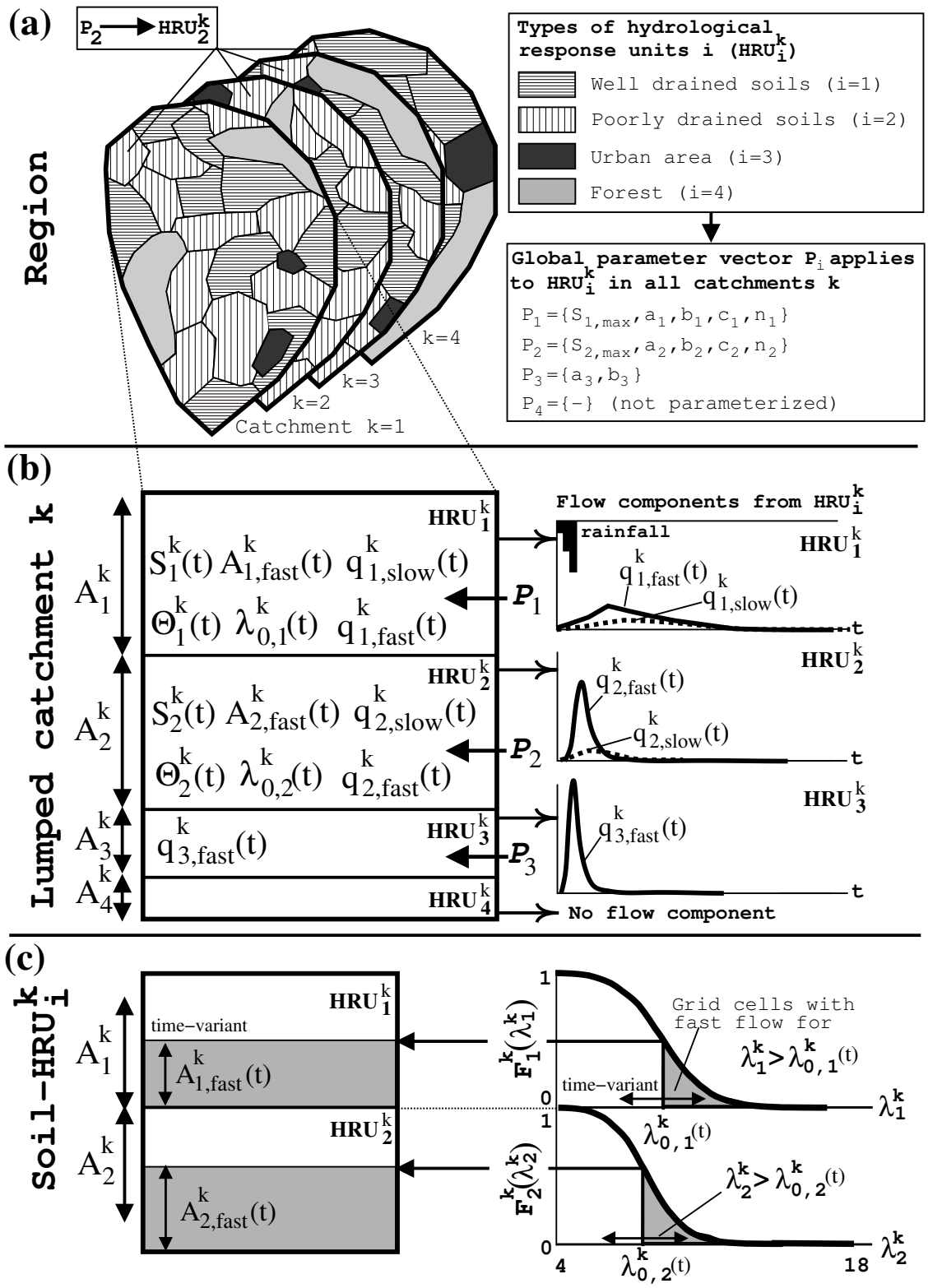

Figure 3.2: *Concept of aggregating different HRU_i^k in four catchments k at three different levels to calculate the local flow components for each HRU_i^k. (a) Assigning a global parameter vector $\boldsymbol{P}_i$ to the same type i of HRU_i^k in all catchments k. (b) Time-variant, local variables $\boldsymbol{V}_i^k(t)$ in HRU_i^k differ in different catchments k and are used to calculate the slow and the fast flow components. The local variables $\boldsymbol{V}_i^k(t)$ are explained in Tab. 3.3. A_i^k are the areal fractions of the HRU_i^k. (c) Threshold concept to determine the respective areal fractions $A_{i,fast}^k(t)$ contributing to fast flow for well and poorly drained HRU_i^k (i=1,2) based on the cumulative distribution functions $F_i^k(\lambda_i^k)$ of the topographic index λ_i^k in catchment k and the time-variant thresholds $\lambda_{0,i}^k(t)$.*

sets to the same types i of $\mathrm{HRU}_{\mathrm{i}}^{\mathrm{k}}$ in all catchments k (Fig. 3.2a,b). For instance, the global parameter vector a_i is composed of a_1, a_2 and a_3 describing the fast flow decline in the three different $\mathrm{HRU}_{\mathrm{i}}^{\mathrm{k}}$ of all catchments $k = 1, \cdots, 4$: (i) a_1 has the same value in all well drained HRU_1^1, HRU_1^2, HRU_1^3 and HRU_1^4, abbreviated as $\mathrm{HRU}_1^{\mathrm{k}=1,\cdots,4}$, (ii) a_2 has the same value in all poorly drained $\mathrm{HRU}_2^{\mathrm{k}=1,\cdots,4}$ and (iii) a_3 the same values in all urban $\mathrm{HRU}_3^{\mathrm{k}=1,\cdots,4}$.

Combining topography with soil-type $\mathrm{HRU}_{\mathrm{i}}^{\mathrm{k}}$ with i=1,2 To account for topographic influences on the flow production we use the topographic index λ (*Kirkby*, 1975) as an indicator for the wetness at a given location. The basic idea is that areas of a given $\mathrm{HRU}_{\mathrm{i}}^{\mathrm{k}}$ with i=1,2 having the same topographic index behave hydrologically similar. Using digital elevation models (DEM) with 25m·25m grid cell elements for the four catchments, the topographic index λ for each grid cell at location [x,y] in the catchment was derived. We defined it as $\lambda = \ln(A_{\mathrm{upstream}}/\tan\beta)$ with A_{upstream} being the upstream area draining through location [x,y] in the catchment k according to the flow direction determined from the DEM (multiple flow direction algorithm of *Quinn et al.* (1991)) and β being the local slope at [x,y]. Note that λ, A_{upstream} and β are time-invariant. Next, we used conventional soil maps to distinguish the well (i=1) and poorly (i=2) drained $\mathrm{HRU}_{\mathrm{i}}^{\mathrm{k}}$. For all catchments, we overlay the λ-maps with those of well and poorly drained $\mathrm{HRU}_{\mathrm{i}}^{\mathrm{k}}$ with i=1,2. This yields, for each soil-type $\mathrm{HRU}_{\mathrm{i}}^{\mathrm{k}}$ the grid-cell based $\lambda_{\mathrm{i}}^{\mathrm{k}}$-maps. These $\lambda_{\mathrm{i}}^{\mathrm{k}}$-maps are used to derive the time-invariant cumulated distribution function $F_{\mathrm{i}}^{\mathrm{k}}(\lambda_{\mathrm{i}}^{\mathrm{k}})$ for each soil-type $\mathrm{HRU}_{\mathrm{i}}^{\mathrm{k}}$ with i=1,2. For i>2, we treat the urban $\mathrm{HRU}_3^{\mathrm{k}}$ and the forested $\mathrm{HRU}_4^{\mathrm{k}}$ as separate lumped HRUs (see below).

3.3.4 Model structure and assumptions

On the one hand, a parameter vector $\mathbf{P}_{\mathrm{i}}$ exists that contains the time-invariant global parameter sets $S_{\mathrm{i,max}}, a_{\mathrm{i}}, b_{\mathrm{i}}, c_{\mathrm{i}}, n_{\mathrm{i}}$ for each $\mathrm{HRU}_{\mathrm{i}}^{\mathrm{k}=1,\cdots,4}$ valid in all catchments k. These global parameters will be simultaneously fitted using parameter constraints to distinguish between flow components from well and poorly drained HRUs. These constraints are derived from catchment data in section 3.3.5.

On the other hand, there are catchment- and HRU-specific (local) variables such as the soil moisture $S(t)$. These local variables are time-variant, calculated in hourly time steps Δt and depend on the local properties of the soil and topography of the individual $\mathrm{HRU}_{\mathrm{i}}^{\mathrm{k}}$. These variables are elements of the variable vector $\mathbf{V}_{\mathrm{i}}^{\mathrm{k}}(t)$. We see from Fig. 3.2b that the number of variables in $\mathbf{V}_{\mathrm{i}}^{\mathrm{k}}(t)$ differs in different $\mathrm{HRU}_{\mathrm{i}}^{\mathrm{k}}$: Six local variables including a

Table 3.3: *Time-variant, local variables that differ for well and poorly drained HRU$_i^k$ (i=1,2) in all catchments k. The label i refers to the HRU-type and k to the catchment index.*

Variable	Property	Surrogate for
$S_i^k(t)$ [mm]	Absolute soil water storage	Soil moisture status
$\Theta_i^k(t)$ [-]	Scaled soil water storage	Soil moisture status
$\lambda_{0,i}^k(t)$ [-]	Threshold of the topographic index λ_i^k for each HRU$_i^k$	-
$A_{i,fast}^k(t)$ [-]	Areal fraction of HRU$_i^k$ contributing to fast flow	Topography
$q_{i,fast}^k(t)$ [mm h^{-1}] ‡	Fast flow component	Fast flow types
$q_{i,slow}^k(t)$ [mm h^{-1}]	Slow flow component	Slow flow types

‡i=1,2,3: Fast flow components calculated for well and poorly drained HRU$_1^k$ and HRU$_2^k$ and the urban HRU$_3^k$ as well

slow and a fast flow component are calculated for the two soil-type HRU$_i^k$ with i=1,2. In addition, a fast flow component for the urban HRU$_3^k$ was calculated, but no flow component for the forested HRU$_4^k$ (Tab. 3.3) for reasons given later. The local variables in $\mathbf{V}_i^k(t)$ are controlled by the global parameters in vector $\mathbf{P}_i$ governing the flow dynamic from a given HRU$_i^k$ and by the different initial values, rainfall and evapotranspiration.

The calculated catchment response $Q^k(t)$ is the sum of all local flow components $q_i^k(t)$ weighted with their respective areal fractions A_i^k of the total catchment area $A^k = \sum_{i=1}^4 A_i^k$.

$$Q^k(t) = \left[q_{1,slow}^k(t) + q_{1,fast}^k(t)\right] A_1^k + \left[q_{2,slow}^k(t) + q_{2,fast}^k(t)\right] A_2^k + q_{3,fast}^k(t) A_3^k \tag{3.2}$$

Local variables $\mathbf{V}_i^k(t)$ for well and poorly drained soil-type HRU$_i^k$ with i=1,2

In the following, local variables referring to well and poorly drained HRU$_i^k$ with i=1,2 will be labeled by the index i without the term i=1,2. E.g. $S_i^k(t)$ is an abbreviation and indicates one local variable $S_1^k(t)$ for well drained HRU$_1^k$ and another $S_2^k(t)$ for poorly drained HRU$_2^k$. This abbreviation is applied to all local variables $\mathbf{V}_i^k(t)$ with i=1,2.

Mass balance The time-variant local water storage term $S_i^k(t + \Delta t)$ is calculated in hourly time steps Δt from the mass balance equation $S_i^k(t + \Delta t) = S_i^k(t) + \Delta S_i^k$ with

$$\Delta S_{\mathrm{i}}^{\mathrm{k}} = \Delta t \Big[r^{\mathrm{k}}(t) - q_{\mathrm{i,slow}}^{\mathrm{k}}(t) - q_{\mathrm{i,fast}}^{\mathrm{k}}(t) - et^{\mathrm{k}}(t) \Big] \tag{3.3}$$

with the local variables of rainfall $r^{\mathrm{k}}(t)$, evapotranspiration $et^{\mathrm{k}}(t)$, the slow and fast flow components $q_{\mathrm{i,slow}}^{\mathrm{k}}(t)$ and $q_{\mathrm{i,fast}}^{\mathrm{k}}(t)$, respectively. For the first time step t_0 (t=0) initial values are assigned to $S_{\mathrm{i}}^{\mathrm{k}}(t_0)$ (Fig. 3.3 top) as explained in section 3.3.5. Next, $S_{\mathrm{i}}^{\mathrm{k}}(t)$ is scaled between zero and one with the global parameters $S_{\mathrm{i,max}}$=$\{S_{1,\mathrm{max}}, S_{2,\mathrm{max}}\}$, the maximum soil water storage capacity of $\mathrm{HRU}_{\mathrm{i}}^{\mathrm{k}}$ (Eq. 3.4 and Tab. 3.2). This yields the local scaled soil water storages $\Theta_{\mathrm{i}}^{\mathrm{k}}(t)$ which are surrogates for the soil moisture status of the $\mathrm{HRU}_{\mathrm{i}}^{\mathrm{k}}$ (Fig. 3.3a).

$$\Theta_{\mathrm{i}}^{\mathrm{k}}(t) = \frac{S_{\mathrm{i}}^{\mathrm{k}}(t)}{S_{\mathrm{i,max}}} \tag{3.4}$$

Based on the following observations we distinguish a slow and a fast flow component: High temporal resolution monitoring studies of P-export from these grassland-dominated catchments showed low P-concentrations during baseflow while they substantially increased during stormflow due to the rapid transport from fields by surface runoff and macropores to tile drains (*Stamm et al.* (1998); *Pacini and Gächter* (1999); *Lazzarotto et al.* (2005)). A fast flow component is also required to explain the dilution of nitrate during stormflow relative to the concentrations observed during baseflow. Hence, the slow flow component stands for baseflow and the fast flow component includes all quickly responding flow types such as preferential flow as well as saturation or Horton overland flow (Tab. 3.3).

We assumed that both soil-type $\mathrm{HRU}_1^{\mathrm{k}}$ and $\mathrm{HRU}_2^{\mathrm{k}}$ produce slow flow $q_{\mathrm{i,slow}}^{\mathrm{k}}(t)$ but with different dynamics defined by the global parameter $c_{\mathrm{i}} = \{c_1, c_2\}$ and the actual soil moisture status $\Theta_1^{\mathrm{k}}(t)$ and $\Theta_2^{\mathrm{k}}(t)$ independent of topography. The global parameters c_i describe how much water is released from $\mathrm{HRU}_{\mathrm{i}}^{\mathrm{k}}$ contributing to local baseflow.

$$q_{\mathrm{i,slow}}^{\mathrm{k}}(t) = \Theta_{\mathrm{i}}^{\mathrm{k}}(t) c_{\mathrm{i}} \tag{3.5}$$

We assumed that the area contributing to fast flow varies in time since local fast flow components $q_{\mathrm{i,fast}}^{\mathrm{k}}(t)$ are influenced by rainfall, soil moisture and topography. They are calculated with an autoregressive term and an exogeneous input.

$$q_{\mathrm{i,fast}}^{\mathrm{k}}(t + \Delta t) = a_{\mathrm{i}} \cdot q_{\mathrm{i,fast}}^{\mathrm{k}}(t) + \Big[b_{\mathrm{i}} \cdot r^{\mathrm{k}}(t - \tau_{\mathrm{i,d}}^{\mathrm{k}}) \cdot A_{\mathrm{i,fast}}^{\mathrm{k}}(t) \Big] \tag{3.6}$$

The global parameters $a_{\mathrm{i}} = \{a_1, a_2\}$ of the autoregressive term describe the temporal flow decline. The input or flow-production term depends on the global parameters $b_{\mathrm{i}} =$

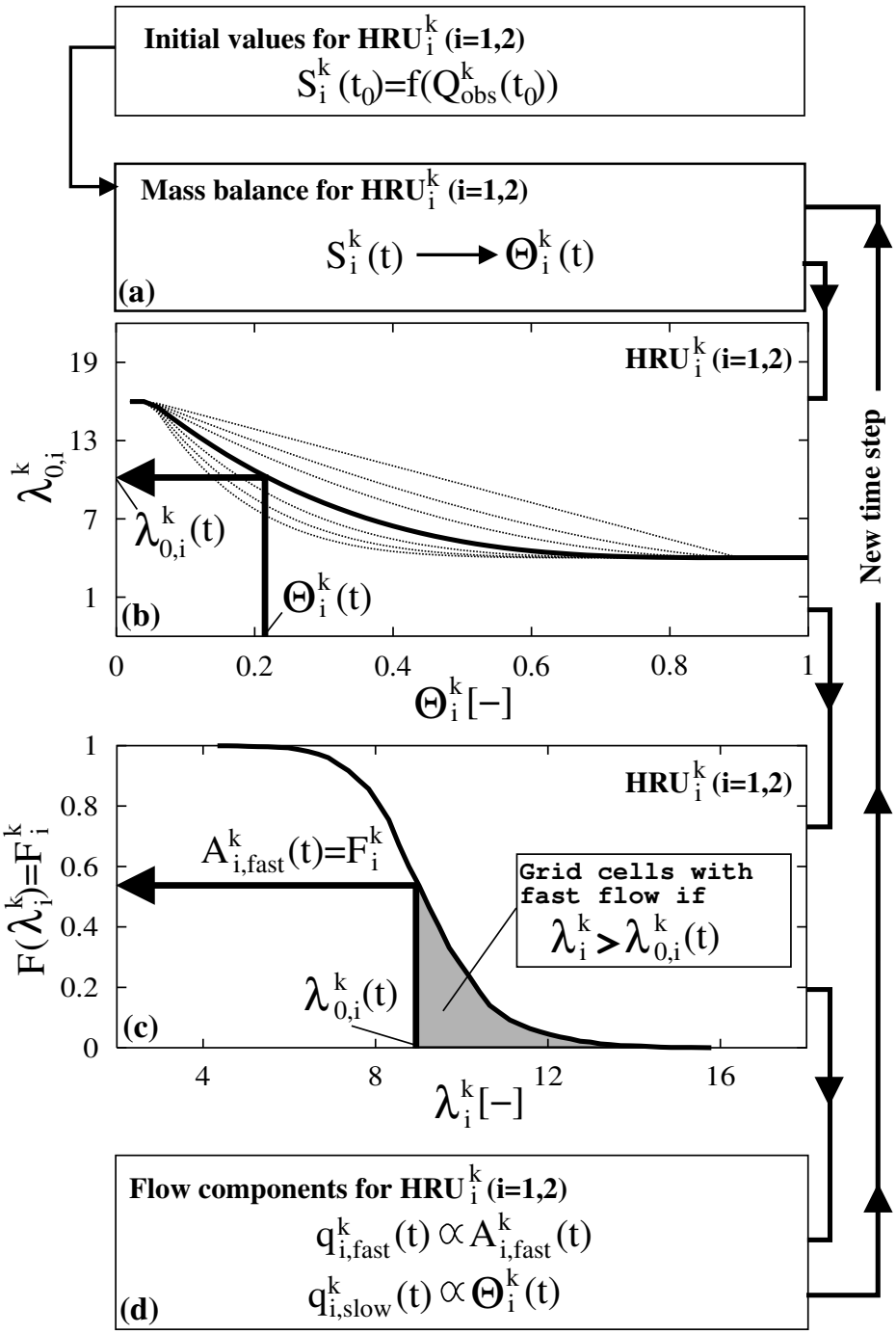

Figure 3.3: *Computational scheme to calculate the local variables including the slow and the fast flow components from well and poorly drained HRU$_i^k$ (i=1,2) of all catchments k. Initial values for $S_i^k(t_0)$ are derived from the optimized relationship between the variables S_i^k and the observed discharge Q_{obs}^k at t_0. (a) The initial value $S_i^k(t_0)$ is used to calculate the first guess of $\Theta_i^k(t_0)$. (b) Local relationships between $\Theta_i^k(t)$ and the threshold of the topographic index $\lambda_{0,i}^k(t)$ for each HRU$_i^k$. Dotted lines are plausible curves and the solid line is the curve selected by calibration. (c) Local cumulative distribution functions $F_i^k(\lambda_i^k)$ defined for each HRU$_i^k$ in each catchment k. Grid cells with $\lambda_i^k > \lambda_{0,i}^k(t)$ contribute to fast flow (grey area). Based on $F_i^k(\lambda_i^k)$ the thresholds $\lambda_{0,i}^k(t)$ define the areal fractions $A_{i,fast}^k(t)$ contributing to fast flow which are then used in (d) to determine the fast flow components $q_i^k(t)$.*

$\{b_1, b_2\}$, that is the fraction of rain converted into runoff on the contributing areas, and local variables such as the rainfall intensity $r^{\mathrm{k}}(t - \tau^{\mathrm{k}}_{\mathrm{i,d}})$ and the calculated areal fractions $A^{\mathrm{k}}_{\mathrm{i,fast}}(t)$ defined below. We used empirically determined local characteristic time lags $\tau^{\mathrm{k}}_{\mathrm{i,d}}$ between the peak of rainfall and discharge as a descriptor for the flow routing through the catchment k.

Estimating the time-variant areal fractions $A^{\mathrm{k}}_{\mathrm{i,fast}}(t)$ with i=1,2 The time-variant local variables $A^{\mathrm{k}}_{\mathrm{i,fast}}(t)$ represent the areal fractions of the soil-type $\mathrm{HRU}^{\mathrm{k}}_{\mathrm{i}}$ from which fast flow is generated (Fig. 3.2c). They account for the role of topography and soil moisture on the flow production. One major assumption of Eq. 3.6 is that the fast flow component $q^{\mathrm{k}}_{\mathrm{i,fast}}(t)$ is linear with $A^{\mathrm{k}}_{\mathrm{i,fast}}(t)$. Since the cumulative distribution of the topographic index $F^{\mathrm{k}}_{\mathrm{i}}(\lambda^{\mathrm{k}}_{\mathrm{i}})$ is a summation of areal elements with λ-values at [x,y] we use it to define the areal fraction $A^{\mathrm{k}}_{\mathrm{i,fast}}(t)$ contributing to fast flow. In addition, a soil moisture dependent time-variant local threshold $\lambda^{\mathrm{k}}_{0,\mathrm{i}}(t)$ with i=1,2 is the topographic index that separates between areas contributing to fast flow.

We assume that areas contributing to fast flow at the location [x,y] have a larger topographic index than the time-variant threshold ($\lambda^{\mathrm{k}}_{\mathrm{i}} > \lambda^{\mathrm{k}}_{0,\mathrm{i}}(t)$) (Fig. 3.2c, right). We postulate that this time-variant local threshold $\lambda^{\mathrm{k}}_{0,\mathrm{i}}(t)$ mainly depends on the soil moisture status $\Theta^{\mathrm{k}}_{\mathrm{i}}(t)$.

$$\lambda^{\mathrm{k}}_{0,\mathrm{i}}(t) \propto \left(1 - \Theta^{\mathrm{k}}_{\mathrm{i}}(t)\right)^{n_{\mathrm{i}}} \tag{3.7}$$

The exponents $n_{\mathrm{i}} = \{n_1, n_2\}$ are global parameters and influence the spatial extent of areas contributing to fast flow (Fig. 3.3b). These areas increase relatively fast for large n_{i} when it rains, a hydrological response that is characteristic for poorly drained soils (i=2). Since well drained soils (i=1) are better buffered these areas expand more slowly and have a smaller n_1. The water storage $\Theta^{\mathrm{k}}_{\mathrm{i}}(t)$ varies with time and is higher in wet than in dry periods. *O'Loughlin* (1981) and *O'Loughlin* (1986) showed that the areal fraction of saturated soil correlates with the average soil moisture. Hence, with increasing soil moisture storage we also expect the areas contributing to fast flow to vary in time and to spatially expand as indicated by declining $\lambda^{\mathrm{k}}_{0,\mathrm{i}}(t)$ and vice versa. This behaviour of $\lambda^{\mathrm{k}}_{0,\mathrm{i}}(t)$ given in Eq. 3.7 yields a convexe function illustrated in Fig. 3.3b.

Once we know the threshold $\lambda^{\mathrm{k}}_{0,\mathrm{i}}(t)$ we pick all grid cells in $\mathrm{HRU}^{\mathrm{k}}_{\mathrm{i}}$ with $\lambda^{\mathrm{k}}_{\mathrm{i}} > \lambda^{\mathrm{k}}_{0,\mathrm{i}}(t)$ and sum up their unit cell area (Fig. 3.2c and 3.3c). This yields the local $A^{\mathrm{k}}_{\mathrm{i,fast}}(t)$ that is the areal fraction of the $\mathrm{HRU}^{\mathrm{k}}_{\mathrm{i}}$ contributing to fast flow at time t. This procedure is equivalent

to using the cumulated distribution function $A^{\mathrm{k}}_{\mathrm{i,fast}}(t)$=$F^{\mathrm{k}}_{\mathrm{i}}(\lambda^{\mathrm{k}}_{\mathrm{i}} > \lambda^{\mathrm{k}}_{0,\mathrm{i}}(t))$. These $A^{\mathrm{k}}_{\mathrm{i,fast}}(t)$ are inserted into Eq. 3.6 to determine the local fast flow components $q^{\mathrm{k}}_{\mathrm{i,fast}}(t)$. For the next time $t = t + \Delta t$, the present-time slow and fast flow components are used to update the local variables of $\mathbf{V}^{\mathrm{k}}_{\mathrm{i}}(t)$ and return again to the mass balance (Fig. 3.3a).

Urban and forested HRUs

Discharge from the urban $\mathrm{HRU}^{\mathrm{k}}_{3}$ is calculated as a fast flow component without delay relative to rainfall.

$$q^{\mathrm{k}}_{3}(t + \Delta t) = q^{\mathrm{k}}_{3}(t)a_3 + \left[b_3 r^{\mathrm{k}}(t)\right] \tag{3.8}$$

The global parameters a_3 and b_3 were pre-calibrated using discharge of eight small runoff events in summer at low antecedent moisture storage when the flow contributions from agricultural soils could be neglected. Discharge contributions from forest were neglected for the following reasons ($q^{\mathrm{k}}_{4}(t)$=0): (i) The forested area is, apart from one catchment, similar ranging from 13 to 15%; (ii) we expect a slow response from forests (large interception effect) compared with the fast response from agricultural and urban areas; (iii) based on a comprehensive study with 94 de- or afforested worldwide selected catchments a reduction in forest cover of less than 20% of the catchment can apparently not be detected by measuring streamflow (*Bosch and Hewlett*, 1982). Hence, we assume that the error introduced by neglecting the forested area is in the same order for all four catchments; (iv) soil maps are not available for the forested area.

3.3.5 Model calibration

Derivation of the initial local soil water storages $S^{\mathrm{k}}_{\mathrm{i}}(t_0)$ The purpose of this step is to find a relationship between the soil moisture storage and an observed local entity that allows an initial guess of the soil water storage $S^{\mathrm{k}}_{\mathrm{i}}(t_0)$ (Fig. 3.3 top) for the calibration as well as the validation periods (see below). Therefore, we used an 11-day record (July 7-17, 2000) of observed discharge $Q^{\mathrm{k}}_{\mathrm{obs}}(t)$ from the four catchments. We optimized the global parameters of vector $\mathbf{P}_{\mathrm{i}}$ and also the initial values of the soil water storage for the well and poorly drained $\mathrm{HRU}^{\mathrm{k}}_{\mathrm{i}}$, $S^{\mathrm{k}}_{\mathrm{i}}(t_0) = \{S^{\mathrm{k}}_{1}(t_0), S^{\mathrm{k}}_{2}(t_0)\}$, with the Metropolis Monte Carlo method (*Metropolis et al.*, 1953), a technique of Simulated Annealing. The value of $S^{\mathrm{k}}_{\mathrm{i}}(t_0)$

is a catchment- and HRU-specific constant that is optimized only in this step. After the optimization the constant $S_{\mathrm{i}}^{\mathrm{k}}(t_0)$ is used as the initial guess to compute the time-series of the $S_{\mathrm{i}}^{\mathrm{k}}(t)$ for the same optimization period. After plotting the computed $S_{\mathrm{i}}^{\mathrm{k}}(t)$ separately for $\mathrm{HRU}_1^{\mathrm{k}}$ and $\mathrm{HRU}_2^{\mathrm{k}}$ as a function of the corresponding $Q_{\mathrm{obs}}^{\mathrm{k}}(t)$ we obtain the data pairs for $[S_{\mathrm{i}}^{\mathrm{k}}, Q_{\mathrm{obs}}^{\mathrm{k}}]$. Then we fit a relationship $S_{\mathrm{i}}^{\mathrm{k}} = f(Q_{\mathrm{obs}}^{\mathrm{k}})$ to these data pairs for each soil-type $\mathrm{HRU}_{\mathrm{i}}^{\mathrm{k}}$ in each catchment. This yields eight separate regression functions that are applied to derive the initial guess $S_{\mathrm{i}}^{\mathrm{k}}(t_0)$ using the observed discharge at t_0 for each soil-type $\mathrm{HRU}_{\mathrm{i}}^{\mathrm{k}}$ in the corresponding catchments.

We optimized $\mathbf{P}_{\mathrm{i}}$ within the ranges given in Tab. 3.2 and $S_{\mathrm{i}}^{\mathrm{k}}(t_0)$ within 0 to 500mm by simultaneously comparing the catchment response of the four catchments k, that is by minimizing the joint objective function $\sum_{\mathrm{k}=1}^{4} \sum_{\mathrm{t}=\mathrm{t}_0}^{\mathrm{t}_{\mathrm{e}}} \left(Q_{\mathrm{obs}}^{\mathrm{k}}(t) - Q^{\mathrm{k}}(t)\right)^2$ from t_0 until t_{e}, the end of the period. Additionally, we constrain the individual parameters: $S_{1,\max} > S_{2,\max}$, $a_1 > a_2$, $b_1 < b_2$ and $n_1 < n_2$ based on the findings from catchment data in section 3.3.5.

Simultaneous model calibration with the Uniform Monte Carlo method Next, we randomly selected values for the global parameters of $\mathbf{P}_{\mathrm{i}}$ as depicted in Fig. 3.2a within a given range (Tab. 3.2) and generated $m = 1, \cdots, 2 \cdot 10^7$ different global parameter vectors $\mathbf{P}_{\mathrm{i}} = \{p_{\mathrm{i},1}, \cdots, p_{\mathrm{i,m}}\}$ assuming that the individual parameters are uncorrelated. We used the derived relationships $S_{\mathrm{i}}^{\mathrm{k}} = f(Q_{\mathrm{obs}}^{\mathrm{k}})$ to determine the initial guess for $S_{\mathrm{i}}^{\mathrm{k}}(t_0)$ with the observed discharge $Q_{\mathrm{obs}}^{\mathrm{k}}(t_0)$ and carried out $m = 1, \cdots, 2 \cdot 10^7$ Uniform Monte Carlo simulations for the July, 7-17, 2000 calibration period. Then, plausible parameter vectors $\mathbf{P}_{\mathrm{i}}$ were retained and further used for validation if they (i) met the above parameter constraints and (ii) lead to acceptable predictions of the observed discharge in all catchments according to the efficiency-criterion E_{m} >0.6 (*Nash and Sutcliffe*, 1970). This is a modified joint objective function for all catchments

$$E_{\mathrm{m}} = 1 - \frac{\sum_{\mathrm{k}=1}^{4} \sum_{\mathrm{t}=\mathrm{t}_0}^{\mathrm{t}_{\mathrm{e}}} \left(Q_{\mathrm{obs}}^{\mathrm{k}}(t) - Q^{\mathrm{k}}(t)\right)^2}{\sum_{k=1}^{4} \sum_{\mathrm{t}=\mathrm{t}_0}^{\mathrm{t}_{\mathrm{e}}} \left(Q_{\mathrm{obs}}^{\mathrm{k}}(t) - \overline{Q}^{\mathrm{k}}\right)^2} \tag{3.9}$$

where E_{m} is the efficiency measure of the m-th global parameter set and $\overline{Q}^k$ is the mean of the observed discharge in catchment k over the period t=$\{t_0, \cdots, t_{\mathrm{e}}\}$.

3.3.6 Validation

As before we used the local relationships $S_{\mathrm{i}}^{\mathrm{k}} = f(Q_{\mathrm{obs}}^{k})$ to estimate the first value of $S_{\mathrm{i}}^{\mathrm{k}}(t_0)$ at the start of the validation periods and all accepted global parameter vectors $\mathbf{P}_{\mathrm{i}}$ to

validate the model with (i) longer discharge records from April to October 1999-2002 in the Lippenrütibach and (ii) two shorter periods in all four catchments. The first of the two short periods was the 11-day major flood period in May 5-15, 1999 caused by intense rainfall combined with unusually wet conditions in April, the second one a 10-day summer period with initially dry soil conditions followed by small runoff events. All calculated time-series of total discharge that are produced with accepted $\mathbf{P}_{\mathrm{i}}$ are illustrated with prediction bands excluding the minimum and maximum 10%-quantiles of the cumulated distribution of the hourly calculated discharge.

3.4 Results

3.4.1 Discharge calibration

Figure 3.4 illustrates the recalculated level-discharge curves (LDC) calculated according to Eq. 3.1 and the available original LDC for all four catchments. The grey areas indicate the 95% quantiles of all observed weir levels derived in the entire monitoring period.

On the top of the figures the bars show the range of the weir levels where discharge was actually calibrated (black bars) and the range for which discharge was extrapolated (grey lined bars). The black lines represent the original and the grey lines the recalculated LDC. Note that after recalculating the LDC the error bars indicate the predicted discharge and the 95% confidence intervals at those weir levels where discharge was actually measured.

In the case of the Lippenrütibach and Rotbach catchment, the actually calibrated range of the weir levels (black bars) covered a much smaller range than the 95% quantiles-range of all weir levels recorded during the monitoring period. When recalculating the LDC, they closely matched the measured discharge in the calibrated range (black bars) yielding small errors and $\mathrm{R}^2 > 0.99$. These small deviations between the observed and recalculated discharge are due to the approximation errors of the cross-section A_{profile}. The recalculated LDC (grey lines) deviated only little from the original LDC (black lines) in three catchments while in case of the Lippenrütibach the recalculated discharge at high weir levels is reduced by 30 to 40%. To investigate the uncertainty effects of distinct LDC on the calibrated parameters we used the observed discharge time-series derived from the recalculated LDC, denoted by $Q^{\mathrm{k}}_{\mathrm{obs,recalc}}(t)$ and those derived from the original LDC, denoted by $Q^{\mathrm{k}}_{\mathrm{obs,orig}}(t)$. For the validation periods, however, we only used the time-series of $Q^{\mathrm{k}}_{\mathrm{obs,recalc}}(t)$.

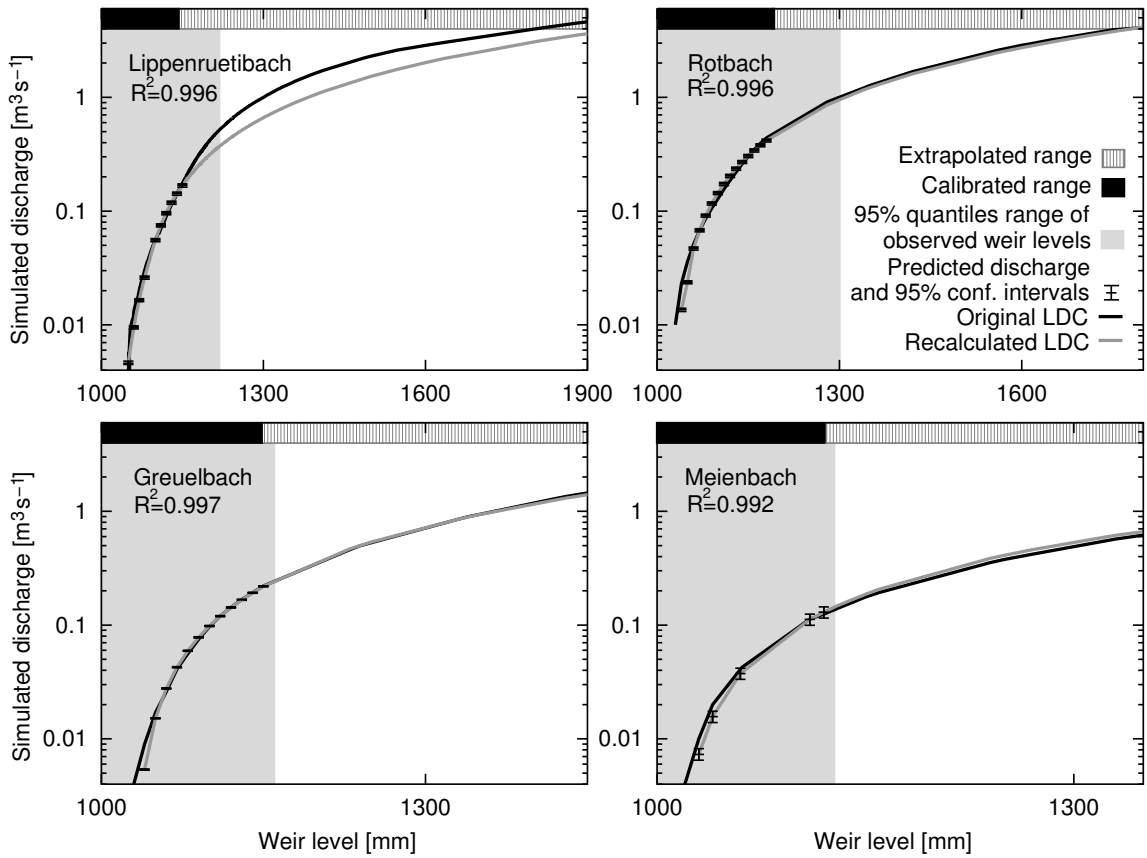

Figure 3.4: *Level-discharge curves (LDC) for the weirs at the outlets of the four catchments. The area shaded in lighter grey indicates the 95% quantile of discharge observed in these catchments during 17 selected periods for 1999 and 2000. The other lines, bars and symbols are explained in the text.*

3.4.2 Soil properties and catchment response

We hypothesize that the different areal fractions of soil types (Tab. 3.1) in these catchments largely control the catchment response. This is confirmed when we calculate the variation coefficient of the daily discharge for each catchment over a 2.5 year period from April 1992 to December 1994 and plot it against their areal fractions of well drained soils. The discharge regime of these catchments is significantly correlated with the areal fractions of permeable soils relative to the area that has been pedologically mapped (Fig. 3.5).

This suggests that in catchments with larger areal fractions of well drained soils, the average variation of daily discharge is smaller and the average hydrograph smoother. On the one hand, in the Lippenrütibach and Rotbach with the smallest areal fractions of well drained soils as given in Fig. 3.5 the variation of daily discharge is higher compared with the other catchments (Fig. 3.6). On the other hand, less extreme discharge rates occur in catchments dominated by well drained soils due to their larger buffer capacities

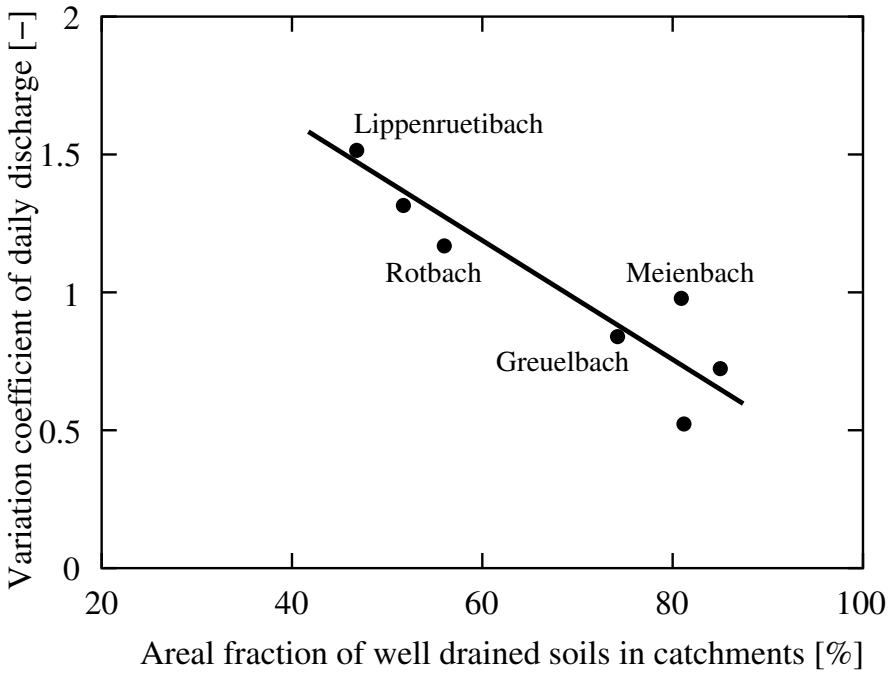

Figure 3.5: *Relationship between the areal fractions of well drained soils and the variation coefficient of observed daily discharge from seven catchments from 1992 to 1994 (R^2=0.91). These areal fractions refer to the mapped soil area. Since no soil maps exist for forests the areal fractions given in Tab. 3.1 differ from those used here.*

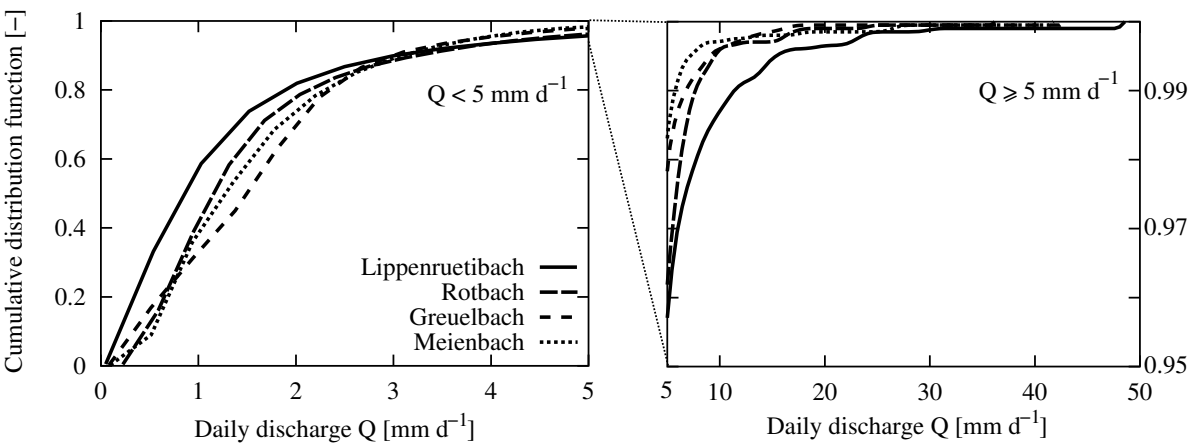

Figure 3.6: *Cumulative distribution of daily discharge below (left) and equal or above 5 mm d^{-1} (right) shown for the four catchments.*

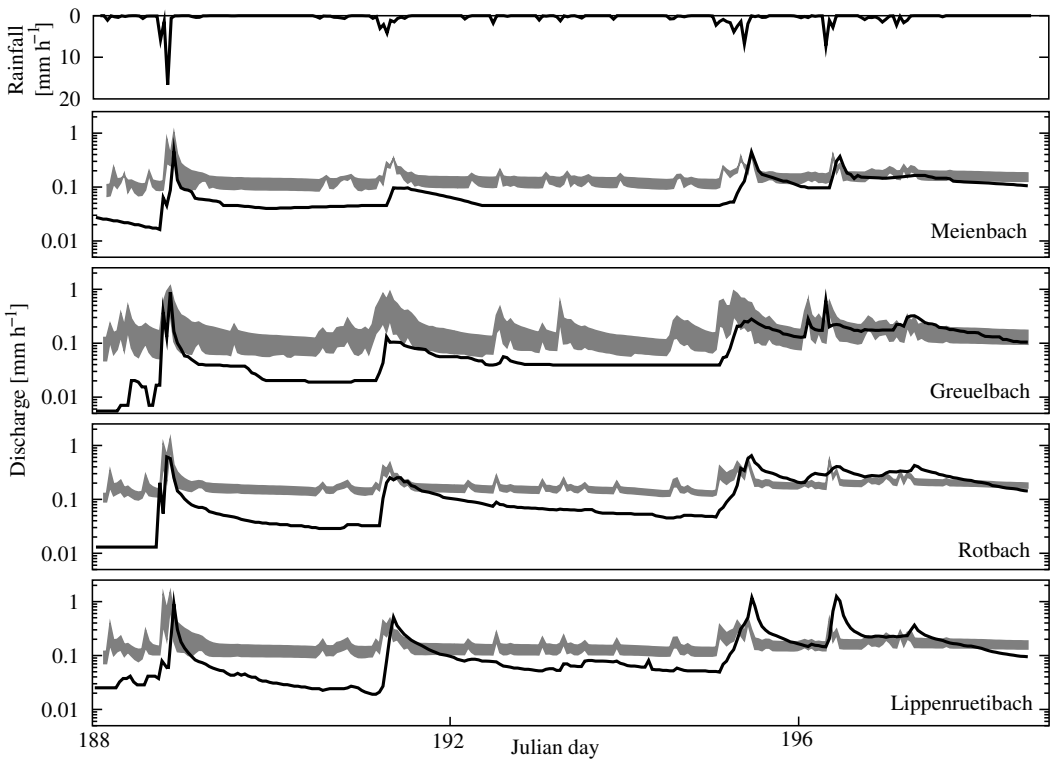

Figure 3.7: *Separate calibration of the 1-soil-HRU-model in each catchment to the observed discharge (black lines) for the period July 7-17, 2000 with* $E_{\mathrm{m}} > 0.1$. *The 1-soil-HRU-model treats the two soil-type HRUs as one single non-specific soil-type HRU. The observed discharge was derived from the recalculated level-discharge curve. The grey bands are the prediction bands excluding the minimum and maximum 10%-quantiles of the cumulated distribution of the hourly calculated discharge. Rainfall is given at the top.*

($S_{1,\max}$>$S_{2,\max}$). For a given rainfall peak (Fig. 3.2b, right) a smoother (a_1>a_2) and more delayed response ($\tau^{\mathrm{k}}_{1,\mathrm{d}} > \tau^{\mathrm{k}}_{2,\mathrm{d}}$) is expected from well drained soils compared with the more pronounced peaks (b_1<b_2) and quickly responding flow from poorly drained soils.

3.4.3 Simultaneous model calibration with Uniform Monte Carlo simulations

We used the same short 11-day period from July 7-17, 2000 for the simultaneous model calibration since this period (i) had complete discharge records for all catchments, (ii) had data of two rainfall gauges and (iii) contained a wide range of observed hydrological variability within a short time: Initial large discharge peaks at low antecedent moisture followed by a small peak, three days with little rainfall and finally two high discharge peaks (>1 mm h^{-1}).

We tested the postulated hypothesis with two models. In the simplest version we lump

the two soil-type $\mathrm{HRU}_{\mathrm{i}}^{\mathrm{k}}$ with i=1,2 to one mixed non-specific HRU. This model version is called the 1-soil-HRU-model having only one slow and one fast flow component. The final model version, however, is that described above distinguishing the two soil-type $\mathrm{HRU}_{1}^{\mathrm{k}}$ and $\mathrm{HRU}_{2}^{\mathrm{k}}$. We calibrated the 1-soil-HRU-model separately for each catchment with four separate parameter vectors. As is evident from Fig. 3.7 the 1-soil-HRU-model fails to explain the observed catchment response demonstrating that its structure cannot reflect the discharge dynamic of those catchments.

Distinguishing the two soils improves the calibration performance substantially. However, the original and the recalculated LDC lead to different numbers of accepted global parameter vectors, diverse parameter values and to a fairly distinct model performance: Figure 3.8 illustrates the prediction bands (grey bands) based on the Uniform Monte Carlo simulations with all accepted global parameter vectors $\mathbf{P}_{\mathrm{i}}$ and the first value $S_{\mathrm{i}}^{\mathrm{k}}(t_0)$ derived from the $S_{\mathrm{i}}^{\mathrm{k}} = f(Q_{\mathrm{obs}}^{\mathrm{k}})$ relationship.

Basically, the model calibrated on the basis of the recalculated LDC performed best (figures B). In this case the grey bands of predicted discharge embrace, with a few exceptions, the observed flow discharge $Q_{\mathrm{obs,recalc}}^{\mathrm{k}}(t)$ (black lines) in all catchments even for high discharge peaks. The exception was Julian day 196 in the Rotbach catchment with overrated peaks. The model also reproduced the observed discharge dynamic in the Lippenrütibach well, that catchment with the largest discharge variation and highest areal fractions of poorly drained soils. The calibration yielded 8100 accepted global parameter sets with individual medians of the efficiency criterion ranging from 0.7 to 0.8 in all catchments (Tab. 3.4).

When plotting the observed discharge $Q_{\mathrm{obs,orig}}^{\mathrm{k}}(t)$ derived from the original LDC for the calibration period there are minor deviations between $Q_{\mathrm{obs,orig}}^{\mathrm{k}}(t)$ and $Q_{\mathrm{obs,recalc}}^{\mathrm{k}}(t)$ in three catchments. For the other, the Lippenrütibach catchment, the observed discharge $Q_{\mathrm{obs,recalc}}^{\mathrm{k}}(t)$ was up to 30 to 40% smaller than $Q_{\mathrm{obs,orig}}^{\mathrm{k}}(t)$ at high discharge levels, indicated by the encircled peaks in Fig. 3.8, bottom. These smaller discharge peaks substantially influenced the calibration performance: Observations and predictions partly deviate dramatically as for instance at day 195 to 198 (box frames) in the Meienbach and Greuelbach. This suggests that the model assumptions in Eq. 3.6 are less compatible with the observed discharge $Q_{\mathrm{obs,orig}}^{\mathrm{k}}(t)$ than with $Q_{\mathrm{obs,recalc}}^{\mathrm{k}}(t)$. In the model, the fast flow $q_{\mathrm{i,fast}}^{\mathrm{k}}(\mathrm{t})$ linearly depends on the areal fractions $A_{\mathrm{i,fast}}^{\mathrm{k}}(t)$. However, in the Lippenrütibach, the areal fraction of the poorly drained $\mathrm{HRU}_{2}^{\mathrm{k}}$ (40%) is apparently too small to explain the observed

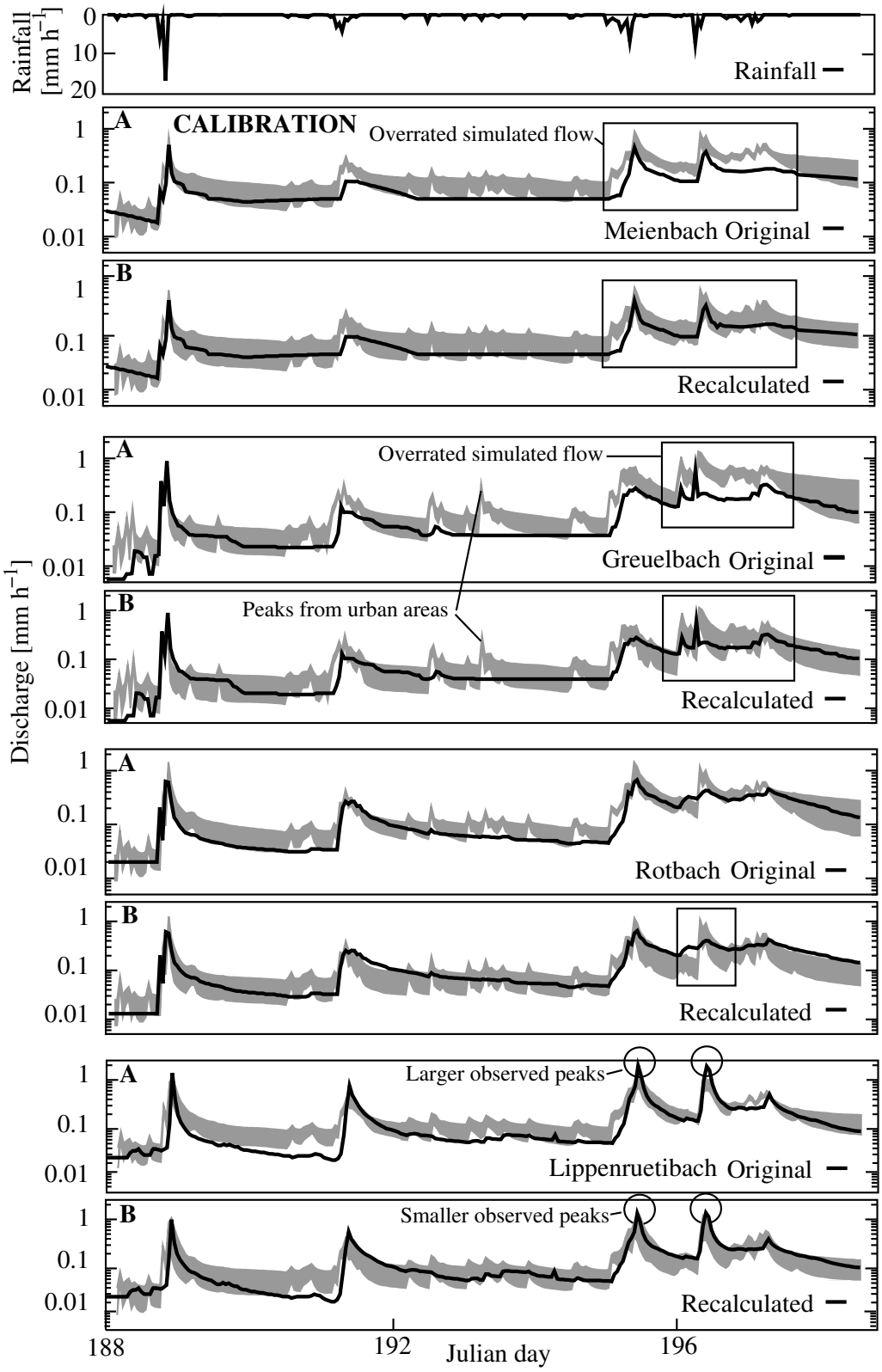

Figure 3.8: *Discharge simultaneously calibrated for the four different catchments to the observed discharge (black lines) for the period of July 7-17, 2000 with* $E_{\mathrm{m}} > 0.6$. *Two types of observed discharge was used for the simultaneous calibration: Observed discharge* $Q^{\mathrm{k}}_{\mathrm{obs,orig}}(t)$ *(figures A) and observed discharge* $Q^{\mathrm{k}}_{\mathrm{obs,recalc}}(t)$ *(figures B). The grey bands are the prediction bands excluding the minimum and maximum 10%-quantiles of the cumulated distribution of the hourly calculated discharge. Some of the significant deviations between the simulated (boxed insets) and observed (circled) discharge are highlighted. Rainfall is given in the top figure.*

Table 3.4: *Median, lower and upper quartiles of the efficiency measure E_{m} in the four catchments for the calibration (C) and validation (V) periods based on the observed discharge $Q^{\mathrm{k}}_{\mathrm{obs,recalc}}(t)$ obtained from the recalculated level-discharge curves.*

Period		Lippenrütibach			Rotbach			Meienbach			Greuelbach		
Quartile limits		25%	50%	75%	25%	50%	75%	25%	50%	75%	25%	50%	75%
July 7-17 2000	C	0.62	0.78	0.84	0.61	0.71	0.76	0.65	0.79	0.85	0.63	0.75	0.80
May 5-15 1999‡	V	0.62	0.75	0.81	0.57	0.74	0.79	0.58	0.71	0.75	0.50	0.57	0.60
Aug. 20 - Sep. 5 2000	V	0.20	0.40	0.49	0.22	0.42	0.52	0.23	0.43	0.51	0.24	0.44	0.52
May - October 1999	V	0.65	0.76	0.80	-			-			-		
May - October 2000	V	0.64	0.73	0.77	-			-			-		
May - October 2001	V	0.54	0.65	0.72	-			-			-		
May - October 2002	V	0.64†	0.71†	0.81†	-			-			-		

‡Only one rainfall gauge available †Efficiency measure obtained after excluding the poor simulations of stormflows in June and July 2002 (see text)

high discharge peaks ($Q^{\mathrm{k}}_{\mathrm{obs,orig}}(t)$ >2 mm h^{-1}) at day 195 to 197 mainly by the fast flow component. As a compromise, the fast flow was overrated to approximate the discharge peak in the Lippenrütibach and this caused an overrating of the peaks <1 mm h^{-1} in other catchments. This drastically limited the number of accepted global parameter vectors $\mathbf{P}_{\mathrm{i}}$ to 1900 when using $Q^{\mathrm{k}}_{\mathrm{obs,orig}}(t)$.

3.4.4 Validation

We tested the calibrated model with other discharge data of the four catchments over two periods of 10 and 11 days and, in case of the Lippenrütibach catchment, over four 6-month periods. Generally, the model produced reasonable agreement with the measured records despite the fact that the validation periods were up to 15 times longer than the calibration period. However, the model systematically yields sequences of good as well as of poor performance. A good agreement was found for intermediate and high discharge periods at medium to high antecedent moisture. For the flood period May 5-15, 1999, especially from day 131 to 135, the discharge dynamic was well reproduced with the exception of the initial peaks (Fig. 3.9).

Obviously, the model performed better for the major flood period (day 131-135) than for smaller isolated runoff events at day 126 and 128. The only exception was the Greuelbach

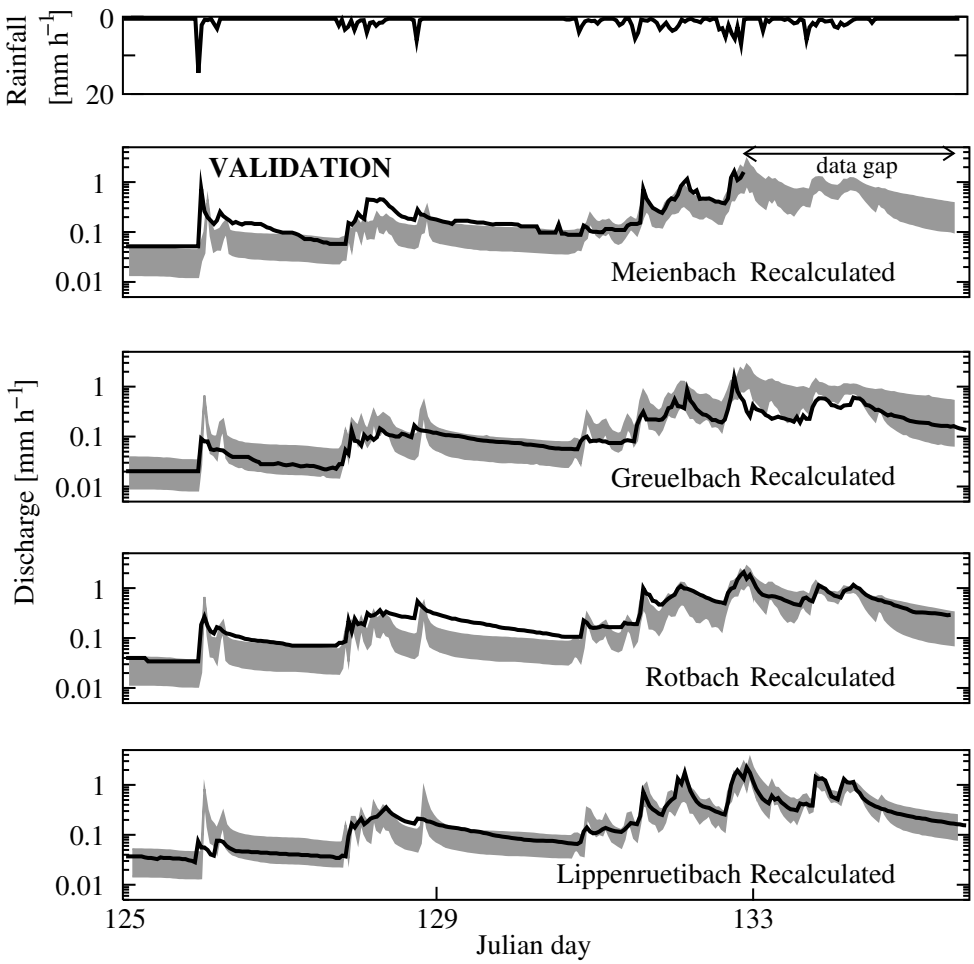

Figure 3.9: *Validation of the calibrated model with observed discharge (black lines) in the four catchments Meienbach, Greuelbach, Rotbach and Lippenrütibach (from top to bottom) for the flood period May 5-15, 1999. Observed discharge was derived from the recalculated level-discharge curves. The grey bands are the prediction bands of the calibrated discharge as described in the caption of Fig. 3.8. Rainfall is presented in the top figure.*

with overestimated discharge for the days 133 onwards primarily because it was predicted based on rainfall data from the only gauge 10km away. The performance was also better during high discharge or for longer wet periods in the period May to October 1999-2002 in the Lippenrütibach (Fig. 3.10): The prediction bands matched the observed peaks well during high discharge periods as given by the efficiency measures in Tab. 3.4.

However, the observations could occasionally not be reproduced in periods of high discharge: An extreme case occurred in June and July 2002 with discharge peaks > 3 mm h^{-1} which were about three times the calculated peak. A possible explanation for such mismatches are local thunderstorms frequently occurring during summer in this region. In such cases the real rainfall amounts may not be properly measured by the rainfall

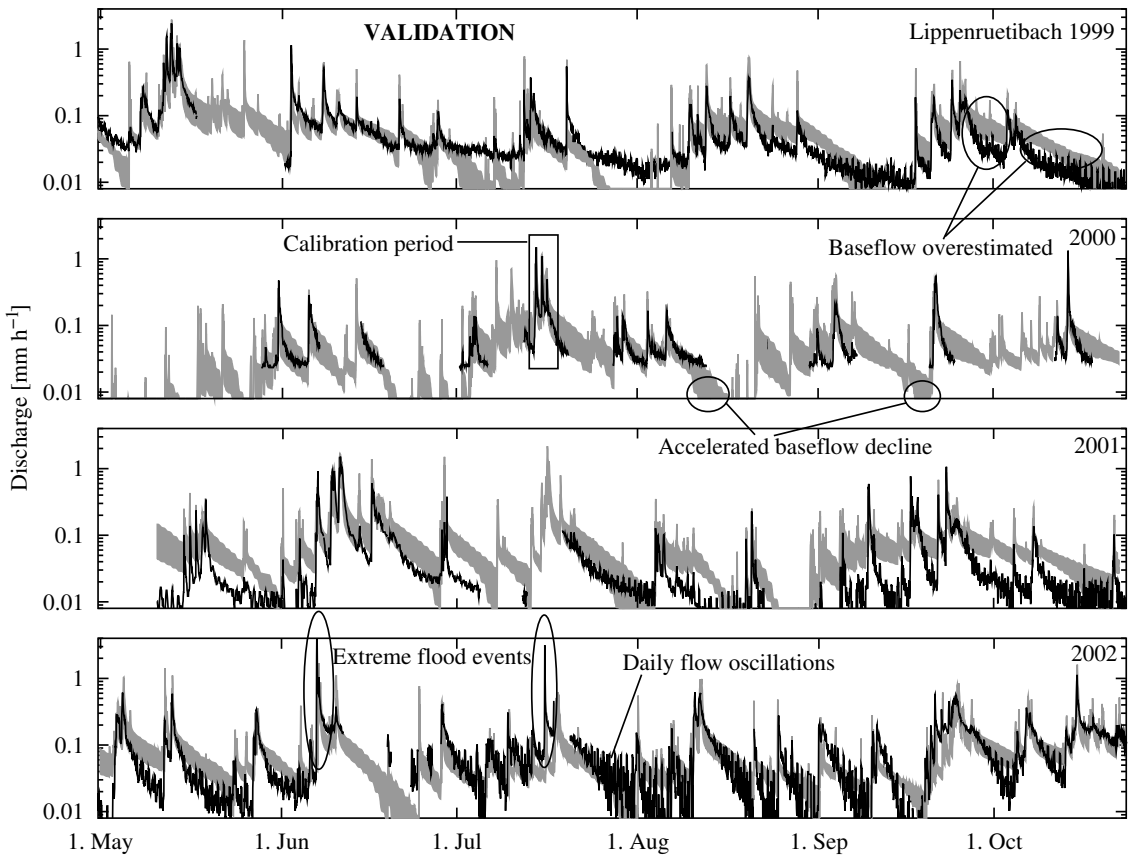

Figure 3.10: *Validation of the calibrated model with observed discharge (black lines) in the Lippenrütibach from May to October for the years 1999 to 2002 (from top to bottom). Observed discharge was derived from the recalculated level-discharge curves. The grey bands are the prediction bands of the calibrated discharge as described in the caption of Fig. 3.8. Note that the monitored discharge record was incomplete in all four years.*

gauge. Excluding these two events in 2002 for this reason, the model performance markedly increased.

Apart from these two extreme cases, poor agreements were consistently found for drier periods and events at low antecedent soil moisture. One example is the validation period from Aug. 20 to Sep. 5, 2000 (Fig. 3.11) with a small antecedent moisture and poor efficiency measures (Tab. 3.4): The initial peaks were mostly overrated while the following peaks were better predicted at day 238, but the predictions clearly mismatched the observations at day 245 to 247 possibly with the exception of the Lippenrütibach and Greuelbach. Especially in longer drought periods (>3-5 days) the poor model performance became evident (Fig. 3.10). For those periods, the calculated baseflow was mostly overestimated while the baseflow decline was much too pronounced below 0.02 to 0.04 mm h^{-1}.

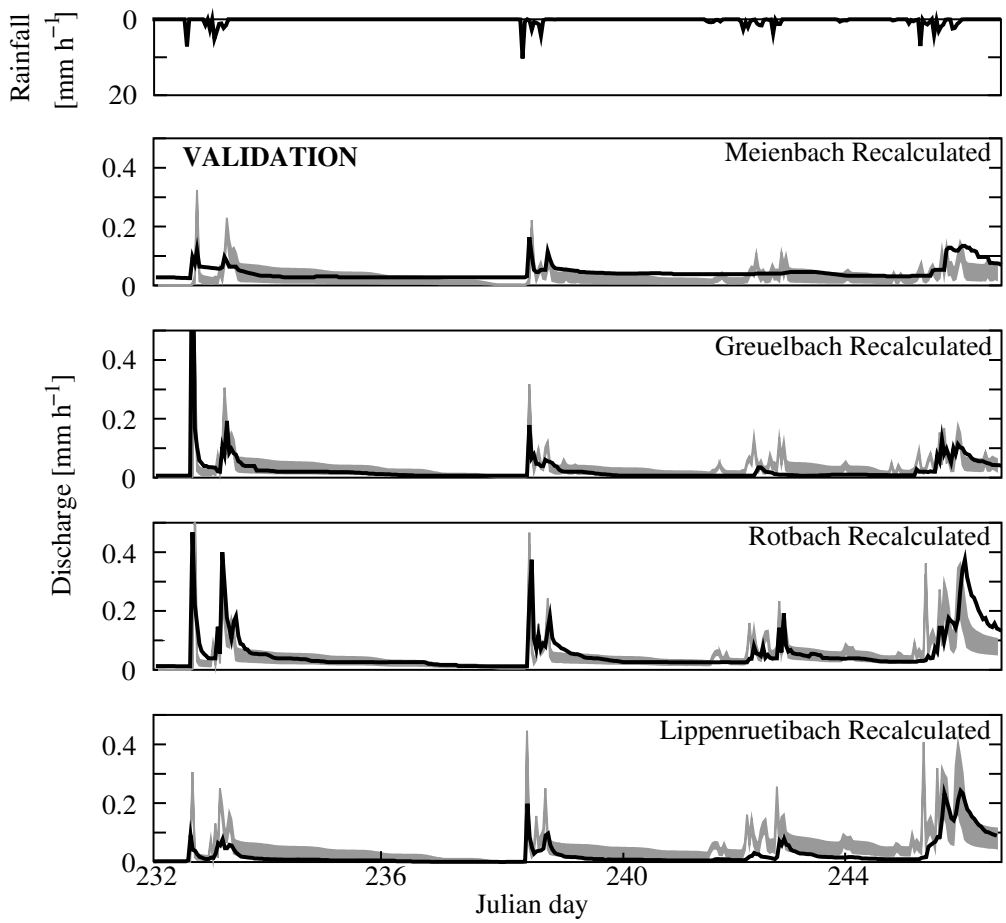

Figure 3.11: *Validation of the calibrated model with observed discharge (black lines) in the four catchments Meienbach, Greuelbach, Rotbach and Lippenrütibach (from top to bottom) for the period August 20 - September 5, 2000. Observed discharge was derived from the recalculated level-discharge curves. The grey bands are the prediction bands of the calibrated discharge as described in the caption of Fig. 3.8.*

3.5 Discussion

The generally satisfying model results are encouraging for using this model in other catchments in this region and confirm the postulated hypothesis that the areal fractions of the well and poorly drained soils govern the catchment response. At least, this is the case for these grassland-dominated catchments where surface and subsurface flow types are the dominant flow processes. However, a good agreement between observations and predictions was commonly achieved for periods with intermediate to high discharge peaks and a high antecedent soil moisture. This is also the case for validation periods up to 15 times longer than the calibration period since the short 11-day calibration record covered a substantial range of the hydrological variability observed in validation periods. This suggests that the

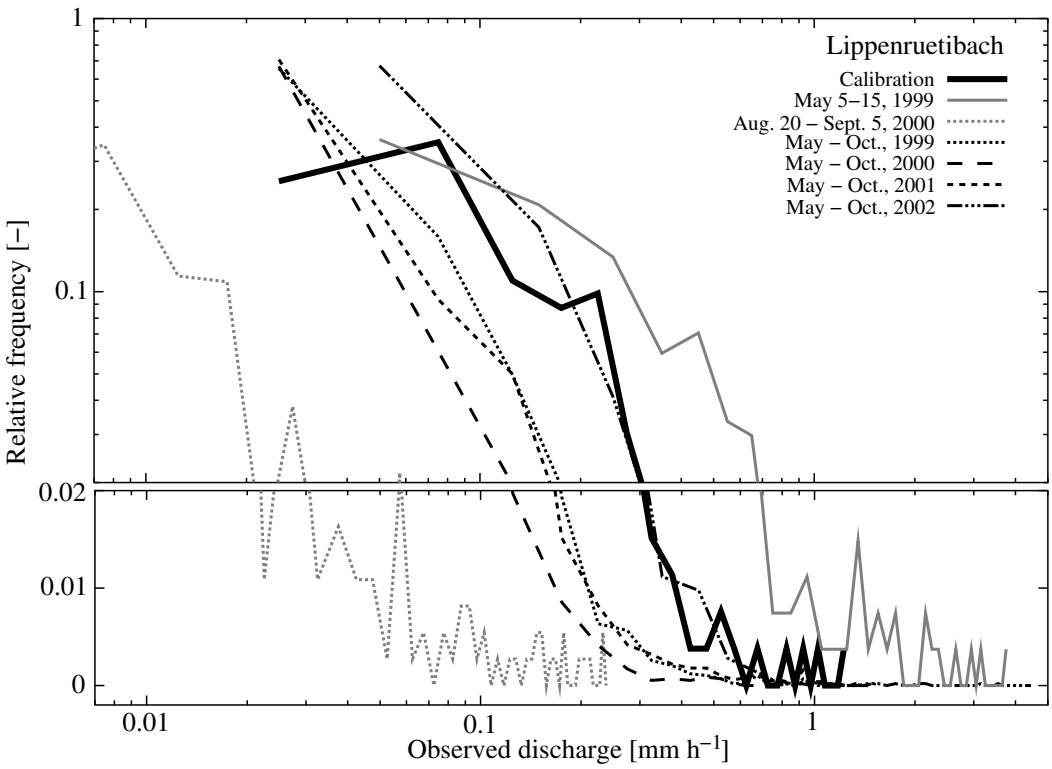

Figure 3.12: *Relative frequency of observed discharge* $Q^1_{\mathrm{obs,recalc}}(t)$ *for the calibration and validation periods in the Lippenrütibach catchment. These frequencies are similar to those of the other catchments. Note that observed discharge was derived from the recalculated level-discharge curves.*

variability of streamflow events is more important than the length of the calibration period (*Yapo et al.* (1996) and *Gupta and Sorooshian* (1985b)). However, long dry periods were still underrepresented in the calibration record. Although the short 3-day drier period during calibration was sufficiently well reproduced it was still too short to allow sound baseflow simulations for dry periods >3 days. One reason is the mismatch in the relative frequencies between the calibration and validation periods (Fig. 3.12).

Compared with the calibration record (bold black line), the drier period (Aug. 20 to Sept. 5, 2000, grey dotted line) contained many more lower discharge rates while high rates were more frequent in the wet period from May 5 to 15, 1999 (grey solid line). This mismatch potentially explains the poor agreement for dry periods while other explanations are needed to account for the good agreement in the wet period. Generally, the relative frequencies of the calibrated record partially covers those of the four 6-month validation periods but the absolute number of low discharge rates was nine times larger than in the calibration record.

The second reason for the occasional poor performance is related to the model structure. For dry conditions at low soil moisture storage we noticed an accelerated baseflow decline:

The soil water storage excessively declined as soon as the losses by evapotranspiration dominated those of baseflow. In reality, evapotranspiration only reduces the soil moisture in the top soil while the saturated zone feeding baseflow reacts with a much larger delay. This effect is a conceptual misrepresentation solely affecting the baseflow. Since this model was designed to simulate the intermediate and high flow dynamics during the growing season, the baseflow simulations are less important for our purpose.

For periods with little antecedent moisture the model calculated small discharge peaks although no peak was observed. This was mostly due to fast flow contributions from urban areas. We assumed that the fast flow from urban areas was unbuffered and linear with rainfall. With an interception storage the immediate discharge peaks could be delayed and smoothed.

It has been argued in the literature that models using the concept of the topographic index perform better for wet periods when lateral surface and subsurface flow dominate and adjust soil moisture to the topography, and thereby improving the hydrological connectivity between fields. Under drained conditions, however, *Western et al.* (1999) argued that reduced lateral flow may reduce the lateral connectivity between fields. Hence, the poor discharge prediction for periods with little antecedent soil moisture possibly indicates that topography is less important and the topographic index is a poor descriptor for such conditions. Model limitations may also be related to catchments themselves if DEMs may not include information relevant to determine flow paths (*Beven*, 1997).

This model is strongly data-driven since the average flow rate from well and poorly drained HRUs was derived from the simultaneous comparison of the four catchment responses. Hence, the results depend strongly on the data quality. The level-discharge curves (LDC) substantially influence the calculated flow contributions from those soil types and the number and values of the accepted global parameter sets as well. This is a serious aspect in hydrological modeling. Errors in the LDC are not obvious because the shape and the discharge volume of the resulting hydrographs often seem reasonable. Second, the real precipitation a catchment received may differ from that observed at one of the two rainfall gauges. Thunderstorms in summer may be especially critical due to their sometimes very limited spatial extent. Besides, flow contributions from forest were neglected and this certainly affected the parameter calibration. However, we cannot quantify this effect without adequate discharge data of paired forest and de-forested catchments.

3.6 Conclusions

The results suggest that it is necessary to differentiate well and poorly drained soil types, assign a slow and a fast flow component to each soil type and weight these flow rates with their respective areal fractions to reasonably simulate the catchment response. Without this pedologically distinction using the 1-soil-HRU-model, the dynamic of the catchment response is not reproducible. Hence, the well and poorly drained soil types may be reasonable hydrological units. So far, the average hydrological response of different types of HRUs are statistically described by the HOST-classification. However, at the time scale of single events no study is known to us showing how to derive parameter sets for distinct types of HRUs valid in several catchments. Therefore, at the event time-scale we presented a method using four catchments and the information of various areal fractions of distinct HRUs in catchments to characterize the average hydrological response of soil types by simultaneously comparing the catchment response. In this way, it is possible to derive parameter sets that can be used to predict discharge in other catchments in this region and to spatially identify fields contributing to fast flow. This is of special importance for assessing the diffuse P-losses and is the issue in a forthcoming paper.

Acknowledgments This paper is part of the project C00.0104 "Modeling P runoff at the catchment level" and is financially supported by the COST 832 action within the scope of "Agricultural contribution to eutrophication". We are grateful for the discharge data provided by E. Butscher from the Environmental Protection Agency of the Cantone Lucerne (Switzerland).

Chapter 4

Spatial classification of hydrological risk areas and their soil-type response

P. Lazzarotto, V. Prasuhn, H. Flühler and C. Stamm

To be submitted to Hydrological Processes

We report on a study to quantify the hydrological contribution from two soil-classes (well and poorly drained soils) from four small agricultural catchments in the Lake Sempach region in Switzerland. To match the hydrological response of those catchments we assigned one slow and one fast flow component to each lumped well and poorly drained hydrological response unit (HRU) influenced by topography. These flow components were quantified by simultaneously fitting the simulated catchment response of four catchments having different areal fractions of well and poorly drained soils. The flow from well drained HRUs was smoother and responded delayed to rainfall as compared with the instant and marked rise of the peak flow from poorly drained HRUs. Despite the fact that poorly drained HRUs produced more fast flow per unit area the well drained HRUs substantially contributed to discharge during long and large runoff events at high soil moisture levels in catchments with large areal fractions of well drained soils. We pixel-wise identified the areas contributing to fast flow in all four catchments and derived a probability p for fast flow production at every soil-pixel. These probabilities were grouped into hydrological risk classes. During a small runoff event less than 1% of the catchment areas clearly contributed to discharge with a probability larger than 0.9 and this fraction increased to 7 to 14% of the catchment

area during a major flood in May 1999. However, 40 to 48% of the catchment area was clearly non-contributing (p <0.1) even during this extreme flood period. In terms of risk classification, as we move from a small to a large runoff event the catchment fraction with a low risk declined from 75 to 50% while the catchment fraction with a very high risk increased from 1 to 18%. The fact that fast flow originating only from a small part of these catchments is particularly relevant for assessing the risk by diffuse pollutant sources.

4.1 Introduction

Changes in land management can significantly modify stormwater discharge, groundwater recharge, and pollution of these water bodies. This effect on the hydrological behaviour of catchments can be quantified with distributed models serving as a tool to test hypotheses and to calculate scenarios for different management practices. In addition, models can explicitly account for distributed predictions of the flow conditions at distinct locations in catchments. This requires distributed data and parameters to characterize the spatially varying state variables.

However, distributed data and input parameters are often missing at the catchment scale. As a result, major problems emerge in computing the spatially and temporally highly varying soil properties. These soil properties are crucial to describe water flow and mass transport since their variability causes an even more highly variability of the flow conditions (*Mosley* (1979) and *Flury et al.* (1994)). Another problem related to spatial data is the scale issue. The properties of hydrological processes span about eight orders of magnitude in space and time (*Blöschl and Sivapalan*, 1995). However, the spatial data are often aggregated from the scale of measurement to that of the model resolution. Despite aggregation the scale of available information does often not match the scale on which hydrological models parameterize the average soil properties.

The strategy to tackle this problem is to reduce the complexity of models without neglecting the major factors or processes that dominate the catchment response. Such a strategy is not only convenient due to the lack of adequate distributed data and parameters but is also unavoidable given the uncertainty in model structure and measurement errors (*Beven* (1993); *Freer and Beven* (1996); *Beven and Freer* (2001a)). Therefore, a simplified process description should still capture the first order controls in catchments (*Seibert and McDonnell*, 2002) with as little parameters as possible while parameters should be mostly assessable from available field data (*Refsgaard*, 1997).

To describe the hydrological processes governing the catchment response it is reasonable to simplify the spatial representation of processes to catchment units containing the relevant hydrological variability. The basic idea is that catchment units represent areas where the variance of soil properties is smaller than the variance between different classes of catchment units. A wide-spread approach amongst others, proposed by *Leavesley and Stannard* (1995), is the concept of hydrological response units (HRU) which assume hydrological similarity for a given type of HRU. Such spatial units have often been combined with topographic information (*Beven and Kirkby* (1979) and *Beven and Freer* (2001b)).

The question is how the soil properties of distinct HRUs can be determined in catchments where discharge is largely controlled by soil types. One option to determine the pertinent soil properties of HRUs is local sampling of point measurements within given HRUs (*Scherrer and Naef* (2003) and *Schmocker-Fackel* (2004)). A promising approach to describe the hydrological soil properties is based on the HOST classification (Hydrology Of Soil Type) (*Boorman et al.*, 1995). *Lilly et al.* (1998) defined a characteristic average flow response for each HOST class. The flow response was calibrated by comparing the areal fractions of the HOST classes per catchment with a flow index of the corresponding catchments using multivariate statistics. Although this approach is useful in the long-term it is limited for dynamic event-based modeling.

Our approach is comparable with the HOST classification with two main differences: We only distinguished well and poorly drained HRUs and derive the parameters for these two HRUs by a simultaneous calibration to discharge time-series. These parameters describe the characteristic flow dynamics of distinct HRUs at the event time-scale and allow to model the flow dynamic for single runoff events (see Chapter 3). At the same time, based on a saturation-dependent storage threshold the model spatially identifies contributing (risk) areas where fast flow is produced. Such areas are of particular interest for diffuse agrochemical losses since such inputs are generally lost to surface waters by fast transport mechanisms like surface runoff and preferential flow into tile drains. Conceptually, these mechanisms can be represented by a single fast flow component.

Commonly, multiple combinations of individual soil-parameters produce equally good descriptions of the catchment hydrograph but also lead to various distributed model state variables. As a result, the spatial distribution of contributing areas varies with the different parameter combinations and makes it difficult to pin down and identify the hydrological risk areas in a catchment. This requires to quantify the parameter variation and to estimate

the probabilities of distributed predictions as well.

In this chapter, we quantify the average flow dynamic from well and poorly drained HRUs and investigate their parameter variation. In addition, we try to unravel the influence of different level-discharge curves on the calibrated parameters. Finally, we present a method with which risk areas can be identified in catchments and show how these risk areas can be further classified into risk classes according to their probabilities of occurrence.

4.2 Material and Methods

4.2.1 Model description

We developed a parsimonious dynamic rainfall-runoff model at the catchment scale based on the hydrological contribution of two lumped hydrological response units (HRU) including the effects of topography. This model is described in detail in Chapter 3. A slow and a fast flow component is assigned to each well (i=1) and poorly (i=2) drained HRU, where i is the index for the type of HRU i. For each HRU i, the slow and the fast flow component is described within five parameters. Conceptually, each HRU i has its soil water storage $S_{\mathrm{i}}(\mathrm{t})$ with a maximum water storage capacity $S_{\mathrm{i,max}}$. The soil moisture $\Theta_{\mathrm{i}}(\mathrm{t})$ of the HRU i is obtained by dividing $S_{\mathrm{i}}(\mathrm{t})$ by $S_{\mathrm{i,max}}$. The soil water storage is depleted by evapotranspiration and by the slow and fast flow components and filled by rainfall. Parameter c_{i} indicates the proportion of $S_{\mathrm{i}}(\mathrm{t})$ being transformed into slow flow. The fast flow component is an autoregressive model with an exogeneous input: Parameter a_{i} describes the fast flow decline rate and the exogeneous input accounts for fast flow production due to precipitation and topography. In the following, areas where fast flow is produced will be called contributing areas. The rate of fast flow production within the contributing areas is assumed to be linear with b_{i} (proportion of rainfall converted into fast flow), the rainfall intensity and the time-variant $A_{\mathrm{i,fast}}(\mathrm{t})$ (areal fraction of each HRU i contributing to fast flow, depending on the soil water storage $S_{\mathrm{i}}(\mathrm{t})$ and topography).

Four catchments were divided into 25m $\cdot$ 25m pixels and the topographic index λ_{i} (*Beven and Kirkby*, 1979) was calculated for each soil-pixel as a measure for the influence of topography on soil-wetness. A time-variant saturation-dependent threshold $\lambda_{0,\mathrm{i}}(\mathrm{t})$ for topography determines the areal fraction $A_{\mathrm{i,fast}}(\mathrm{t})$ of the contributing areas and allows to spatially identify the contributing areas with $\lambda_{0,\mathrm{i}}(\mathrm{t}) < \lambda_{\mathrm{i}}$. This threshold $\lambda_{0,\mathrm{i}}(\mathrm{t})$ is computed for each HRU i by a non-linear function based on the soil moisture Θ_{i} of the HRU i and

the curvature of this function is governed by the parameter n_{i}.

These 10 parameters were jointly calibrated by simultaneously comparing the modeled and observed total catchment response of four neighbouring catchments over a short 11-day calibration period. The parameters were constrained to compute the expected flow components from well and poorly drained HRUs as defined a priori in Chapter 3: $S_{\mathrm{well,max}}>S_{\mathrm{poor,max}}$, $a_{\mathrm{well}}>a_{\mathrm{poor}}$, $b_{\mathrm{well}}<b_{\mathrm{poor}}$ and $n_{\mathrm{well}}<n_{\mathrm{poor}}$ while no constraints were assumed for c_{i}.

4.2.2 Soil parameters

Results in Chapter 3 demonstrated that level-discharge curves (LDC) strongly influence the calibrated parameters. Such LDC are usually derived from discharge measurements at low and intermediate water levels and extrapolated to high levels at the weirs when measurements are mostly lacking. In our case, the extrapolation method and errors of the original LDC of the four catchments were unknown. For comparison, we recalculated a second type of LDC by fitting the Darcy-Weisbach equation to discharge measurements at low and intermediate water levels and extrapolated discharge to high levels. The recalculated LDC were similar with the original LDC for three catchments while discharge differed by 30% to 40% at high water levels in the fourth catchment.

To investigate the influence of different types of LDC on the calibrated parameter distributions we used discharge time-series obtained from the original and from the recalculated LDC. From $2{\cdot}10^7$ parameter estimation runs we retained those parameter sets producing simulations better than a modified efficiency measure E>0.6. We obtained 1900 and 8100 retained parameter sets associated with the original and the recalculated LDC, respectively. An unpaired two-sided non-parametric Wilcoxon rank sum test was applied to detect significanct differences between individual parameter distributions for different types of LDC. A global sensitivity analysis of the soil parameters was conducted for each type of HRUs and LDC by classifying the 1900 and 8100 retained parameter sets into 10 subsets of equal size according to their efficiency measures. We only plotted three of 10 subsets: Subset 10 contains those with the highest, subset 5 those with intermediate and subset 1 those parameters with the lowest efficiency measures. Insensitivity was expressed by similarity between the cumulative distributions for two subsets while strong differences between the distributions suggest a sensitive parameter.

4.2.3 Hydrological response from soil types

The slow and the fast flow components from each HRU were simulated, using the retained parameter sets, and were expressed as prediction bands by excluding the minimum and maximum 10%-quantiles of their respective cumulative distributions at each time step as a measure for uncertainty. The same procedure was applied to define the prediction bands of the areal fractions $A_{i,fast}(t)$ contributing to fast flow for each type of HRU i. To illustrate how the areal fraction $A_{i,fast}$ changed with the rising average soil moisture Θ_i of each HRU i we combined them to the so-called Θ_i-$A_{i,fast}$-curves. Using the retained parameter sets the values for $A_{i,fast}$ were determined over the whole range of soil moisture of each HRU i ($0< \Theta_i <1$ with $\Delta\Theta_i$=0.02). These $A_{i,fast}$-values were expressed as ranges by excluding the lower and upper 10%-quantiles of the cumulative distributions of $A_{i,fast}$ for each $\Delta\Theta_i$.

4.2.4 Hydrological risk areas for fast flow production

All pixels belonging to well and poorly drained HRUs were classified as pixels contributing ($\lambda_{i,0}(t)< \lambda_i$) or non-contributing ($\lambda_{i,0}(t)> \lambda_i$) to fast flow at time t based on the dynamic threshold of the topographic index, $\lambda_{i,0}(t)$. Furthermore, we generated probability-maps of the four catchments for a small runoff event (time t_1) and for a major flood in May 1999 at time t_2. For each of the 8100 accepted parameter sets, different $\lambda_{i,0}(t)$-values were obtained for both HRUs at time t_1 and t_2. This led to 8100 various maps of contributing pixels of well and of poorly drained soils in the catchments and, overlaid at time t_1 and t_2, defined the corresponding probability p. This probability represents the relative frequency of how often fast flow was produced from each soil-pixel compared to the 8100 retainted parameter sets. We further classified the probabilities p into four risk classes irrespective of the soil-types ($0< p <0.2$: low risk, $0.2< p <0.5$: medium risk, $0.5< p <0.8$: high risk and $0.8< p <1$: very high risk).

4.2.5 Study area

We used data of four agricultural catchments in the Lake Sempach region in Switzerland (Fig. 4.1) which had been described in Chapter 3. Poorly drained soils such as water-logged gleyic Cambisols and eutric Gleysols cover 16% to 40% while well drained soils (permeable eutric and dystric Cambisols and eutric Regosols) dominate and vary from 42% to 78% of the total catchment area, respectively. Roughly 30% of the soils are tile-drained and terrasses alternate with steeper hillslopes. Annual rainfall varies from 1100-1200 mm y^{-1}.

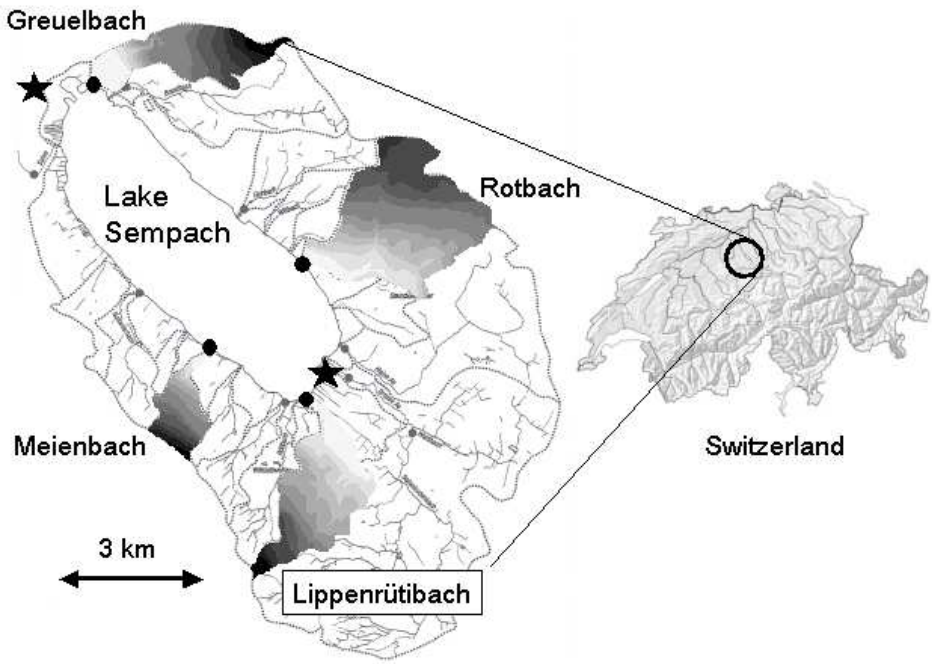

Figure 4.1: *Catchments of the Lake Sempach region (modified map of the Environmental Protection Agency, Cantone Lucerne, Switzerland). The four selected catchments are shaded. The catchment outlets are denoted as black dots. The two rainfall gauges are indicated as black asterisks.*

4.3 Results and discussion

4.3.1 Soil-type parameters

We obtained significantly different individual parameter distributions for the same type of HRUs when the model was jointly calibrated to discharge obtained with the original (empty boxplots) and the recalculated LDC (grey boxplots) in Fig. 4.2. It was shown in Chapter 3 that both types of LDC led to similar discharge values at low and high water levels in three catchments but substantial differences (30 to 40%) in discharge emerged at high water levels in the Lippenrütibach catchment only. This data constellation yielded substantial discrepancies in the individual parameter distributions for the two types of LDC and highlights how sensitive the parameters respond to uncertainty of the discharge data during the joint calibration.

Irrespective of the type of LDC the soil parameters for well and poorly drained HRUs clearly differed as indicated by the parameter distributions in Fig. 4.2 and Tab. 4.1. This

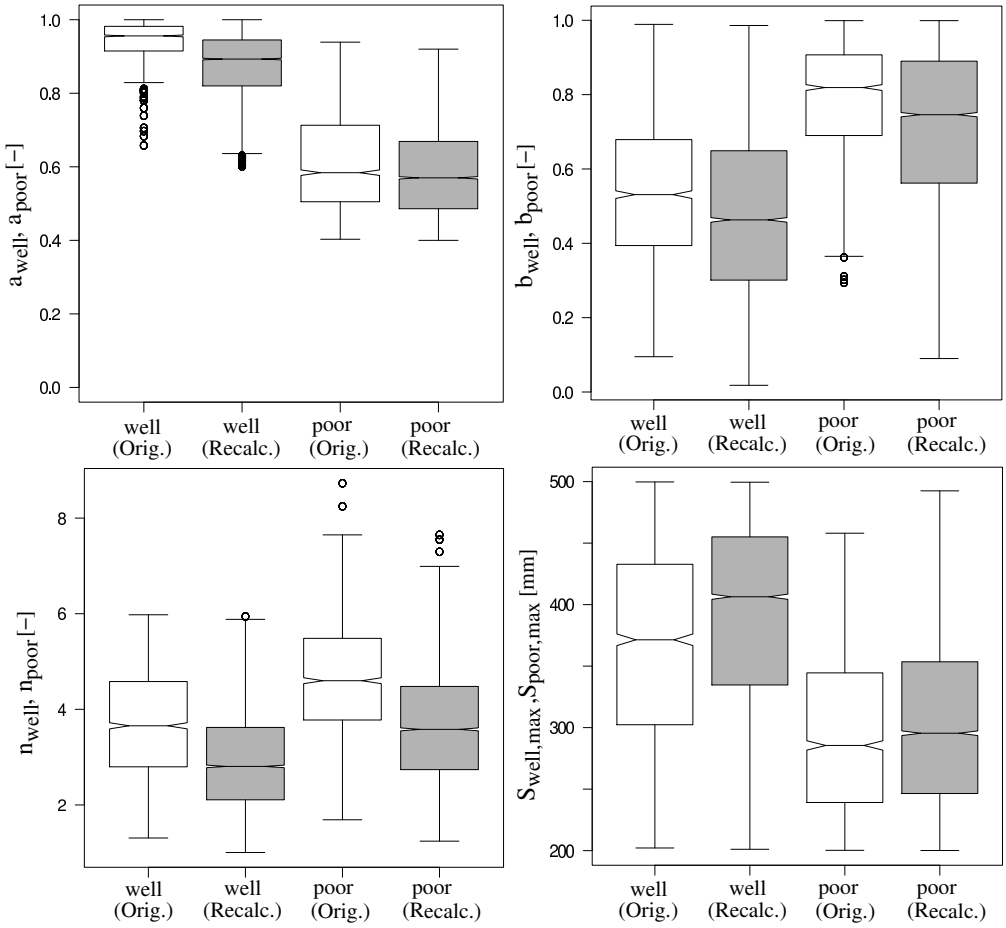

Figure 4.2: *Box-and-whisker plots for the model parameters a_i, b_i, n_i and $S_{i,max}$ for the well (i=1) and poorly (i=2) drained HRUs. These parameter sets were calibrated to observed discharge derived from the original (Orig.) and the recalculated (Recalc.) level-discharge curves. Outliers (circles) are values that are more than 1.5 times the box range away from the top or bottom of the box.*

can be seen, for the example of the parameter a_i (with i=1,2) that defines the fast flow decline rate. Following the parameter constraints (section 4.2.1) the medians of a_i were much smaller for poorly (a_{poor}=0.57) than for well drained HRUs (a_{well}=0.89). Also the medians for the maximum soil water capacity $S_{i,max}$ for well (406 mm) and poorly (295 mm) drained HRUs substantially differed. Compared with the area-weighted mean soil-thickness of 70 cm in the Lippenrütibach catchment these values correspond to a drainable porosity of $\Theta_{d,well}$=0.57 for well and $\Theta_{d,poor}$=0.42 for poorly drained soils. Here, $\Theta_{d,i}$ is defined as $S_{i,max}$ divided by the soil-thickness. Despite that these values were obtained by completely independent estimates they are close to real values of the drainable porosity.

Physically, the fast flow components, described as $q_{i,fast}(t + \Delta t)$=a_i $q_{i,fast}(t)$, have the character of a linear reservoir and the decline rate a_i accounts for physical soil-properties. The relation between a_i and the physical variables is given by $a_i = exp(-K_i \nabla h_i (\Theta_{d,i} w_i)^{-1})$

Table 4.1: *Quantiles (Qntl.) of the estimated parameters for well and poorly drained HRUs obtained from the recalculated level-discharge curve. The Median* gives the median of the parameter distributions without using parameter constraints*

	$S_{\text{well,max}}$ [mm]	$S_{\text{poor,max}}$ [mm]	a_{well} [-]	a_{poor} [-]	b_{well} [-]	b_{poor} [-]	c_{well} [mm/h]	c_{poor} [mm/h]	n_{well} [-]	n_{poor} [-]
25%-Qntl.	335	247	0.82	0.49	0.30	0.56	0.37	0.46	2.11	2.73
Median	406	295	0.89	0.57	0.46	0.75	0.59	0.63	2.81	3.58
75%-Qntl.	455	354	0.95	0.67	0.65	0.89	0.80	0.80	3.62	4.48
Median*	401	263	0.79	0.75	0.51	0.59	0.67	0.68	3.55	2.54

where K_{i} is the hydraulic conductivity, ∇h_{i} the hydraulic gradient, w_{i} the area of the storage i and $\Theta_{\text{d,i}}$ the drainable porosity of the corresponding storage i. Accordingly, with increasing hydraulic conductivity K_{i} and hydraulic gradient ∇h_{i} and decreasing area w_{i} and drainable porosity $\Theta_{\text{d,i}}$ the fast flow component should decline quicker, expressed as a small value for a_{i}.

This concept is supported by the parameter estimates listed in Tab. 4.1: Assuming that ∇h_{i} and w_{i} are similar for both types of HRUs the fast flow decline rate a_{i} is then influenced by the fraction $K_{\text{i}}/\Theta_{\text{d,i}}$. This fraction is larger for poorly drained soils (with $\Theta_{\text{d,poor}}$=0.42) than for well drained soils (with $\Theta_{\text{d,well}}$=0.57) and results in a smaller value for a_{i} for poorly than for well drained HRUs. These estimates were obtained without parameter constraints for c_{i} during calibration and suggest that the distribution of the estimated soil properties was reasonable. The larger values for b_{poor} imply more runoff being produced on poorly drained soils due to their high water tables and reduced infiltration capacity. The values for the empirical parameter n_{i}, governing the spatial extent on areas contributing to fast flow can, however, not be judged for plausibility.

Correlations between parameter pairs were mostly weak (Tab. 4.2) because it is the entire parameter combination that produces acceptable results during calibration. However, some parameter pairs were still correlated but some were also biased by the parameter constraints (e.g. $a_{\text{well}} > a_{\text{poor}}$) imposed to separate the flow dynamics from the two HRUs. As a result, these parameters were artificially concentrated at these constraint-boundaries and

Table 4.2: *Cross correlation matrix of the estimated parameters based on the recalculated level-discharge curve. Correlation coefficients r<0.20 are replaced by a. Coefficients with (+) indicate enforced correlations due to parameter constraints.*

	a_{poor}	a_{well}	b_{poor}	b_{well}	c_{poor}	c_{well}	$S_{\text{well,max}}$	$S_{\text{poor,max}}$	n_{well}	n_{poor}
a_{poor}	1	(+)	a	a	a	a	a	a	a	a
a_{well}	-	1	a	-0.23	a	a	a	a	-0.20	a
b_{poor}	-	-	1	(+)	a	a	a	a	a	a
b_{well}	-	-	-	1	a	a	a	a	a	a
c_{poor}	-	-	-	-	1	0.66	a	a	a	a
c_{well}	-	-	-	-	-	1	a	a	a	0.20
$S_{\text{well,max}}$	-	-	-	-	-	-	1	(+)	0.50	0.59
$S_{\text{poor,max}}$	-	-	-	-	-	-	-	1	0.37	0.49
n_{well}	-	-	-	-	-	-	-	-	1	(+)
n_{poor}	-	-	-	-	-	-	-	-	-	1

yield highly enforced correlations (indicated by + in Tab. 4.2). Other unbiased parameters correlated such as c_{well} and c_{poor} (r=0.66) and n_{i} and $S_{\text{i,max}}$ (0.37<r<0.59) which partially compensated each other within a certain parameter range.

The main parameters a_{i}, b_{i}, n_{i}, and $S_{\text{i,max}}$ for both HRUs, when determined with the recalculated level-discharge curves (LDC), exhibited a stronger sensitivity in the cumulative parameter distributions than for the original LDC (Fig. 4.3). The reason is that in the Lippenrütibach catchment only, the higher observed discharge peaks obtained with the original LDC were only reproducible with a peaky fast flow component from poorly drained HRUs. This limited the number of retained parameter combinations to 1900 sets and the variation in the cumulative distributions remained small. With the recalculated LDC, the smaller observed discharge peaks in the same catchment could be reproduced as a mixture of fast flow from both HRUs, thereby allowing 8100 parameter combinations to be accepted. This led to a larger variation in the cumulative distributions. For the recalculated LDC, the parameters b_{i}, n_{i} and $S_{\text{i,max}}$ were more sensitive than a_{i}.

These parameters also govern the spatial extent of contributing areas for each HRUs. The

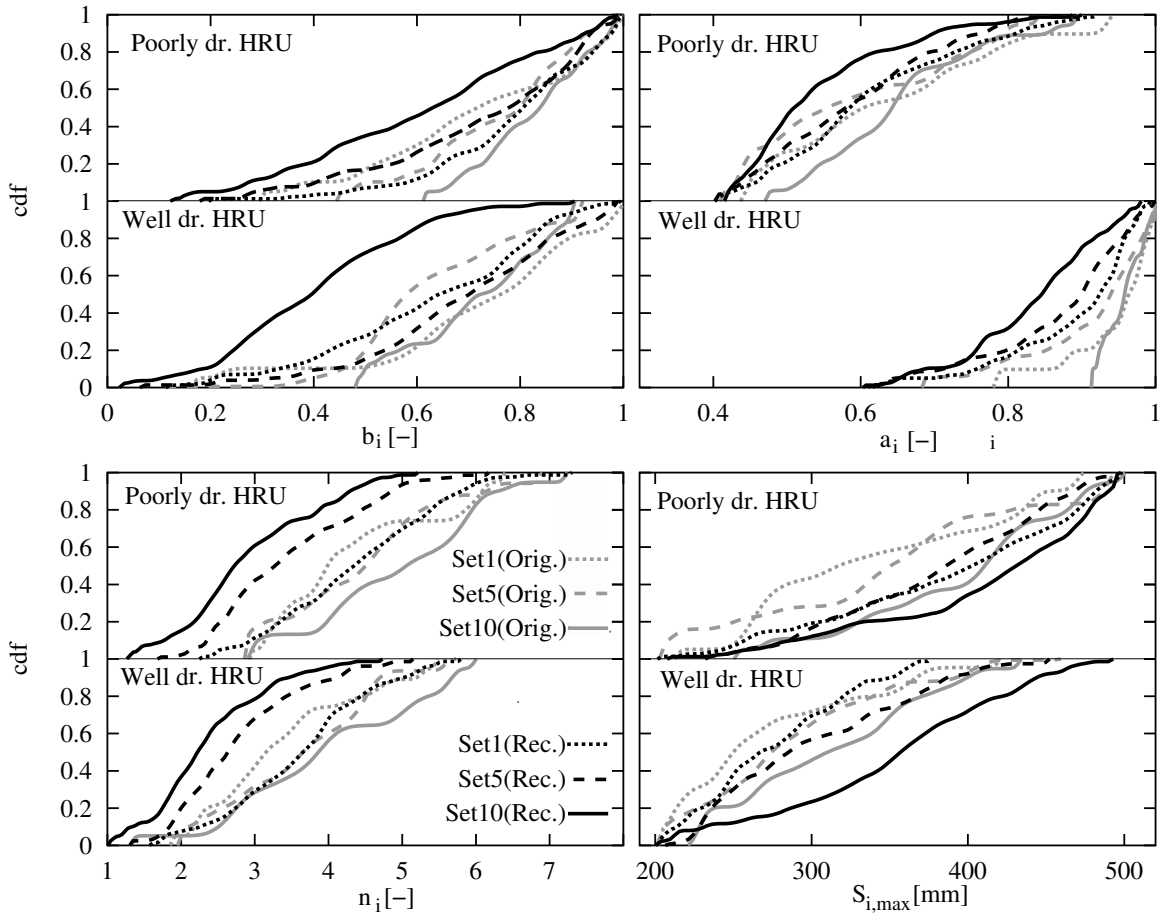

Figure 4.3: *Global sensitivity analysis with the cumulative distributions of the HRU-parameters a_i (top right), b_i (top left), n_i (bottom left) and $S_{i,max}$ (bottom right) for well and poorly drained HRUs. Each of those four figures is subdivided into two subfigures for the well (bottom) and poorly drained HRUs (top). The grey and black lines represent the parameter distributions obtained with the original (Orig.) and the recalculated (Rec.) level-discharge curves, respectively.*

Θ_i-$A_{i,fast}$-curves indicate for each HRU i the areal fraction $A_{i,fast}$ that contributes to fast flow for a given average soil moisture Θ_i. These curves were plotted for the original (left) and the recalculated LDC (right) in Fig. 4.4. Based on all accepted parameter sets, the solid lines represent the potential range of contributing areas (shown only for the Lippenrütibach catchment) when the average soil moisture of the HRUs varied from zero storage (Θ_i=0) to full saturation (Θ_i=1). The non-linear shape of these potential ranges is similar for both types of LDC but the ranges of $A_{i,fast}$ varied stronger in case of the recalculated than of the original LDC. This is because more parameter sets were accepted during calibration when applying the recalculated LDC. Under fully drained soil conditions (Θ_i <0.1) less than 5% of both HRUs contributed to fast flow. This areal fraction, however, markedly increased with increasing Θ_i: About 5 to 80% of the well drained HRUs produced fast flow

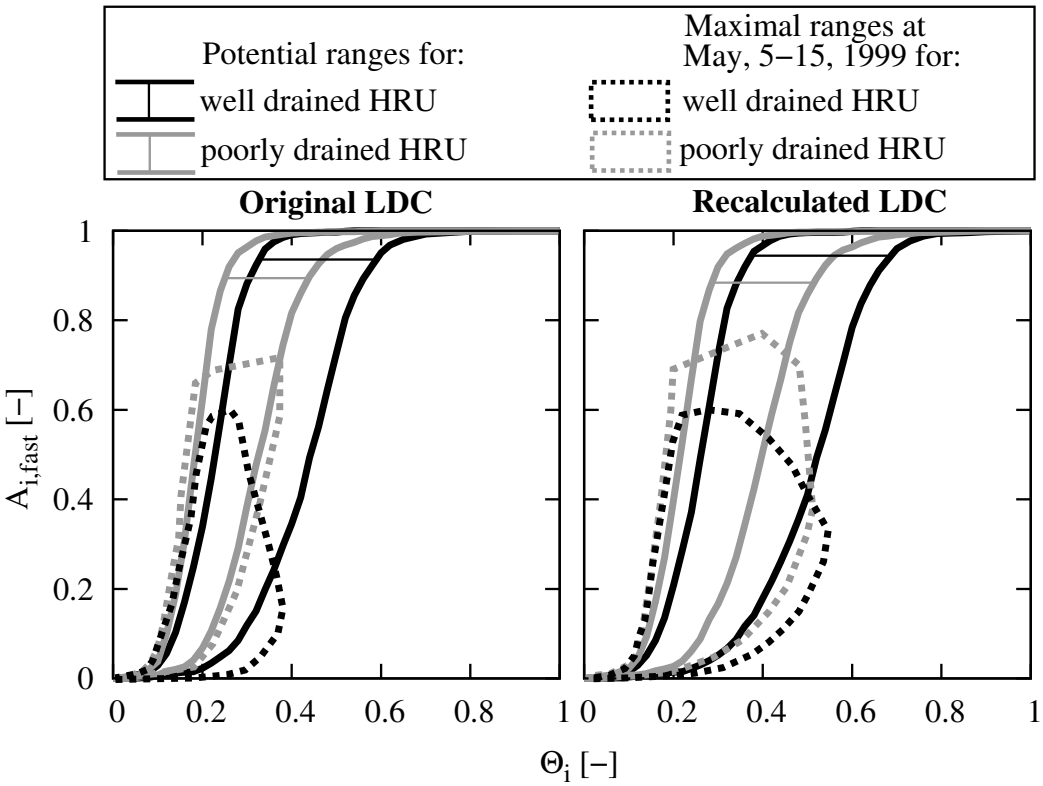

Figure 4.4: *Relationship between the areal fraction $A_{i,fast}$ of areas contributing to fast flow and the soil moisture Θ_i for well and poorly drained HRUs in the Lippenrütibach catchment. Solid lines represent the 10% and 90% quantiles of the cumulative distribution of $A_{i,fast}$ over the whole potential range from a dry (Θ_i=0) to a saturated (Θ_i=1) HRU i. Dotted lines envelope the maximum extent of the Θ_i-$A_{i,fast}$-pairs for the flood period of May 5-15, 1999, simulated with the same parameter sets. These curves refer to the original (left) and the recalculated (right) level-discharge curve.*

for an average soil moisture of Θ_{well}=0.3 while even 20 to 90% of the poorly drained HRUs produced fast flow at similar soil moisture levels (Θ_{poor}=0.3). The overall large variation of $A_{i,fast}$ - even at low soil moisture levels - clearly illustrated the uncertainty accounted for by the parameters sets. Note that $A_{i,fast}$ was even higher when using the original LDC.

Clearly, $A_{i,fast}$ was larger for poorly than for well drained HRUs at a given soil moisture Θ_i. This may be primarily due to the topographic location of the soils in the four catchments. Figure 4.5 shows the cumulative distributions of the topographic index for well (λ_{well}) and poorly drained soils (λ_{poor}). For similar cumulated frequencies we found higher λ values associated with the poorly drained soils. This indicates that flow accumulation is more likely to occur on poorly than on well drained HRUs and demonstrates the influence of topography on soil development. However, the distributions of λ were quite similar in the four catchments due to their similarity in alternating hillslopes and terrasses.

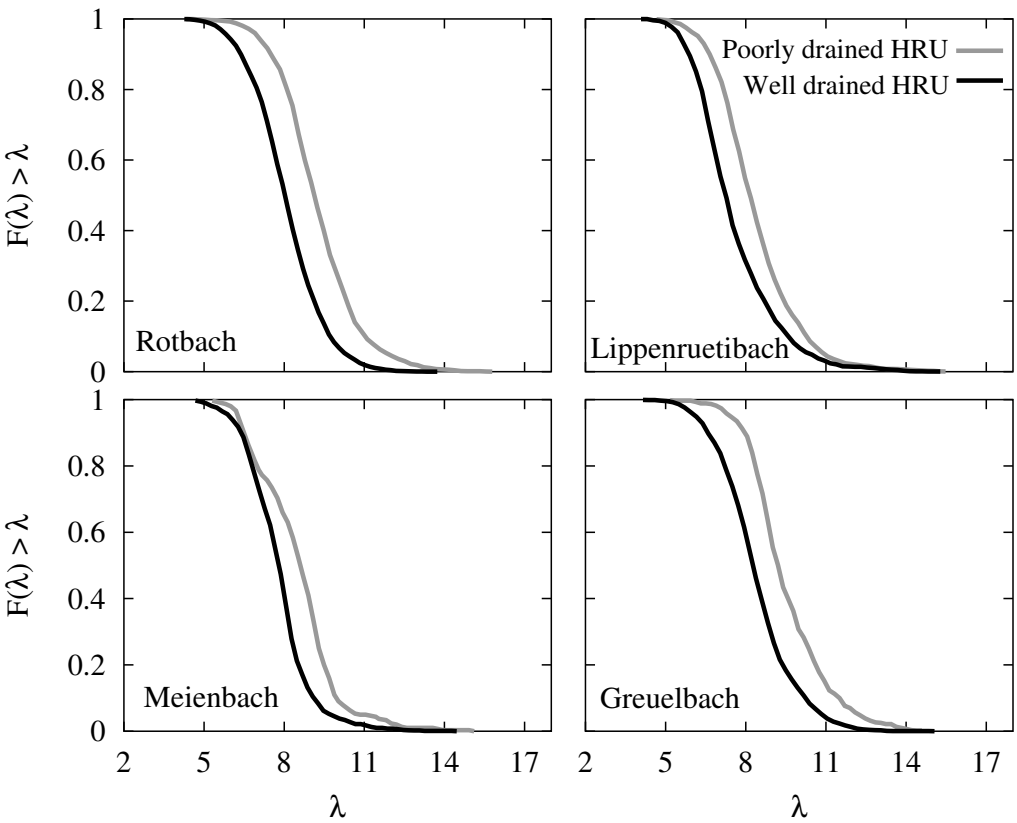

Figure 4.5: *Cumulative distribution of the topographic index λ for well (black) and poorly (grey lines) drained HRUs of the four catchments.*

To compare the maximum extent of contributing areas during a flood period in May 1999 we calculated $\Theta_i(t)$ and $A_{i,fast}(t)$ for both HRUs i in the Lippenrütibach catchment with the same parameter sets as were used to derive the potential ranges of $A_{i,fast}$ over the whole range $0< \Theta_i <1$ (solid lines in Fig. 4.4). The simulated Θ_i-$A_{i,fast}$-pairs from the May-1999-flood period are enveloped by dotted lines for each HRU and inserted into Fig. 4.4. The dotted lines indicating the maximum expansion of contributing areas show that at most 60% of the well and close to 80% of the poorly drained area contributed to this major flood in the Lippenrütibach catchment. This suggests that at most 50% of the total catchment area potentially contributed to fast flow during that major flood.

4.3.2 Soil type responses

The fast flow components from well and poorly drained HRUs were calculated in four catchments for two 11-day periods. These components are illustrated as grey prediction bands in Fig. 4.6 and 4.7. Well drained HRUs (solid black lines) responded delayed to rainfall showing smaller and smoother peaks while poorly drained HRUs (solid grey lines)

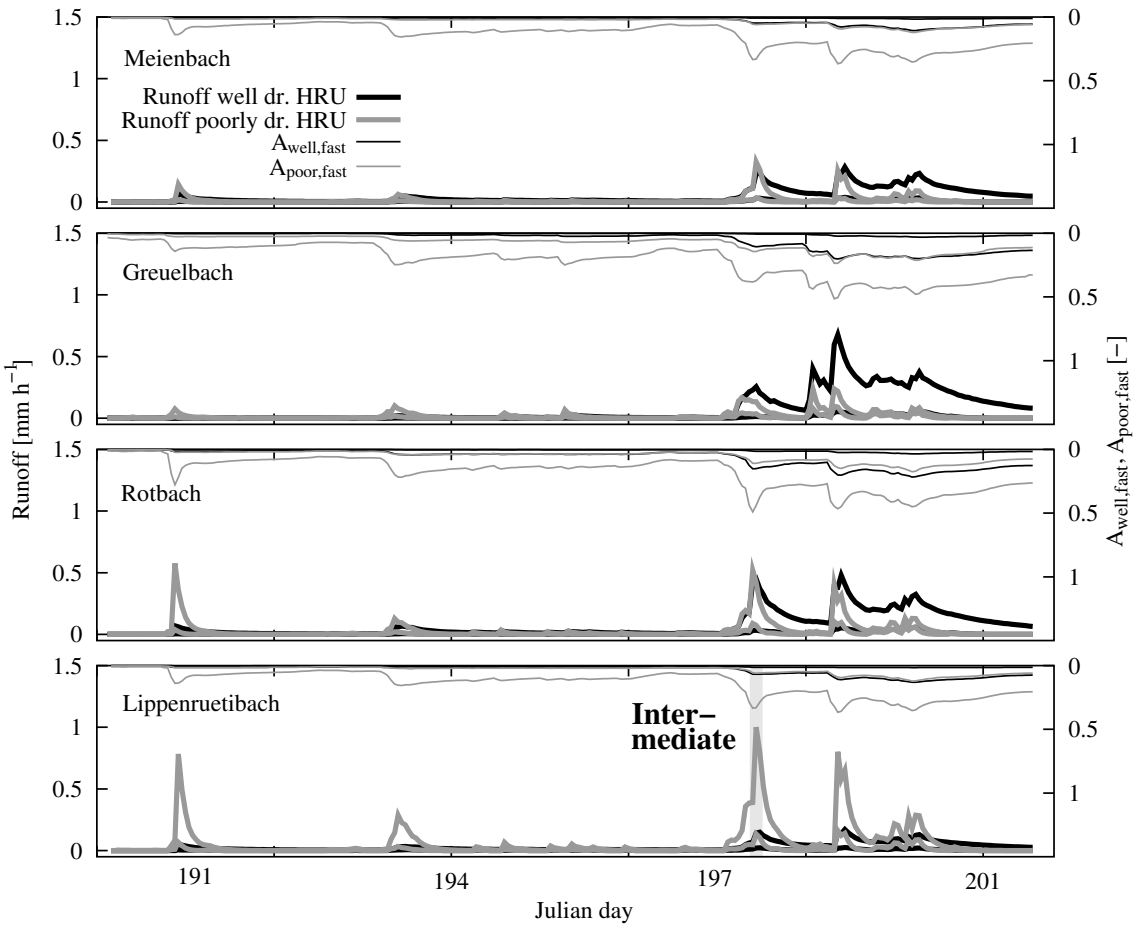

Figure 4.6: *Upper and lower boundaries of the simulated fast flow components (thick lines) and the areal fractions $A_{\mathrm{well,fast}}(t)$ and $A_{\mathrm{poor,fast}}(t)$ of areas contributing to fast flow (thin lines at the top figures) for well (black lines) and poorly (grey lines) drained HRUs in the four catchments shown for the period of July 7-17, 2000. The range between the respective upper and lower boundaries represent the fast flow components or $A_{\mathrm{i,fast}}(t)$ when the minimum and maximum 10%-quantiles of their hourly cumulated distributions are excluded. They refer to the recalculated level-discharge curves. Intermediate indicates the intermediate runoff event on day 197 referred to in Fig. 4.11.*

instantly reacted to rainfall with stronger increases and declines in peaks. The cumulated flow from the two HRUs substantially varied between catchments having different areal fractions of well and poorly drained soil-types. In the Lippenrütibach, the catchment with the largest areal fraction of poorly drained soils (40%), fast flow from this soil-type dominated the catchment response. The fast flow contribution from the well drained HRUs was markedly smaller despite comparable areal fractions.

In the other catchments (Rotbach, Greuelbach and Meienbach) having larger areal fractions of well drained soils (>60%) the fast flow from these HRUs dominated, especially during prolonged wet periods such as that starting on day 132 (Fig. 4.7).

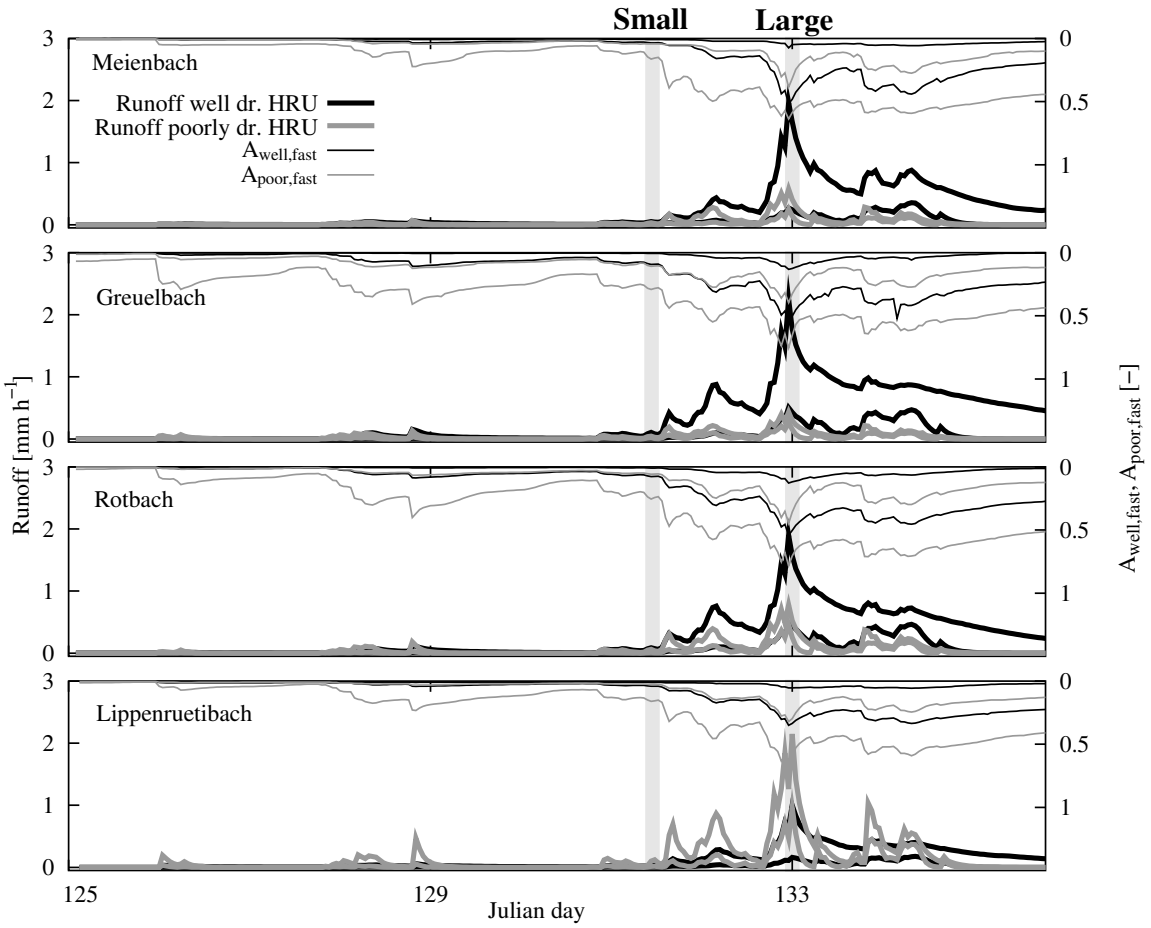

Figure 4.7: *Upper and lower boundaries of the simulated fast flow components (thick lines) and the areal fractions $A_{\mathrm{well,fast}}(t)$ and $A_{\mathrm{poor,fast}}(t)$ (thin lines at the top figures) for well (black) and poorly (grey) drained HRUs in four catchments for the flood in May 5-15, 1999. Small refers to a small runoff event and Large to the peak discharge period. See Fig. 4.6 for more explanation.*

The influence of antecedent moisture on the fast flow production from the two soil types is illustrated for the Lippenrütibach. For a rainfall peak of 10 mm h^{-1} at day 197 when antecedent moisture was relatively low the poorly drained HRUs responded by 0.2 to 1 mm h^{-1} while the well drained HRUs hardly produced fast flow (Fig. 4.6). On day 133 with the largest peak during the flood period in May 1999, antecedent moisture was extremely high and a rainfall intensity of 5 mm h^{-1} generated 1 to 2 mm h^{-1} from the poorly and 0.2 to 1 mm h^{-1} from the well drained HRUs (Fig. 4.7). This corresponds to runoff coefficients around 40% for poorly and 20% for well drained HRUs for this event. Hence, although the poorly drained HRUs produced more fast flow per unit area for small and large runoff events, the well drained HRUs dominate the catchment response under two conditions: (i) If small areal fractions of poorly drained HRUs are present in a catchment and (ii) if the soil water storage of well drained HRUs is sufficiently large, such as during longer intermediate

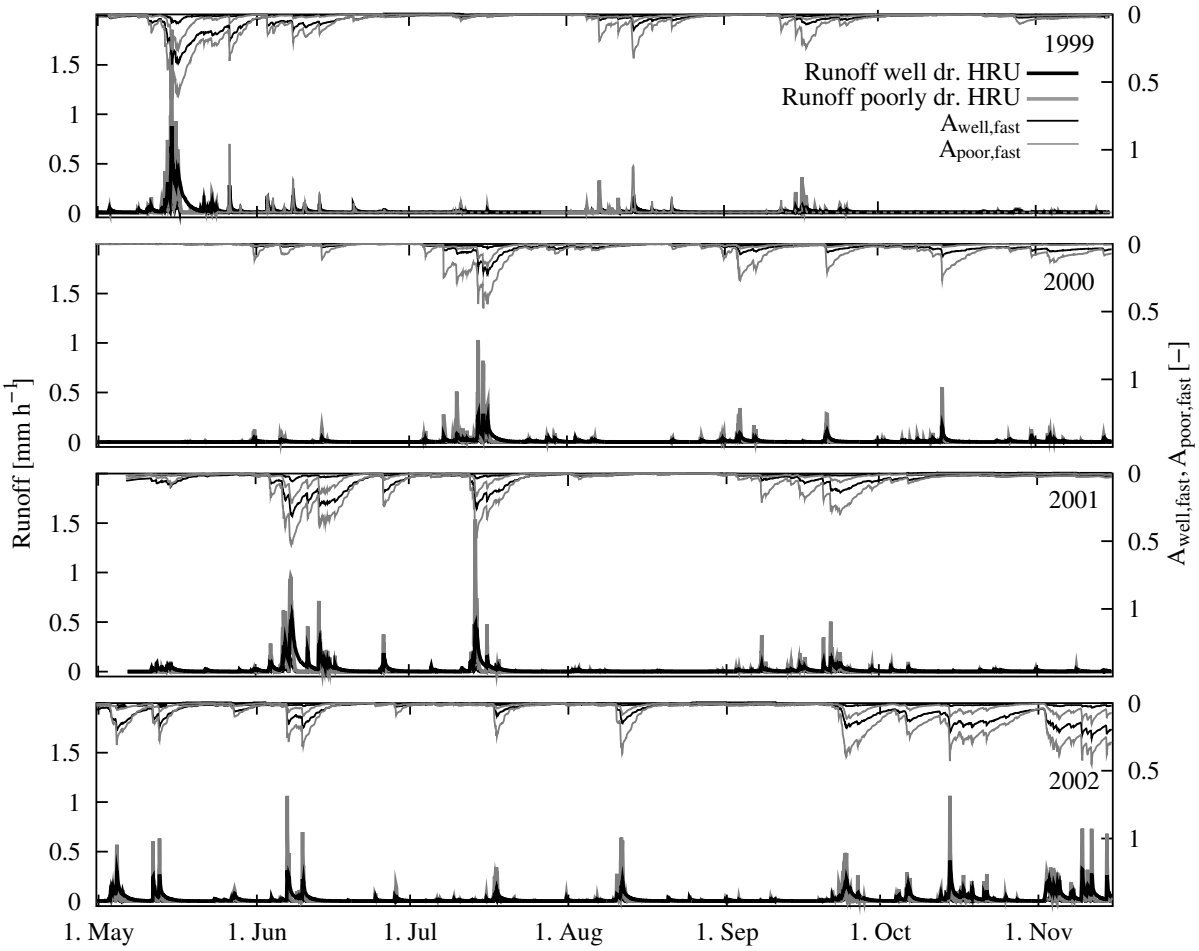

Figure 4.8: *Upper and lower boundaries of the simulated fast flow components (solid thick lines) and the areal fractions $A_{\mathrm{well,fast}}(t)$ and $A_{\mathrm{poor,fast}}(t)$ (solid thin lines at the top figures) for well (black) and poorly (grey) drained HRUs in the Lippenrütibach from May until November 1999-2002. See Fig. 4.6 for more explanation.*

and large runoff events.

The temporal evolution of the areal fraction $\mathrm{A_{i,fast}}$ of contributing areas is indicated at the top of each subfigure in Fig. 4.6 and 4.7 and their respective ranges are plotted as lower und upper boundaries (solid thin lines). We see that $\mathrm{A_{i,fast}(t)}$ always increased in response to rising fast flow although $\mathrm{A_{i,fast}(t)}$ rose faster at high soil moisture levels due to the non-linear dependency of $\mathrm{A_{i,fast}}(\Theta_\mathrm{i})$ in Fig. 4.4. For the July 2000 period (Fig. 4.6) the maximum expansion of contributing areas amounted from 13 to 22% of the well and 35 to 45% of the poorly drained HRUs, or from 16 to 24% of the total catchment area. These fractions increased during the flood in May 1999 (Fig. 4.7) from 35 to 55% of the well and up to 65 to 78% of the poorly drained HRUs corresponding to 40 to 52% of the total catchment area at the maximum. These values seem rather large but refer to an extreme

period when the spatial expansion of contributing areas was largest.

In the Lippenrütibach catchment, with 40% of poorly drained soils, the fast flow contributions from this soil-type clearly dominated the catchment response from May until November 1999 to 2002 (Fig. 4.8). Fast flow contributions from well drained HRUs were less relevant at low soil moisture but made up to 30 to 40% of the fast response from poorly drained HRUs during larger stormflows such as in May 1999, July 2000, June and July 2001. Interestingly, the areal fractions $A_{i,fast}(t)$ were unusually large in autumn 2002 (Fig. 4.8 bottom) when frequent stormflows and less evapotranspiration caused elevated soil moisture. Although the ranges in soil moisture and $A_{i,fast}(t)$ were comparable with those for longer stormflows in summer 2001 the fast flow components in autumn 2002 were smaller because of the smaller rainfall intensity in autumn 2002.

4.3.3 Hydrological risk areas for fast flow production

We were also interested in the distributions of hydrological risk areas. Thus, each soil-pixel contributing to fast flow was further classified into clearly, unclearly or clearly non-contributing according to its probability p. We illustrate the maps of this probability p for well and poorly drained soil-pixels in four catchments at two times for the period May 5-15, 1999 (Fig. 4.9). The first time t_1 refers to a small runoff event at day 131 (denoted by *Small* in Fig. 4.7) with intermediate antecedent moisture before the flood. Very high antecedent moisture was present for the second time t_2 on day 133 (Q>1 to 3 mm h^{-1}) for one of the largest flood in six years (denoted by *Large* in Fig. 4.7).

For the small runoff event at time t_1 only a few soil-pixels were contributing in the catchments (Fig. 4.9 left). These contributing soil-pixels with a probability $p > 0$ are colored in red and blue and get darker with increasing probability. Obviously, no fast flow was produced at most locations (white pixels) because high thresholds ($11 < \lambda_{0,well}(t_1) < 14$ and $10 < \lambda_{0,poor}(t_1) < 13$) were obtained as a result of the low soil-moisture status of both HRUs. Such low $\lambda_{0,i}(t_1)$-values limited the development of contributing pixels to terrasses or valley bottoms. Consistently, the poorly drained HRUs exhibited a higher probability for fast flow production than the well drained HRUs as the cumulative distributions (thin solid and thin dotted lines) in Fig. 4.10 indicate: A high probability $p > 0.9$ was calculated for 2 to 8% of all poorly but for only 1% of all well-drained soil-pixels. This suggests, that less than 1% of the total catchment areas were highly likely to produce fast flow and therefore represent the "hot spots" in case of such small runoff events. About 3 to 8% of the total

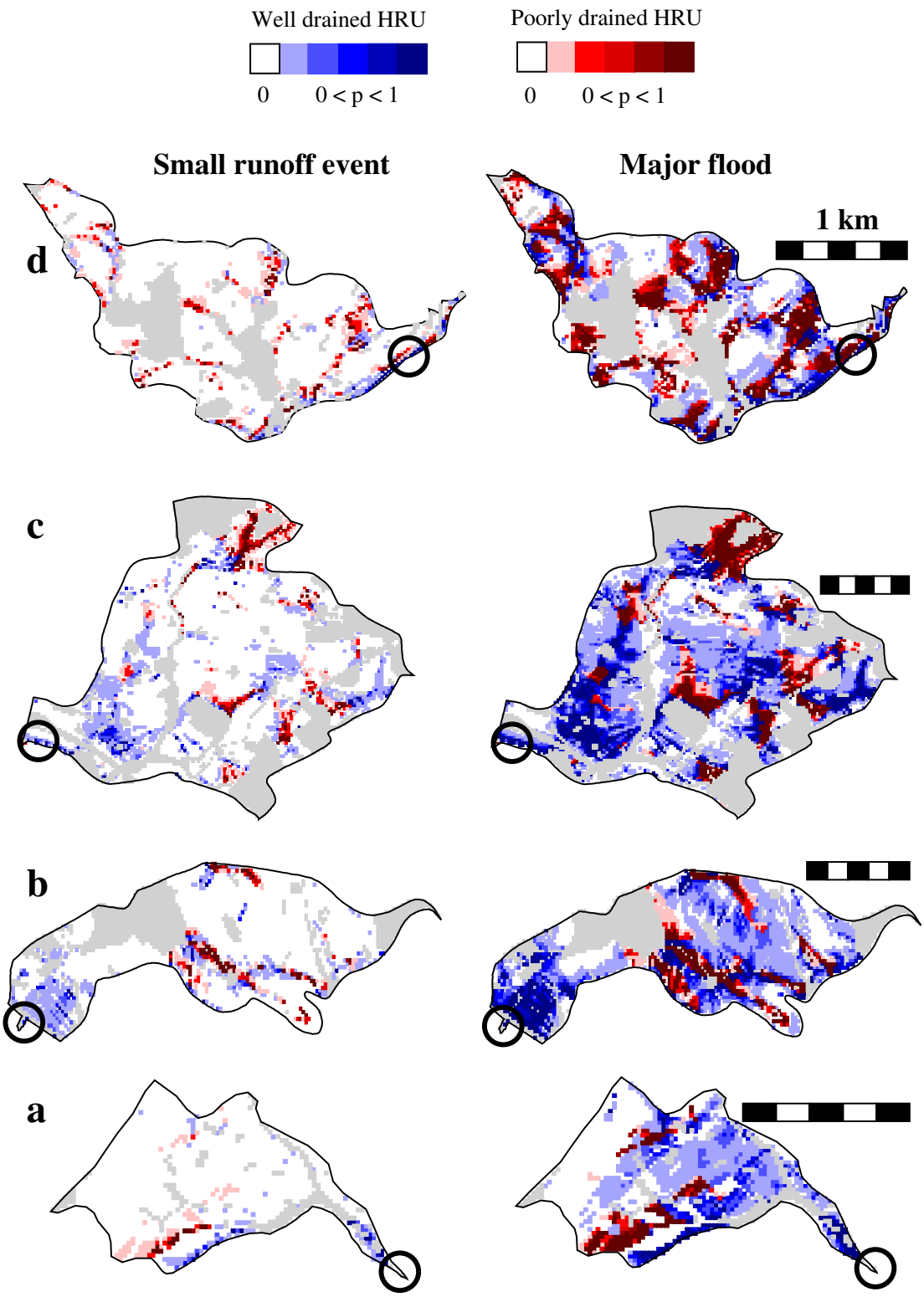

Figure 4.9: *Maps indicating the probability p that well and poorly drained soil-pixels contribute to fast flow in the Meienbach (a), Greuelbach (b), Rotbach (c) and the Lippenrütibach (d) catchment for a small (left) and a large runoff event (right). Grey shaded areas represent forested and urban area. The small runoff event refers to day 131 (indicated by Small) and the large runoff event to day 133 (Large) in the period of May 5-15, 1999 in Fig. 4.7. Circles show the discharge gauges at the catchment outlets.*

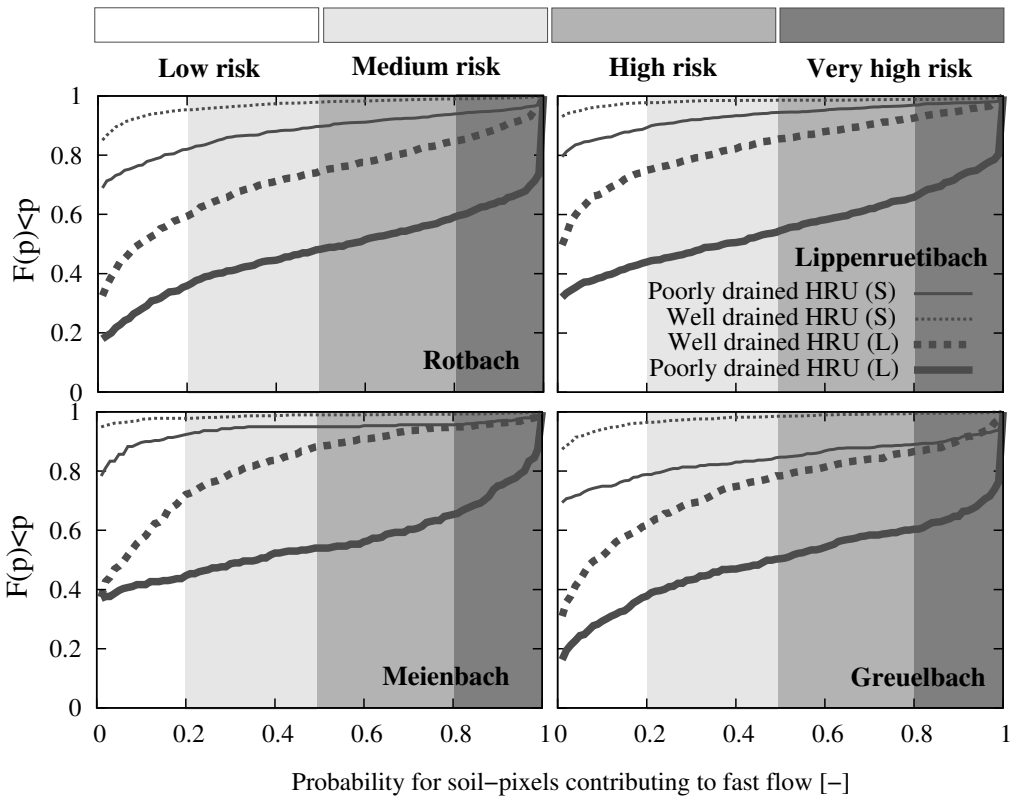

Figure 4.10: *Cumulative distribution of the probability p of soil-pixels contributing to fast flow for well (dotted lines) and and poorly drained HRUs (solid lines) for the small (thin lines) and the large runoff event (bold lines) in four catchments. S refers to the small and L to the large runoff event.*

catchment areas include soil-pixels with 0.1< p <0.9. Such a wide probability range makes it difficult to classify soil-pixels as being contributing or not. However, soil-pixels having a very low probability of p <0.1 can be treated as soil-pixels not contributing to fast flow production: About 60 to 90% of the four catchments had p <0.1 indicating that most of the catchment was clearly not contributing at low soil moisture.

For time t_2 during the major flood substantially more soil-pixels were contributing in the four catchments (Fig. 4.9 right). The reason was an exceptionally high soil moisture status of both HRUs i for which low thresholds of the topographic index were calculated (8< $\lambda_{0,\mathrm{well}}(\mathrm{t}_2)$ <11 and 8< $\lambda_{0,\mathrm{poor}}(\mathrm{t}_2)$ <9). For such wet soil conditions, the probabilility increased in all catchments as the cumulative distributions of p (thick lines) for both HRUs in Fig. 4.10 illustrate: In average, only 30 to 40% of all poorly and 51 to 68% of all well drained soil-pixels, respectively had a low probability p<0.1. This means that even during a major flood when the spatial expansion of contributing areas was maximal, 40 to 55% of the total area of these catchments can be excluded as potential risk areas since they were predicted as clearly non-contributing. Clearly contributing areas with p >0.9, however,

covered a remarkable area of 25 to 33% of all poorly and 4 to 11% of all well drained soil-pixels, or 14% of the Lippenrütibach and Rotbach, 13% of the Greuelbach and 7% of the Meienbach catchment area. Hence, the main risk areas for fast flow correspond to those soil-pixels which probably represent the maximal expansion of clearly contributing areas for such large runoff events and are in line with bulk estimates of 20%. However, most soil-pixels, expressed as 40 to 48% of the total catchment area, were still unclearly predicted with $0.1 < p < 0.9$.

Hence, probabilities allow to classify soil-pixels and to further limit the number of possible hydrological risk areas in a catchment. A more comprehensive picture of the hydrological risk areas is obtained when the probability p in Fig. 4.9 from both soil-types were pooled into four risk classes ($0 < p < 0.2$: low risk, $0.2 < p < 0.5$: medium risk, $0.5 < p < 0.8$: high risk and $0.8 < p < 1$: very high risk). The spatial distribution of these risk classes is illustrated in Fig. 4.11 for a wetting-up sequence from low to high soil-moisture levels for the small runoff event at day 131 in May 1999 (top), an intermediate runoff event at day 197 in July 2000 (middle) and the flood event at day 133 in May 1999 (bottom) in the Lippenrütibach. For a low soil-moisture status (top), only a few soil-pixels had a very high risk but most had a low risk. As the soils wet up (middle), the risk areas spread and the number of poorly drained soil-pixels with a medium, high and very high risk increased from below 5% up to 10% of the areal fraction. This increase was counterbalanced by less poorly drained soil-pixels with a low risk while the distribution of the risk-classes for well drained soil-pixels remained basically unchanged. For the large runoff event (bottom) the contributing areas substantially spread in the catchment: Such wet soil-conditions caused a very high risk on 34% of all poorly and on 8% of all well drained soil-pixels and also the number of well-drained soil-pixels with a medium and high risk markedly increased. However, low risk was still present for 74% of all well and 43% of all poorly drained soil-pixels. This suggests that 18% of the total Lippenrütibach area had a very high risk but 50% still exhibited a low risk during this major flood period. This is in line with results from *O'Loughlin* (1981) and *O'Loughlin* (1986) who observed saturated areas of less than 5% for a drier period but 5 to 20% for a wet Australian catchment.

Generally, the distributions of the risk classes suggest that with increasing soil-moisture the dominance of soil-pixels with low risks shifts towards a constellation when soil-pixels with a low and a very high risk prevail. This is important since even during wet soil-conditions a large part of the catchments had a low risk. Hence, such low risk areas can be

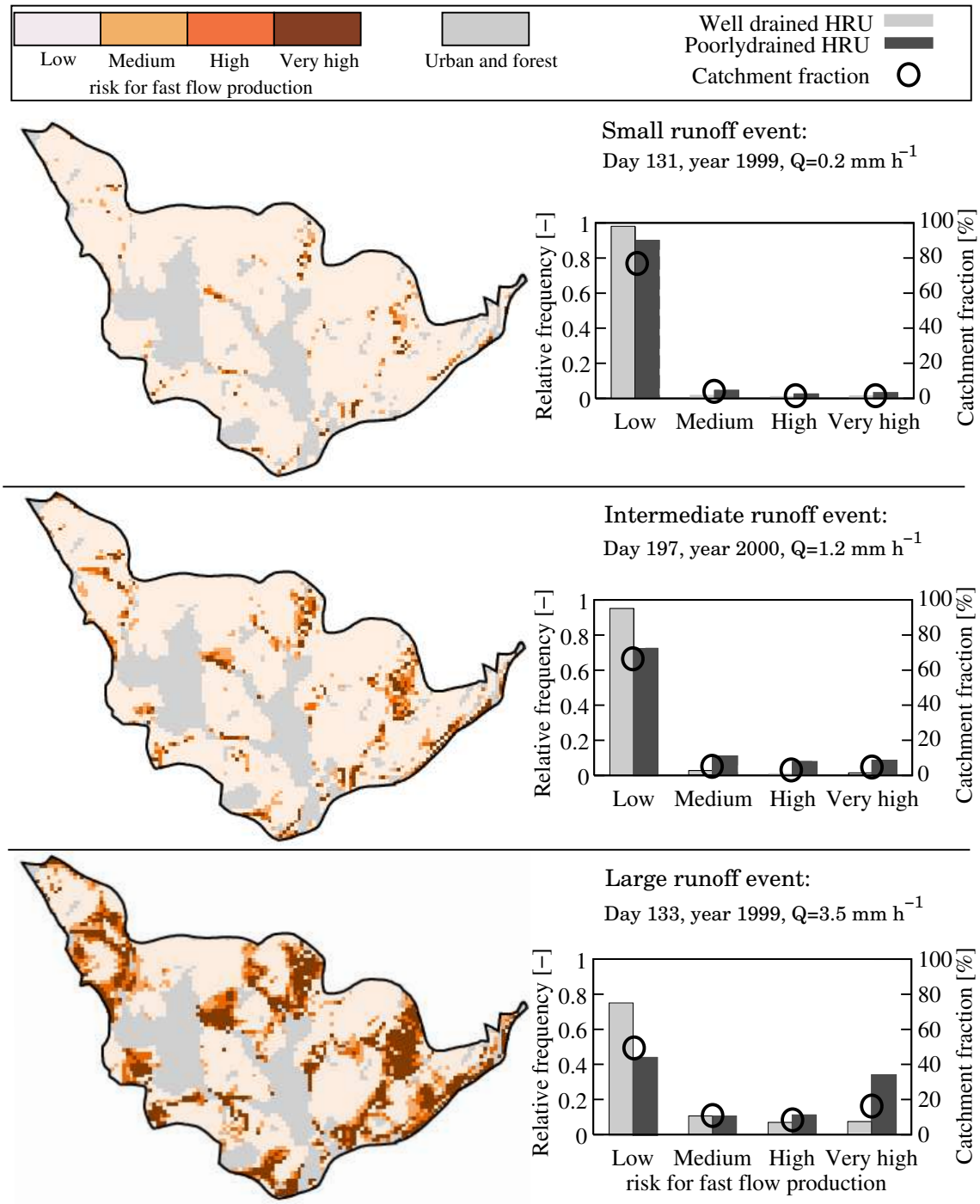

Figure 4.11: *Risk maps for soil-pixels contributing to fast flow for a small (top), for an intermediate runoff event (bottom) and for a major flood (bottom) in the Lippenrütibach catchment. Frequency distributions indicate for each runoff event the risk class contributing to fast flow for well and poorly drained HRUs, expressed as the areal fraction of each HRU (boxes) and expressed as the catchment fraction (circle).*

excluded and areas with a very high risk should be targeted with measures against diffuse agrochemical losses.

4.3.4 Ignoring the parameter constraints

We also tested the hypothesis if parameter constraints were necessary to separate between fast flow from well and poorly drained HRUs. The results (not shown) revealed that the general picture of the fast flow components did not strongly change and remained comparable as if parameter constraints were set. However, the fast flow component from the well drained HRUs stronger increased and declined while the fast flow component from poorly drained HRUs became smoother. This suggests that the dynamics of the fast flow components became similar irrespective of the soil-type as the parameter-medians (Median*) in Tab. 4.1 indicate: The parameter values for both HRUs were similar in case of a_{i}, b_{i} and c_{i}. Without constraints the maximum soil water storage of the poorly drained HRU, $S_{\mathrm{poor,max}}$, declined from 295 mm to 263 mm and n_{well} became larger than n_{poor}. Even with this new constellation $n_{\mathrm{well}} > n_{\mathrm{poor}}$ the new parameter distributions still warranted a peaky response from the poorly and a smoother response from the well drained HRUs. Such a constellation $n_{\mathrm{well}} > n_{\mathrm{poor}}$ means a larger expansion of contributing areas for well than for poorly drained HRUs but seemed unreasonable since fast flow production is more likely on poorly than on well drained soils. Despite of that the areal fractions of the poorly drained contributing areas $\mathrm{A}_{\mathrm{poor,fast}}(\mathrm{t})$ remained still higher than $\mathrm{A}_{\mathrm{well,fast}}(\mathrm{t})$ for the following reason: A higher areal fraction is related to a smaller threshold $\lambda_{0,\mathrm{i}}(\mathrm{t})$ which depends on $S_{\mathrm{i,max}}$ and n_{i} (Fig. 3.3b in Chapter 3). The same $\lambda_{0,\mathrm{i}}(\mathrm{t})$ values can be obtained with a small $S_{\mathrm{i,max}}$ and a small n_{i} or reverse. Without constraints, $S_{\mathrm{poor,max}}$ was small and this led to higher values of the soil moisture $\Theta_{\mathrm{poor}}(\mathrm{t})$. Since n_{poor} was also small this combination still allowed smaller thresholds $\lambda_{0,\mathrm{poor}}(\mathrm{t})$ and thus, higher areal fractions $\mathrm{A}_{\mathrm{poor,fast}}(\mathrm{t})$ for poorly drained HRUs. With parameter constraints, the similar values for $\lambda_{0,\mathrm{i}}(\mathrm{t})$ were obtained with a larger $S_{\mathrm{poor,max}}$ and a larger n_{poor}. Hence, this example shows that various parameter combinations yield similar results.

Without parameter constraints, the accepted parameter sets matched the individual parameter constraints by 100% for $S_{\mathrm{well,max}} > S_{\mathrm{poor,max}}$, by 67% for $a_{\mathrm{well}} > a_{\mathrm{poor}}$, by 53% for $b_{\mathrm{well}} < b_{\mathrm{poor}}$ but only by 33% for $n_{\mathrm{well}} < n_{\mathrm{poor}}$. Only 10% of all parameter sets passed all constraints and produced similar efficiency measures $\approx$0.80 during calibration as those parameter sets violating at least one of these constraints. However, ignoring the parameter

constraints impacts the number of clearly contributing soil-pixels with $p > 0.9$: For the flood event the areal fractions of poorly drained soil-pixels in all catchments declined in average from 30 to 22% but increased from 8 to 11% for well drained soil-pixels. Hence, if ignoring the parameter constraints the spatial distribution of clearly contributing soil-pixels with $p > 0.9$ differed but not as strongly as probably expected. Without parameter constraints the well drained HRUs slightly gained in importance for fast flow production. These results suggest that parameter constraints may not be absolutely necessary to reproduce the catchment response since the areal fractions of different soil-types are a strong natural constraint to separate the flow components in these catchments. In terms of the spatial classification of risk areas, however, the probability-distributions differed. Since no hard data was available for validation it remains unclear which type of predictions (ignoring or following the constraints) better approximates the real-world distribution of the contributing areas. A close fit between observed and simulated discharge is still no proof that the model structure is correct and the internal state variables of the model actually correspond with the distributed variables in catchments (*Grayson et al.* (1992); *Beven* (1996); *Beven* (1997); *Refsgaard* (1997)).

4.4 Conclusions

We conclude that the hydrology of the well and poorly drained HRUs differed clearly despite the uncertainty related to various types of level-discharge curves. However, discharge exerts a relevant influence on the parameter calibration and highlights the need to test level-discharge curves. Most of the conceptual parameters can be physically interpreted and the parameter distributions seem realistic. Interestingly, it is not absolutely necessary to impose parameter constraints to separate the flow components from different soil-types to reproduce the catchment response although the fast flow components became similar irrespective of the soil-types. It seems that the areal fractions of soil-types in these catchments are a strong constraint to separate the flow components anyway. The subjective judgement of the flow dynamics from both soil-types suggests reasonability. So far, we assumed that poorly drained soils were the main soils for fast flow generation. Despite that poorly drained HRUs produced more fast flow per unit area a large fraction of well drained soils became contributing to fast flow. This applies to prolonged intermediate and high runoff events in catchments with large areal fractions of well drained soil-types. Besides poorly drained HRUs the well drained HRUs may become hydrological risk areas

too, under very wet conditions and may contribute to diffuse agrochemical losses. The further classification of soil-pixels into risk classes according to their probabilities clearly demonstrated that the major part of the catchment had a low risk, even during very wet conditions. However, the risk areas in catchments spread with increasing catchment wetness but even during a major flood only 18% of the total catchment had a very high risk. It also turned out that the prediction of clearly non-contributing areas was easier than the clearly contributing areas. Unfortunately, the validation of the spatial results remained difficult since no hard validation data was available. This would be important since spatial predictions of contributing areas are crucial for modelling diffuse agrochemical losses.

Acknowledgments This paper is part of the project C00.0104 "Modeling P runoff at the catchment level (Lake Sempach)" and was financially supported by the COST 832 action within the scope of "Agricultural contribution to eutrophication" and by the Institute of Terrestrial Ecology, ETH Zurich. We are grateful to E. Butscher (UWE Luzern) for making the discharge data of those catchments available.

Chapter 5

Event-based modeling of diffuse phosphorus losses from topsoils and manure in an agricultural catchment

P. Lazzarotto, V. Prasuhn, H. Flühler and C. Stamm

To be submitted to Journal of Environmental Quality

5.1 Abstract

Diffuse losses of phosphorus (P) by surface runoff or preferential flow into surface waters may cause eutrophication problems. These P-losses can be substantially reduced by reducing P-inputs into risk areas within catchments. This project aimed to identify such risk areas for P-loss in catchments and to quantify the P lost from soils and from manure by event-based modeling using temporally and spatially high-resolution data. The study area is a small grassland catchment (3.3 km^2) in the Lake Sempach region (Switzerland) where discharge and dissolved reactive P (DRP) were measured in hourly time steps since 1998. Since 1998 we also collected data of each manure application from 30 farmers for each of the 250 fields and assessed the soil-P status for all fields in 2000. Because risk areas for P-loss are fields with fast flow occurring, a high soil-P status or recent additions of manure we applied a semi-distributed parsimonious model which accounts for the dominant hydrological and P-mobilization processes. Despite that all P-parameters were solely derived from avail-

able field-data the model well reproduced the hourly DRP-loads of some stormflow periods during the growth period in 1999 using 500 Monte-Carlo simulations. However, the high peaks in the DRP-load were mostly underestimated for most stormflow periods. The simulations indicated that most of the DRP-loss during the growth period in 1999 originated from topsoils with 23 to 110 kg DRP-loss depending on the scenarios to describe P-mobilization from soils and from manure. The DRP-loss from manure for that period was less relevant (5 to 7 kg DRP) and amounted to <30% of the total DRP-loss. However, irrespective of the used scenarios to describe DRP-mobilization the DRP-loss from soils dominated over the DRP-loss from manure for that period. The reason was the high DRP-concentrations being mobilized from a large number of P-enriched topsoils in this catchment which overran those concentrations from manure during most of the growth period. These results suggested that measures are primarily needed to reduce the high soil-P status in this catchment.

5.2 Introduction

Elevated phosphorus (P) concentrations pose severe risks for eutrophication in surface waters (*Foy and Withers* (1995) and *Sharpley et al.* (2000)). During the middle of the last century, P-loss from diffuse sources (agriculture) and from non-point sources (households, sewage water treatment plants) into surface waters markedly increased in Switzerland (*Bundesamt für Landwirtschaft*, 2001). One of these lakes confronted with eutrophication problems is Lake Sempach in the Swiss Plateau, which received public attention in 1984 after a massive fish kill (*Stadelmann*, 1988). As one of the main measures to reduce the P-concentrations the waste water treatment plants were extended in the 1980s to connect all households to a sewer system. Despite these measures the P-inputs into the lake did not decrease as predicted since the reduced loss from waste water was replaced by increased diffuse loss from agriculture. Before measures to reduce diffuse P-loss are efficiently implemented in catchments two questions arise: Which are the fields relevant for P-transport during runoff events and which type of P-source (topsoils or manure) is responsible for mobilising P? These questions can be target by models if adequate data for manure and soil-P data is available and the dominant processes for P-mobilization and the P-sources are known.

In agricultural catchments with high stock densities, diffuse P-sources are derived primarily from the P contained in manure and from the P stored in the topsoils. A high soil-P status develops due to excessive manure application compared with the P-demand

of plants. While the P accumulated in topsoils is a long-term source for P-mobilization freshly applied manure is temporarily important in generating additional P-loss (*Edwards and Daniel* (1993a) and *Withers et al.* (2003)). The dominant P-form in runoff from grassland is the dissolved P (*Sharpley et al.*, 1992) which limits the growth of algae in surface waters. Although agricultural P-loss is economically irrelevant the dissolved reactive P (DRP)-concentrations in runoff amount from 100 to >1000 mg m^{-3} and largely exceed the water quality goal for oligotrophic lakes (10 to 30 mg total-P m^{-3}).

In many soils, the P-mobility is low due to the low solubility of phosphate and the high P-binding capacities of the soil material (*Sharpley and Rekolainen*, 1997). Hence, the DRP-concentrations in solution remain low. Many studies on pastures, however, report on strong correlations between DRP-concentrations in runoff and the soil-P status (SPS) when rainwater interacts with the P-enriched topsoils (*Pote et al.* (1996); *Sibbesen and Sharpley* (1997); *Schoumans and Groenendijk* (2000)). In that case, the P-loss may rapidly increase as soon as a threshold level of P-saturation (change point) is exceeded (*McDowell and Sharpley*, 2001). High P-loss also emerges on peaty, sandy or acid organic soils with low P-sorption capacities (*Sharpley and Rekolainen*, 1997) or by surface runoff or preferential flow when P moves rapidly through the soil with little sorption into near-surface tile-drains and laterally into surface waters (*Stamm et al.* (1998) and *Hesketh and Brookes* (2000)).

Another type of P-loss is related to the direct interaction between rainfall and recently applied manure on fields and the subsequent loss of DRP by surface runoff or macropore flow into tile-drains. This kind of P-transport is known as incidental P-loss (IPL) and may significantly contribute to total P-export (*Withers et al.*, 2003). However, the relative importance of P-loss from soil or IPL is still under debate. Applying manure creates a temporarily large P-pool that is instantly prone for losses if the soil- and weather conditions are not favourable (*Withers et al.*, 2003). The variation of IPL depends mainly on the method, rate and timing of application (*Withers et al.* (2001) and *Kleinmann and Sharpley* (2003)), the time between manure application and runoff event (*Braun et al.* (1993); *Sharpley* (1997); *Tabbara* (2004)), the water-soluble P in manure, the rainfall intensity, the presence of runoff and the hydrological connectivity from the fields to the stream. For the first runoff event after the last application DRP in runoff was largest and dropped with increasing duration between manure application and the runoff event at variable rates due to P-loss from previous stormflows, to P-uptake by plants and to longer contact time between manure-P and the soil. *Braun et al.* (1993) showed that (i) DRP was still high

several weeks after the last application and (ii) IPL may temporarily dominate the P-loss irrespective of the SPS. Manure application also reduced the infiltration capacity of soils thereby increasing the extent to which fast transport mechanisms like surface runoff occur (*Smith et al.* (2001); *Stamm et al.* (2002); *Burkhardt et al.* (accepted)).

Although research has aimed to quantify P-transfer from grassland and data exists for a range of agronomic management practices and soils (*Haygarth and Jarvis*, 1999) the quantification of P-loss from soils or from IPL remains difficult since P-transport requires the simultaneous presence of fast flow and a P-source (*Gburek et al.* (1996) and *Gburek et al.* (2000)). Hence, risk areas are fields where (i) fast flow is produced and a hydrological connectivity to the brook is established, (ii) high SPS had developed and/or (iii) manure/fertilizer was recently applied. It was also proposed that a few fields - hot spots - contribute above-average to P-loss during a few stormflows (*Pionke et al.*, 1999). This is supported by findings of field experiments demonstrating that the main herbicide losses within a catchment originated from certain fields only (*Leu et al.*, 2004).

The hydrological risk areas can be identified by semi-distributed models accounting for the dominant hydrological processes and catchment attributes as shown in Chapter 4. However, to determine the P-loss from soils and from manure requires detailed distributed P-data for the SPS and manure which is lacking in most studies. For this study, this data was available to run a semi-distributed P-model.

Physically-based models for transport are often desired but their use at the catchment scale is questionable because (i) vast amounts of required data cannot be collected (i) fast transport mechanisms such as preferential flow are not reproducible by classic transport equations and (iii) the model parameters are scale-dependent as a result from the heterogeneity of soil properties below the scale of application.

Although conceptual models such as CREAMS (*Knisel*, 1980), GLEAMS (*Leonard et al.*, 1987), EPIC (*Sharpley and Williams*, 1990) or ICECREAM (*Tattari et al.*, 2001) were often applied they are too data-demanding and the described P-cycle relies on pre-calibrated site-specific parameters. This prevents to use such models in other catchments with distinct climatic and soil conditions as they were calibrated for. Despite that widespread conceptual rainfall-runoff models such as TOPMODEL (*Beven and Kirkby*, 1979) or HBV (*Lindström et al.*, 1997) were modified to estimate diffuse P-loss they require data and parameters which often cannot be properly derived from available field data.

Alternatives are empirical models that identify relationships between input and output

and neglect how physical mechanisms convert input into output. For example, *Lek et al.* (1996) linked catchment features with the observed P-concentrations and P-loads by using neural networks. A more experimental approach is the export coefficient method to up-scale the exported nutrient loads measured from distinct units by field studies to large catchment sizes (*Johnes* (1996) and *Johnes and Heathwaite* (1997)). This approach has also been combined with the HOST classification (Hydrology of Soil Types, (*Boorman et al.*, 1995)) by *Heathwaite et al.* (2003) to conceive hydrologically effective rainfall to predict mean annual P-export. Other approaches such as the index method (*Gburek et al.* (2000) and *Braun et al.* (2001)) estimated total-risk values for fields based on risk-values for land-use, chemical and hydrological site features influencing P-loss. Although export coefficients were assigned to the total risk-values to estimate mean-annual P-loss this approach is not suitable for event-based predictions.

This short overview suggests to combine lumped and conceptual models to match process complexity with available information from field-experiments (*Russell and Wheater*, 2004). This, however, requires parsimonity in parameters that should be mostly derived from observations while the model structure must be simplified to a degree that still accounts for the dominant processes relevant at the catchment scale (*Hillel* (1986); *Beven* (1989); *Refsgaard* (1997)).

The goal of this study was to spatially predict the risk areas for diffuse P-loss in a grassland catchment and to determine the contribution of P-loss from manure and from soils for single runoff events. This was possible since a semi-distributed hydrological model spatially identified the contributing areas to fast flow based on topography and the hydrologic response of two major soil-types. A semi-distributed P-model, for which the relevant P-parameters were derived from experimental field data, accounts for the temporally and spatially high-resolution P-management data from 30 farmers and detailed data for the soil-P status.

5.3 Material and Methods

5.3.1 Study area

The study area is the Lippenrütibach catchment (334 ha) in the central part of Switzerland (Fig. 5.1). About 255 ha is agricultural land, divided into 250 fields managed by 30 farmers. About 90% of this area is grassland and 10% arable land. Well drained soils amount to

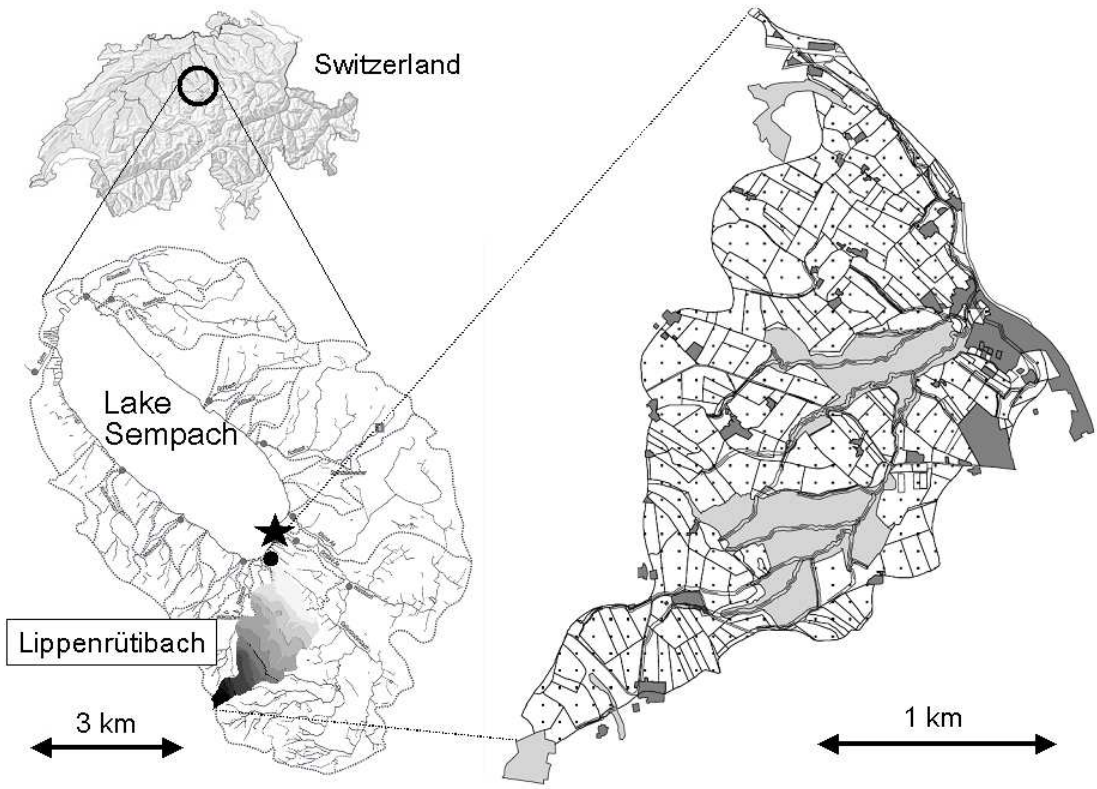

Figure 5.1: *Map of the Lippenrütibach catchment illustrating agricultural fields (white fields with black dots), forested areas (bright grey), urban areas (dark grey) and the brook (double-lined). The monitoring station is indicated by the black point and the rainfall gauge by the black star.*

42%, poorly drained soils 40%, forest 15% and urban areas 3% of the catchment area. Well drained soils represent eutric and dystric Cambisols and eutric Regosols while poorly drained soils include water-logged eutric Gleysols and gleyic Cambisols.

About 30 to 40% of all fields are tile drained enabling fast subsurface P-transport from fields to the brook. Average annual rainfall is 1100 mm y^{-1} and discharge about 600 mm y^{-1}. More than 60% of the annual rain falls during the growth season, which is the main period of manure application and of highest P-loss. The livestock density is high with 2.4 dairy-cow equivalents ha^{-1}. Although most farmers have balanced P-budgets since 2001 the topsoils are still P-overloaded (*Keller and van der Zee*, 2004). The average P-saturation index (*Van der Zee and van Riemsdijk*, 1988) was high with 48% for the top 5 cm and 36% for 5 to 20 cm soil depth. Average P-application rates declined from 40 in 1998 to 35 kg P ha^{-1} y^{-1} in 2002 and the annual DRP-loss varied from 0.3 to 1.3 kg ha^{-1} y^{-1} for the years 1998 to 2002 due to different weather conditions. This was in most years above acceptable

losses (0.5 to 0.9 kg DRP ha^{-1} y^{-1}, *Gächter and Stadelmann* (1993)).

This catchment was selected to test the efficiency of ecological measures to reduce diffuse P-loss (*Forni et al.* (1999) and *Prasuhn and Lazzarotto* (in press)). A first set of ecological measures was introduced in 1993 by the Swiss government. Stricter measures such as a reduction of P-inputs and livestock density, etc. were started in the Lake Sempach region in 1999. Within this scope, a campaign to collect spatially and temporally detailed manure-, soil-P, discharge- and DRP-data had been running in this catchment since 1998. This led to an extensive data-base for a catchment that, in terms of P-data, is unique in Switzerland.

5.3.2 Data sampling

Water quality sampling

For every hour since January 1998, discharge was measured and automated water samples of DRP (*Murphy and Riley*, 1962) and nitrate were taken and analyzed with a flow injection analyser at the catchment outlet (see Chapter 2). Hourly rainfall was measured with a tipping bucket gauge about 500 m outside the catchment.

Manure-P data

Manure data had been collected since 1998 from 30 farmers for each of the 250 fields. They include for each application the time of application, the applied amount, the type of manure (pig or cattle) and the ratio of manure being diluted by water. For each farm, an average annual P-concentration in manure was calculated based on detailed farm-specific nutrient-balances (Appendix A.1.1). Hence, for each application on each field the amount of applied manure was multiplied with this P-concentration to determine the applied P-amounts in kg ha^{-1}. To quantify DRP-concentrations in surface runoff caused by IPL we adopted data from *Braun et al.* (1993) and *von Albertini et al.* (1993) who studied IPL from two grassland sites in the same catchment for various application rates. One site was a permeable soil with permanent pasture and a high soil-P status (27 to 55 mg kg^{-1} CO_2-water extractable P) and the other site was a poorly drained ley with a low soil-P status (4 to 6 mg kg^{-1} CO_2-water extractable P). Both sites received 10 to 11 slurry applications between 108 to 130 kg P ha^{-1} over two years.

Soil-P data

In April 2000 all fields were sampled for the top 10 cm depth and analyzed for the CO_2-saturated water extractable P (*FAL and FAW and RAC*, 1995) as a measure for the soil-P status (SPS). These values were transformed into water-soluble P (WSP)-equivalents for the top 4 cm depth to be comparable with WSP-measurements from other studies (Appendix A.1.2). We empirically determined DRP in surface runoff, mobilized from the P stored in soils, as a function of the WSP-values. Since such a function was lacking for the soils in the Lippenrütibach we adopted data from runoff experiments on grassland plots in the region of Lake Greifen. This region is about 40 km east of our study area with similar climatic conditions, soil-types and soil-P status: Dystric Cambisols with acid topsoils and a strong history of manure application leading to 1300 mg total P kg^{-1} and to mean WSP-levels of 9 mg P kg^{-1} $soil^{-1}$. *Vollmer et al.* (in prep.) and *Schärer et al.* (2005) conducted sprinkling experiments on 15 plots, measured the DRP-concentration (<0.45μm) in surface runoff and analyzed the soils (0 to 4 cm depth) for WSP and the CO_2-saturated water extractable P.

5.3.3 Model description

Main concept

The model accounts for the dominant hydrological patterns observed at the catchment outlet and for those patterns found from runoff experiments. High temporal resolution monitoring studies of P-export at the catchment outlet showed rises in the DRP-concentration with rising discharge (*Stamm et al.* (1998); *Pacini and Gächter* (1999); *Lazzarotto et al.* (2005)). This indicated fast P-transport when high DRP-concentrations were caused by a fast flow component which accounts for surface runoff and preferential flow while the low DRP-concentrations were limited to baseflow. The model considered this typical pattern for fast P-transport although it was replaced by a mechanistically poorly understood new pattern since 2000 (Chapter 2). In Chapter 3 was shown that the areal fractions of well and poorly drained soils in catchments strongly influenced the catchment response: Smoother hydrographs exhibited in catchments with high areal fractions of well drained soils while hydrographs became peakier with increasing areal fractions of poorly drained soils in catchments. Hence, we assigned a slow and a fast flow component to well and poorly drained hydrological response units (HRU). Since the new water produced during runoff events is relevant for P-loss the model assigned the high DRP-concentrations, $DRP_{high}(t)$, to the new water component (Fig. 5.2 a). Here, $DRP_{high}(t)$ include both DRP_{Soil} (the contri-

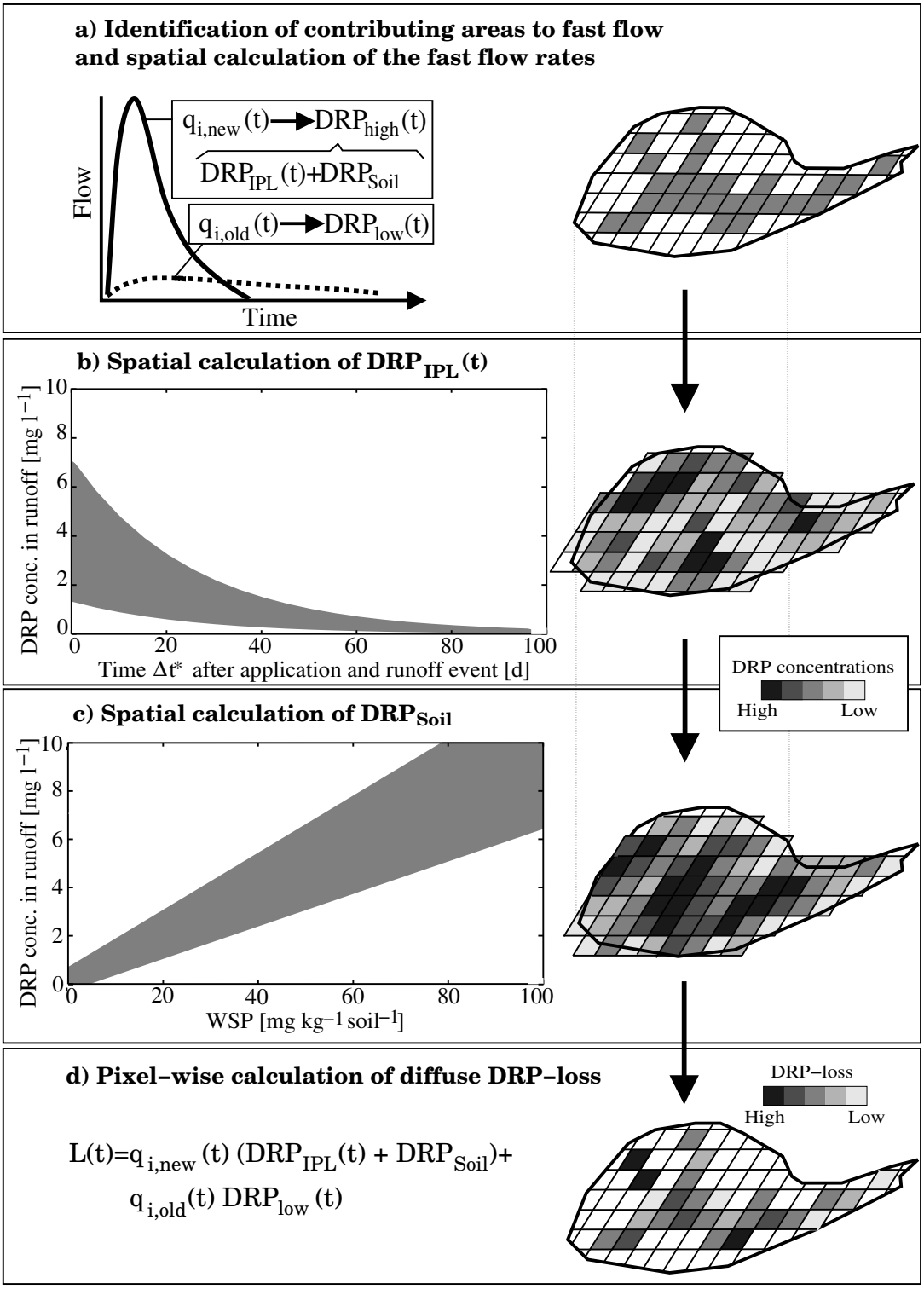

Figure 5.2: *Concept to calculate diffuse DRP-loss in the Lippenrütibach: (a) Quantifying the new and old water flow components for contributing areas for well and poorly drained hydrological response units i. (b) Calculating the DRP-concentrations in surface runoff, $DRP_{\mathrm{IPL}}(t)$, from IPL based on the duration Δt^* between application and runoff event. (c) Function between WSP and the DRP-concentrations in surface runoff, DRP_{Soil}, mobilized from topsoils. (d) Calculation of diffuse DRP-loss for each soil-pixel.*

bution of the P mobilized from soils) and $\mathrm{DRP_{IPL}(t)}$, the contribution from IPL. The low DRP-concentrations $\mathrm{DRP_{low}(t)}$ represent the P slowly percolating through the soil and are related to the old water component. The two terms new and old water will be explained below.

Rainfall-runoff model

We used a parsimonious dynamic semi-lumped rainfall-runoff model (Chapter 3) to calculate time-series of the slow and fast flow components for well and poorly drained soils. Based on a time-variable threshold of the topographic index (*Kirkby*, 1975) the model spatially distinguished contributing areas to fast flow (25m · 25m pixels) which are potential hydrological risk areas for P-loss (Chapter 4). We presumed that those areas with the same soil type and topographic index have the same flow rate. Studies showed that old water commonly dominates the stormflow hydrographs (*Burns et al.* (2001) and *Kirchner* (2003)) but varies with the dominant flow pathways and antecedent moisture in catchments (*Burns and McDonnell*, 1990). To determine the fraction η of new water in the fast flow components we estimated the fraction of the new water in total discharge based on the nitrate concentrations being diluted during stormflows relative to the nitrate levels observed during baseflow. One assumption was that the new water component $q_{\mathrm{i,new}}(\mathrm{t})$ was a constant fraction η of the fast flow component $q_{\mathrm{i,fast}}(\mathrm{t})$. The old water $q_{\mathrm{i,old}}(\mathrm{t})$ represents the slow flow component $q_{\mathrm{i,slow}}(\mathrm{t})$ and that part of the fast flow component that is not new water

$$q_{\mathrm{i,new}}(t) = \eta \cdot q_{\mathrm{i,fast}}(t) \tag{5.1}$$

$$q_{\mathrm{i,old}}(t) = \Big[(1-\eta) \cdot q_{\mathrm{i,fast}}(t)\Big] + q_{\mathrm{i,slow}}(t) \tag{5.2}$$

where the index i denotes well and poorly drained HRU. The old water component $q_{\mathrm{i,old}}(\mathrm{t})$ accounts for baseflow associated with low DRP-concentrations from leaching. The new water component $q_{\mathrm{i,new}}(\mathrm{t})$ summarizes that part of new water contained in fast flow by preferential flow and surface runoff.

P-model and diffuse P-loss

The spatial distribution of the high DRP-concentrations $\mathrm{DRP_{high}(t)}$ on the contributing areas to fast flow was calculated for each soil pixel in hourly time steps. Since $\mathrm{DRP_{high}(t)}$

is the sum of $DRP_{IPL}(t)$ and DRP_{Soil} we quantified both concentrations based on field data from runoff experiments. Note that the estimation of the parameters and their ranges to describe the P-mobilization from soils and from manure is explained in the same section where the modeling results are presented (Section 5.4.2).

Estimation of $DRP_{IPL}(t)$ The time-variant DRP-concentrations $DRP_{IPL}(t)$ were quantified with data of *Braun et al.* (1993) and *von Albertini et al.* (1993). Here, $DRP_{IPL}(t)$ was treated as an exponential function of the duration Δt^*=t-t_a between the time of manure application t_a and the time of runoff onset t (Fig. 5.2 b) and will be called the IPL-function. In the model the time t of runoff onset was replaced by the time when the soil-pixel was contributing to fast flow. When manure was applied $DRP_{IPL}(t)$ sharply increased and the duration Δt^* became zero. With increasing duration Δt^* $DRP_{IPL}(t)$ declined at variable rates h. We assumed that h was the same for well and poorly drained soils.

$$DRP_{IPL}(t) = DRP^0_{IPL} \cdot e^{-(t-t_a)\cdot h} \tag{5.3}$$

After a recent application, the newly estimated DRP^0_{IPL} was added to the previously calculated DRP_{IPL}(t-1) to yield the actual value of $DRP_{IPL}(t)$ at time t. The initial DRP-concentrations DRP^0_{IPL} for each application were derived as a function of the calculated P-amounts contained in the applied manure.

Estimation of DRP_{Soil} The DRP-concentrations in runoff, DRP_{Soil}, due to the mobilization of P stored in topsoils, were treated as a function of the WSP-levels of each field (Fig. 5.2 c). We assumed time-invariant WSP-levels independent from P-accumulation by manure, animal excretions or mineralization and P-removal (plant uptake or P-loss by runoff). This means that the estimated DRP_{Soil} was constant for the same soil pixels over the modeled period.

Diffuse losses For each well and poorly drained HRU the diffuse DRP-loss $L_{i,new}(t)$ on contributing areas was determined as the product of new water and $DRP_{high}(t)$. For each time t the load $L_{i,new}(t)$ was summed up for each soil-pixel in the catchment assuming that the generated DRP-loss was immediatelly lost by fast transport mechanisms irrespective of the location of a pixel

$$L_{\mathrm{i,new}}(t) = \begin{cases} 0 & if \quad q_{\mathrm{i,new}}(t) = 0 \\ \left[DRP_{\mathrm{i,IPL}}(t) + DRP_{\mathrm{i,Soil}}\right] q_{\mathrm{i,new}}(t) & if \quad q_{\mathrm{i,new}}(t) > 0 \end{cases} \tag{5.4}$$

The diffuse DRP-loss by old water $\mathrm{L_{i,old}(t)}$ was related to the old water component and the low DRP-concentrations (0.05 mg $\mathrm{l^{-1}}$) observed during baseflow.

5.3.4 Calibration and uncertainty propagation

All parameters for the rainfall-runoff model had been simultaneously calibrated by jointly comparing the individual hydrological responses of four catchments in advance (Chapter 3) by accepting parameter sets that produced satisfying discharge simulations. In contrast, all P-relevant parameters were derived from field data without additional fitting of parameters (section 5.4.2). We ran 500 Monte-Carlo simulations for the year 1999 and used the calculated time-series of the hydrological variables and randomly varied η and h. The coincidence between total predicted L(t) and observed DRP-loss $\mathrm{L_{obs}(t)}$ was determined by the efficiency measure $\mathrm{E_m}$ (*Nash and Sutcliffe*, 1970). Here, $\overline{L}$ is the mean of the observed load for the period t=$\{t_0, \cdots, t_\mathrm{e}\}$ where $\mathrm{t_0}$ is the start, $\mathrm{t_e}$ the end of the period and m the number of the model run.

$$E_\mathrm{m} = 1 - \frac{\sum_{\mathrm{t=t_0}}^{\mathrm{t_e}} \left(L_\mathrm{obs}(t) - L(t)\right)^2}{\sum_{\mathrm{t=t_0}}^{\mathrm{t_e}} \left(L_\mathrm{obs}(t) - \overline{L}\right)^2} \tag{5.5}$$

The uncertainty of the predicted P-loss in time and space arose from the uncertainty of the modeled hydrological variables and that uncertainty associated with the P-data and the description how P was mobilized. This uncertainty was propagated further to quantify DRP-loss for each soil-pixel.

5.4 Results

5.4.1 Empirical data

We transformed the original values of the CO_2-saturated water extractable P from the top 10 cm of all fields in the Lippenrütibach into WSP-values for the top 4 cm. These WSP-values covered a wide range from 3 to 94 mg $\mathrm{kg^{-1}}$ soil with the 25%-quantiles at 11, the median at 16 and the 75%-quantiles at 24 mg $\mathrm{kg^{-1}}$ soil. This indicated an even higher

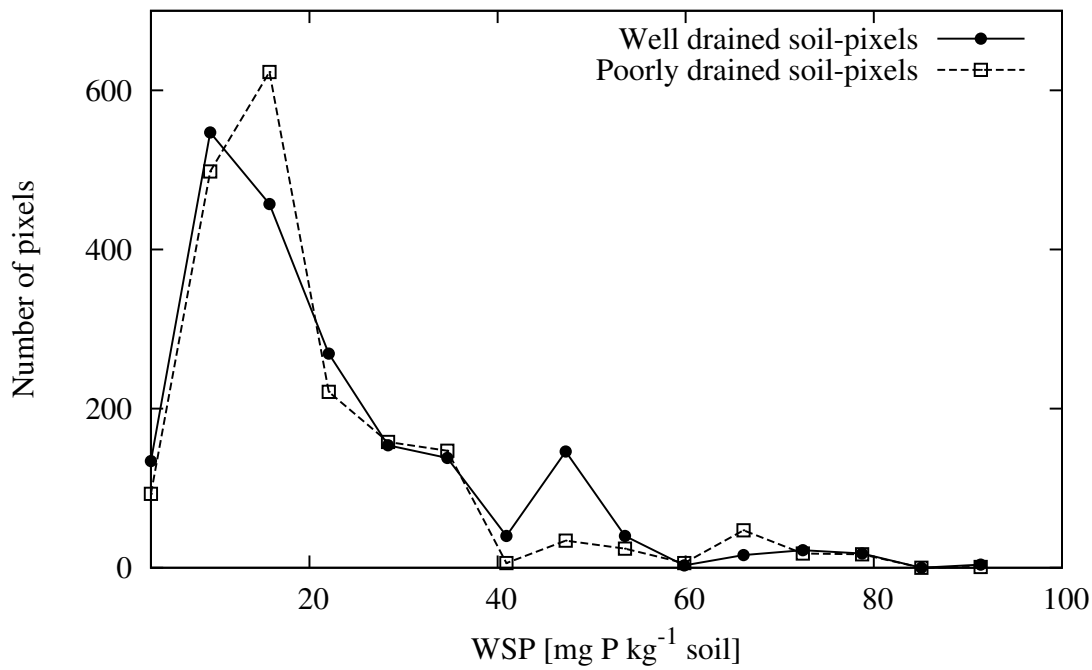

Figure 5.3: *Frequency distribution of the WSP-values (0 to 4 cm soil depth) in the Lippenrütibach based on the originally measured CO_2-water extractable P (0 to 10 cm) for well and poorly drained soil-pixels in the Lippenrütibach.*

soil-P status in the Lippenrütibach compared with the median (9 mg WSP kg^{-1} soil) in the Lake Greifen region. When separating the WSP-values in the Lippenrütibach into well and poorly drained soil-pixels the frequency distributions were similar for both soil-types (Fig. 5.3): The medians of the WSP-values were about 16 mg kg^{-1} soil for both soil types but the 75%-quantiles were higher for well (27 mg kg^{-1} soil) than for poorly drained soils (22 mg kg^{-1} soil). This overall similarity suggests that farmers did not well consider the soil-P status when applying manure. Interestingly, about 5 times more well drained soil-pixels had high WSP-values from 40 to 50 mg kg^{-1} soil than poorly drained soil-pixels and could be the hot spots for P-loss from soils.

For those fields receiving manure in 1999 we compared the WSP-values with the annually applied P-amounts in kg ha^{-1}. Soils being over- and strongly oversupplied with P received markedly more manure (40 to 42 kg P ha^{-1} y^{-1} as the median) than tolerable. Since the annual P-amounts for such soils should be below the norm P-fertilization these exaggerated P-amounts substantially contribute to the P-accumulation of P-oversupplied soils. Figure 5.4 shows the cumulative rainfall and discharge and, separately for both soil-types, the cumulated applied P-amounts from March to November 1999. From March to

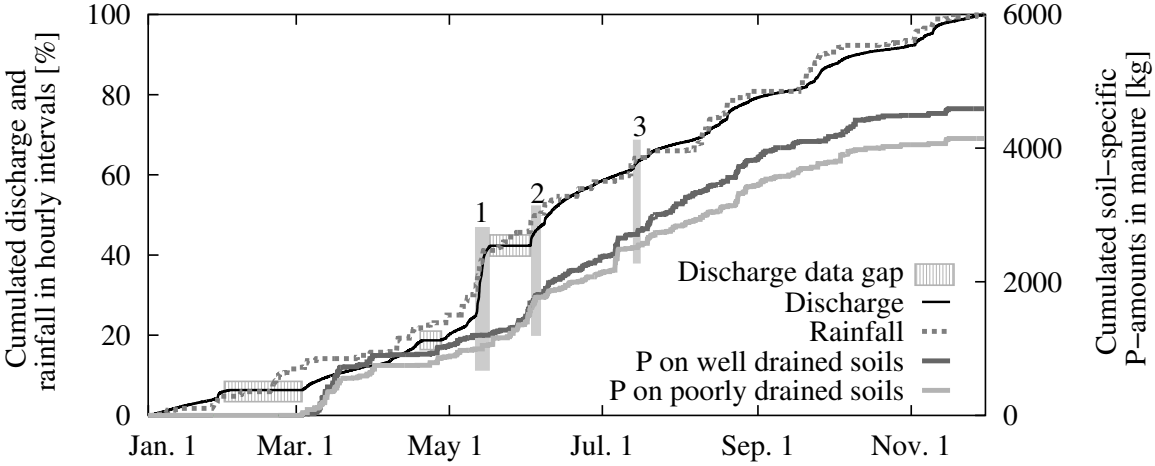

Figure 5.4: *Cumulated rainfall (dotted line), discharge (thin black line) and cumulated P-amounts in manure applied on well (dark grey line) and poorly (light grey line) drained soils from March until November 1999. The grey shaded boxes indicate data gaps in discharge monitoring and grey filled boxes represent periods of interference between stormflows and manure applications.*

July, the applied P-amounts on well and poorly drained sites were comparable while the well drained soils received more P towards the end of the year. This demonstrates that farmers applied manure irrespective of the soil-types. The applied P-amounts averaged 40 kg P ha^{-1} y^{-1} and correspond to volumes of 25 m^3 or 11 kg P ha^{-1} per application. Most manure was spread during baseflow but often shortly before and sometimes even during stormflows (label 1 to 3, grey boxes). This interference was evident for stormflow 2 in June with >600 kg P four days before and even >100(!) kg P applied by three farmers during this event. Manure was also spread on wet soils during the major stormflow 1 in May by a few farmers and during the small runoff event 3.

One may ask if such high applied P-amounts showed impacts on the DRP-loss observed at the catchmet outlet. Figure 5.5 illustrates the monthly distribution of rainfall, discharge, the volume of applied manure and the DRP-load as an average from 1998 to 2002. We see that the highest rainfall coincided with the main application period. However, the DRP-loads (bottom figure) were low until April, then rose in May, peaked in June and remained high until September. The volume of applied manure (above), however, showed a different temporal evolution: It peaked in March with >3000 m^3 when farmers depleted the manure tanks, then remained low in April while much manure was spread from May until August (2500 to 3000 m^3) and correlated with the DRP-loss until September. One explanation for the small DRP-load in March despite high manure volume was low discharge and rainfall intensities combined with the high P-demand of plants at the start of the growth period.

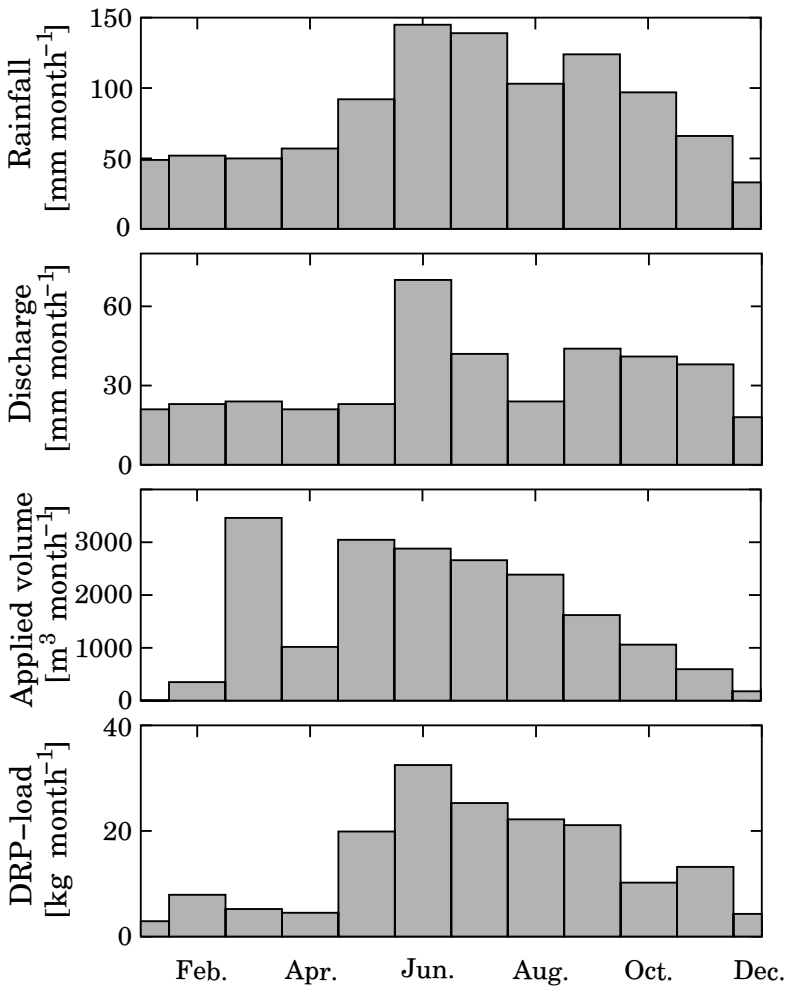

Figure 5.5: *Monthly distributions of rainfall, discharge, volume of applied manure and DRP-load (from top to bottom) in the Lippenrütibach catchment, averaged from 1998 to 2002.*

Possibly, there were hardly contributing areas to fast flow in March while more of those contributing areas were present in May due to higher rainfall intensities. However, the average DRP-loss in May was strongly influenced by a flood in May 1999.

5.4.2 Parameter estimates for the P-model

Estimation of new and old water

We estimated the degree η of nitrate being diluted during runoff events relative to the concentrations during baseflow (data not shown). In average, η varied from 15 to 30%, suggesting that 15 to 30% of the total runoff during stormflow was new water. Hence, by randomly varying $0.15 < \eta < 0.3$ for each model run the fast flow components for each soil-type were split into a new water component while 70 to 85% of the fast flow components was attributed to old water.

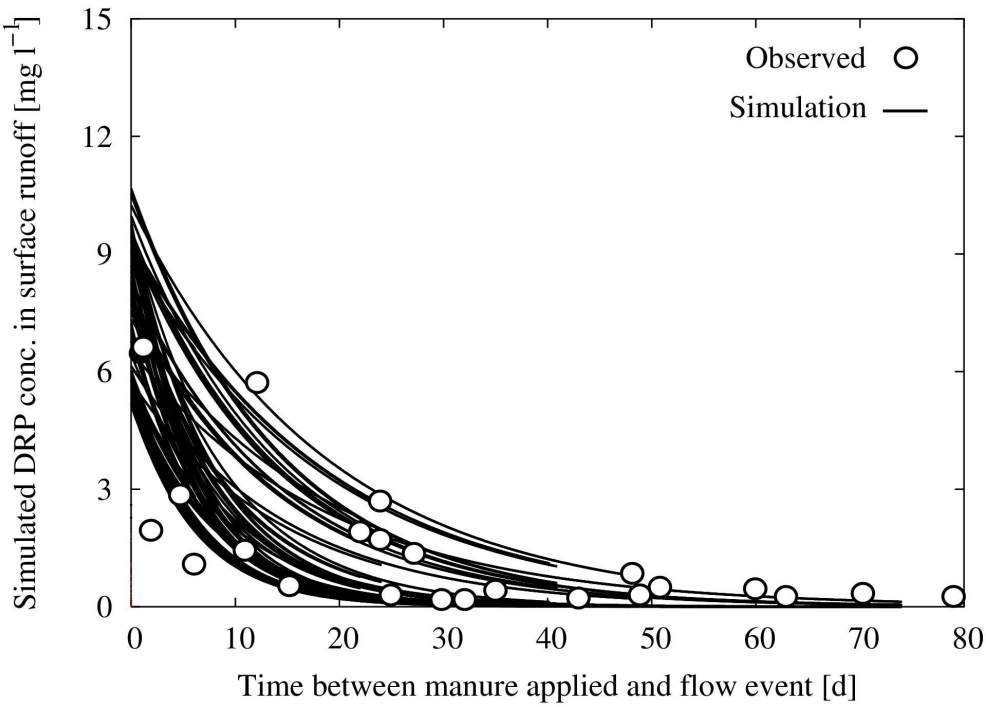

Figure 5.6: *Calibrated IPL-function using 10 Monte-Carlo simulations. Large points are oberved data-pairs and the simulated declines of $DRP_{\mathrm{IPL}}(t)$ are given by lines.*

Estimating $\mathbf{DRP_{IPL}(t)}$

The IPL-function was calibrated by adjusting the decline rate h to observed data for various initial DRP-concentrations $\mathrm{DRP}^0_{\mathrm{IPL}}$ in surface runoff (Fig. 5.6). We randomly varied h within a defined range and calculated the time-series for $\mathrm{DRP_{IPL}(t)}$ based on the application schedules of two soil-pixels for the year 1999. Two soil-pixels were selected to ensure that the variation of distinct $\mathrm{DRP}^0_{\mathrm{IPL}}$ for distinct applications was accounted for. This was carried out by 10 simulation runs until the calibrated IPL-function (lines) approximated the observations (points) for $0.003 < h < 0.011$ h^{-1}. The most sensitive period was until 30 to 40 days after the last application when $\mathrm{DRP_{IPL}(t)}$ was still high and strongly varied due to sorption, P-uptake rates and different $\mathrm{DRP}^0_{\mathrm{IPL}}$. Interruptions in the temporal decline of $\mathrm{DRP_{IPL}(t)}$ occurred when soil-pixels received fresh manure.

Since the initial DRP-concentrations $\mathrm{DRP}^0_{\mathrm{IPL}}$ in surface runoff influenced the temporal evolution of $\mathrm{DRP_{IPL}(t)}$ we set two scenarios (Fig. 5.7): (A) assumed that $\mathrm{DRP}^0_{\mathrm{IPL}}$ was independent from the P-amount that was applied and (B) assumed a linear correlation between $\mathrm{DRP}^0_{\mathrm{IPL}}$ and the P-amounts of the manure applications. Uniform distributions for $5 < \mathrm{DRP}^0_{\mathrm{IPL}} < 10$ mg l^{-1} were presumed for scenario A while $\mathrm{DRP}^0_{\mathrm{IPL}}$ varied up to 20 mg l^{-1} for scenario B. Since the P-amounts per application were most frequent at 11 kg P ha^{-1}

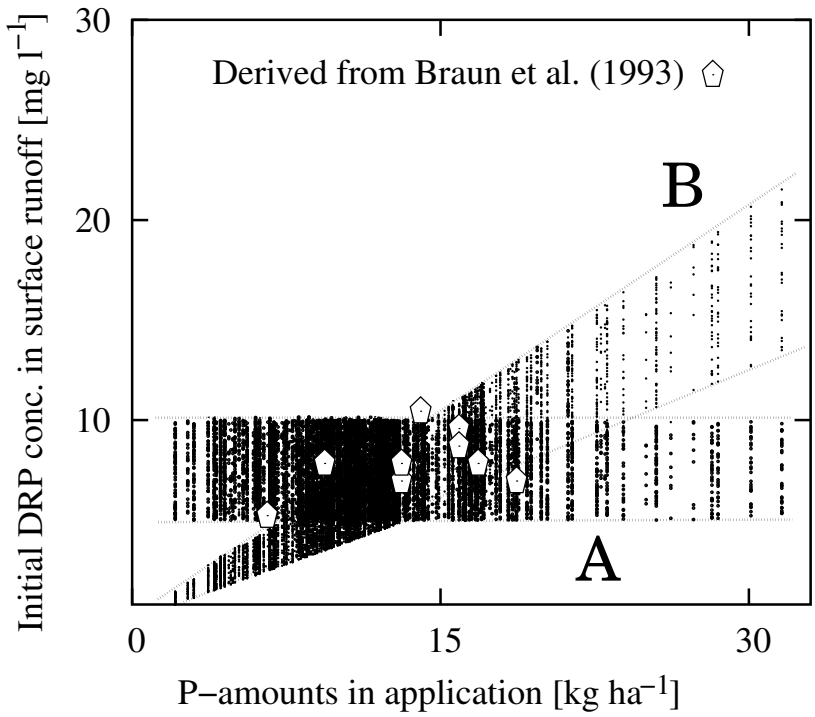

Figure 5.7: *Calibrated ranges of the initial DRP-concentrations DRP^0_{IPL} in fast flow for each soil-pixel (small dots) as a function of the P-amounts per application rate for two scenarios: (A) no correlation, (B) linear function between DRP^0_{IPL} and the the P-amounts per application. The variation of DRP^0_{IPL} for scenario B corresponds to the ranges of the 95%-confidence intervals of the linear regression. The large symbols are observed data.*

most of the calculated DRP^0_{IPL} varied from 4 to 6 mg l^{-1} for scenario B. Hence, smaller DRP^0_{IPL} in surface runoff were estimated in average for scenario B than for A.

Estimating DRP_{Soil}

Since the WSP-values in the Lippenrütibach strongly exceeded those in the Lake Greifen region and the ranges of DRP_{Soil} were uncertain at elevated WSP-levels we applied three different relationships (scenarios) between DRP_{Soil} and WSP-levels: (1) a linear function with the parameters being obtained from *Vollmer et al.* (in prep.), (2) a logarithmic function with smaller maximum DRP_{Soil} and (3) a scenario where DRP_{Soil} was independent from WSP. Parameters for scenario 2 were not required since we apriori defined minimum and maximum DRP_{Soil}-values for 20 distinct WSP-values, so the DRP_{Soil}-values were linearly interpolated between those 20 WSP-values. The minimum and maximum values for DRP_{Soil} were obtained from observed data from the plots in the Lake Greifen region.

Figure 5.8 illustrates the functions between WSP and DRP_{Soil} in runoff, including their

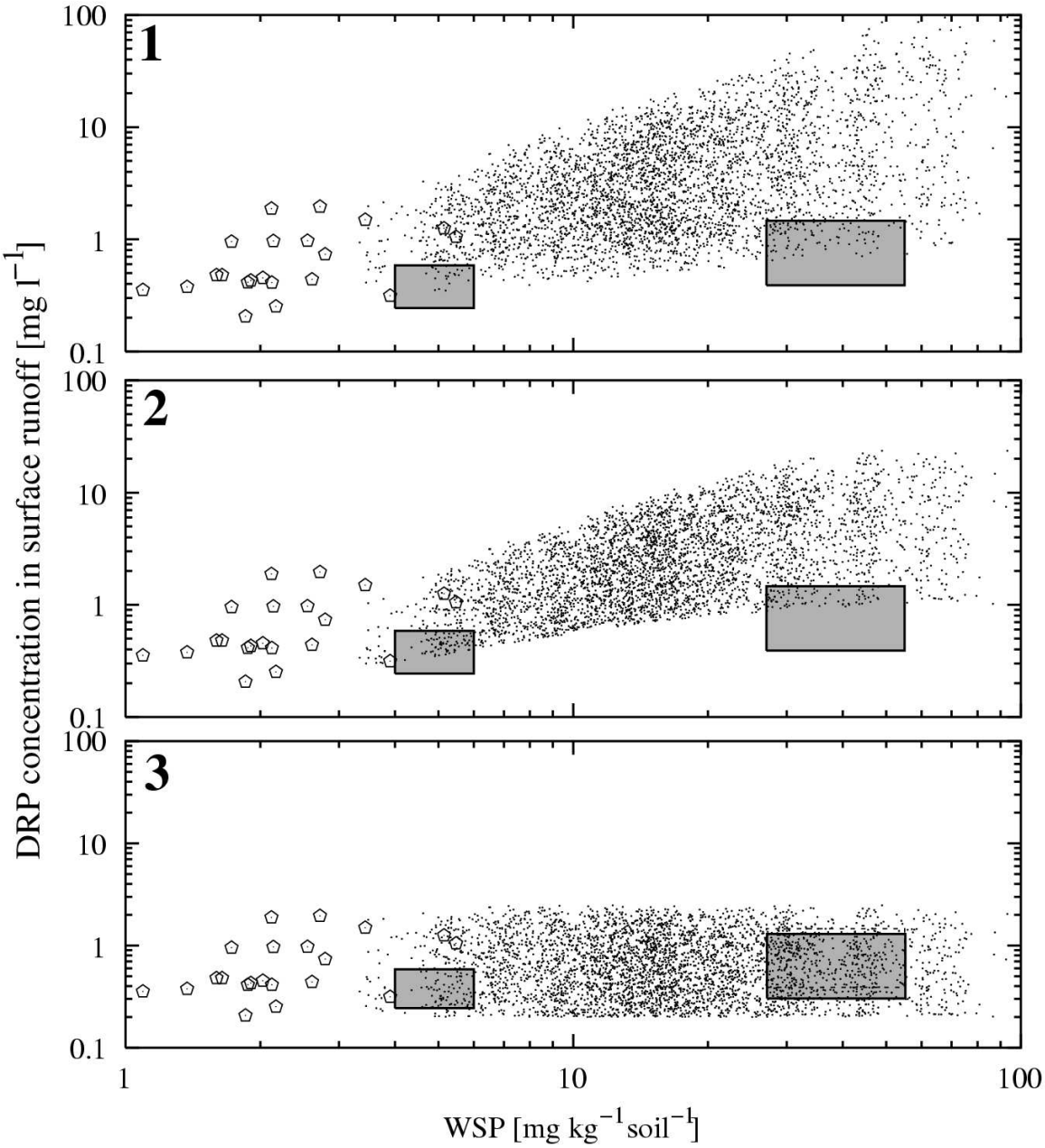

Figure 5.8: *Scenarios for the function between WSP in the soil and DRP_{Soil}-concentrations in surface runoff. Large points are observed data from the plots in the Lake Greifen region. Grey boxes indicate the observed ranges from manured runoff experiments in the Lippenrütibach for $\Delta t^* > 50$ days after the last application. Small dots represent the simulated ranges of DRP_{Soil} for each soil-pixel in the Lippenrütibach based on a linear (scenario 1), a logarithmic (scenario 2) and an uncorrelated (scenario 3) function between WSP and DRP_{Soil}.*

ranges, for scenario 1 (top), 2 (middle) and 3 (bottom) as log-log diagrams. The large points denote the observed WSP-DRP_{Soil}-pairs from the Lake Greifen region that scatter without exhibiting a clear trend. The observed range for DRP_{Soil} was between 0.2 and 2 mg l^{-1}. As a control we inserted observed DRP_{Soil}-WSP-pairs collected by *Braun et al.* (1993) which were taken after a long duration >50 d between applied manure and runoff (grey boxes) when the influence of the last application on DRP_{Soil} was neglectable. These DRP_{Soil}-ranges were comparable with those from the Lake Greifen region but WSP was far higher. The small dots represent the calculated DRP_{Soil} of each soil-pixel for 500 simulation runs. For all scenarios for WSP-levels<10 mg l^{-1}, DRP_{Soil} were in comparable ranges as the observed DRP_{Soil} from the Lake Greifen region. Above this WSP-value, however, the calculated DRP_{Soil} markedly varied for different scenarios, especially for the highest WSP-values: For scenario 1, DRP_{Soil} were sometimes >30 mg l^{-1} while the maximum DRP_{Soil} converged to 25 mg l^{-1} in scenario 2 and never exceeded 2 mg l^{-1} for scenario 3.

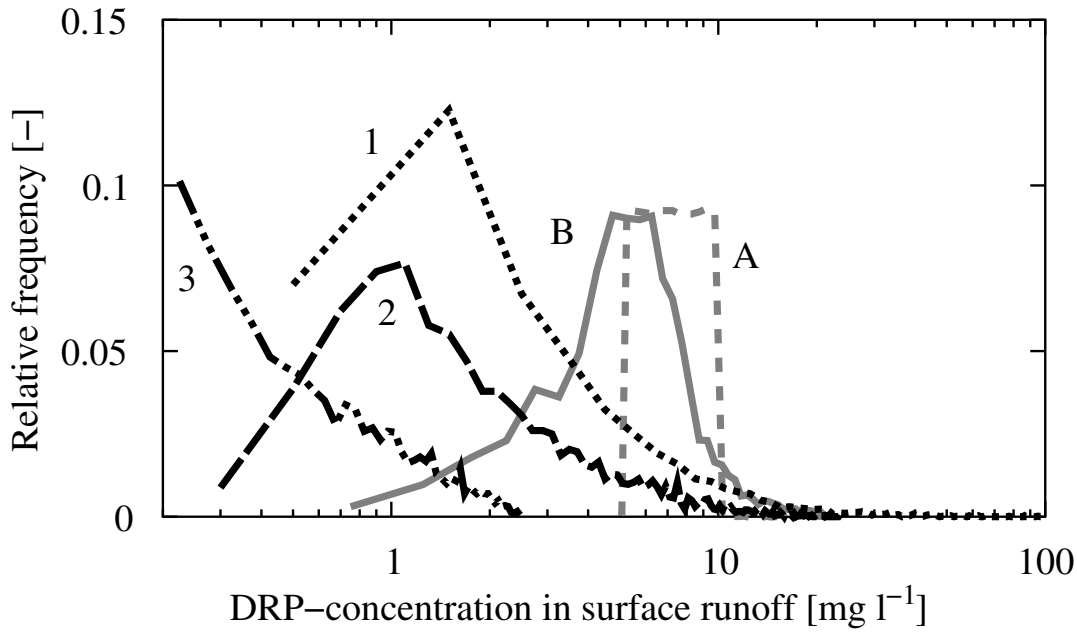

Figure 5.9: *Frequency distributions of DRP_{Soil} (scenarios 1 to 3) and of the initial DRP-concentrations DRP^0_{IPL} for scenario A and B.*

Figure 5.9 compiles the frequency distributions of the calculated DRP-concentrations in runoff for all scenarios. Although the medians of DRP^0_{IPL} for scenario A (7.6 mg l^{-1}) and B (5.8 mg l^{-1}) were clearly higher than those of DRP_{Soil} for scenario 1 to 3 (2.8 to 0.6 mg l^{-1}) it must be noted that DRP^0_{IPL} were initial concentrations which declined with time while DRP_{Soil} were assumed to be constant. After a certain duration Δt_p the influence of IPL will be overriden as DRP_{Soil} will dominate (section 5.4.3).

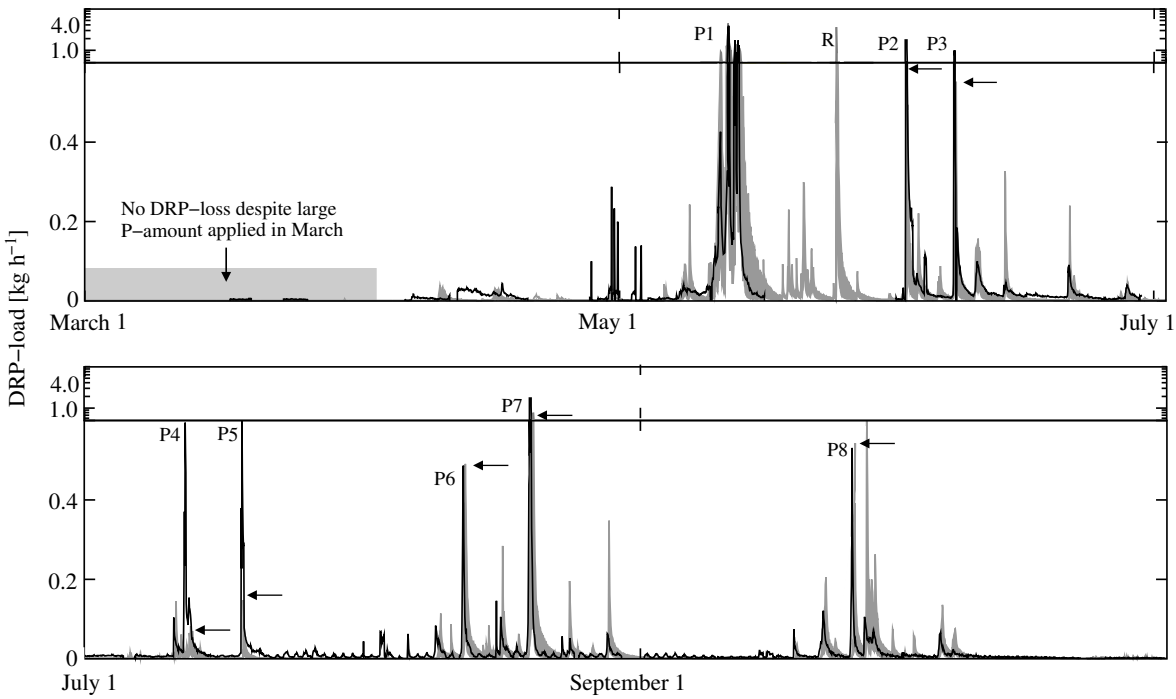

Figure 5.10: *Simulated ranges (grey bands) and observed (black line) DRP-loss during the growth period in 1999. Arrows indicate the peak of the prediction bands for the DRP-loads. The prediction bands are based on the combined scenario 2-A (see text).*

5.4.3 Simulation results

Model validation

To account for the uncertainty in the predictions of $DRP_{IPL}(t)$ and DRP_{Soil} we combined each scenario A and B (Fig. 5.7) with each scenario 1 to 3 (Fig. 5.8). For each of these six combined scenarios 1-A, 2-A, 3-A, 1-B, 2-B and 3-B we applied 500 Monte-Carlo runs to simulate the DRP-loss in hourly time steps for the period March to October 1999. For example, 1-A means that scenario 1 with the linear function between WSP and DRP_{Soil} and scenario A ($DRP_{IPL}(t)$ independent from the P-amounts in manure) were combined.

Figure 5.10 illustrates for scenario 2-A the simulated DRP-loads L(t) as prediction bands excluding the minimum and maximum 10% quantiles of the cumulative distribution of all hourly simulated loads. Although the model predictions for DRP were purely based on the modeled flow components and the P-parameters derived from plot/field-scale observations the model well reproduced the dynamic of the DRP-loss for the August period (event P6) and for the first peak in September (P8). The very large peaks for the flood in May (P1) and for the June events (P2 and P3) were markedly underestimated by scenario 2-A, especially for the July period (P4 and P5). This general underestimation led to markedly smaller

Table 5.1: *Comparison between the total observed and simulated DRP-loss and the contributions of DRP-loss from soil and from IPL for all combined scenarios for the period March until November 1999 in the Lippenrütibach.*

Scenario	Measured DRP-loss [kg]	Total DRP-loss [kg]	Soil-P loss [kg]	IPL [kg]
1-A	135	117	110	7
2-A	135	80	73	7
3-A	135	30	23	7
1-B	135	115	110	5
2-B	135	78	73	5
3-B	135	28	23	5

calculated loads (80 kg) compared with the observed loads of 135 kg for this scenario (Tab. 5.1).

Despite of that the medians of the efficiency measures for the May (E_m=0.60) and the August period (E_m=0.46) were relatively high (Tab. 5.2) while those for other periods were low (0.10<E_m<0.38). The poor model performance for some periods is related to underrated peak-loads and explained in the discussion. The simulations also indicated that a large event in May (R) produced substantial P-loss which had not been measured. The simulations also confirmed the empirical observations in Fig. 5.5 that due to the lack of contributing areas in the catchment no substantial DRP-loss emerged in in March when >2000 kg P were applied (Fig. 5.10).

Model sensitivity

We tested how sensitive the predicted DRP-loss and its contribution from manure-P and soil-P responded to changing scenarios. Since the simulation of IPL was marginally affected when using scenario A or B we only displayed in Fig. 5.11 the simulated DRP-loads for the flood in May 1999 for the scenarios 1-A (top), 2-A (middle) and 3-A (bottom).

For the combined scenario 1 (linear function) with scenario A the prediction bands closely enveloped the observations, even the huge peaks at May 13. Despite this good match (Tab. 5.2) the prediction bands strongly varied due to the wide ranges in the estimated DRP_{Soil} for soil-pixels at high WSP-levels and due to the propagation of uncertainty from

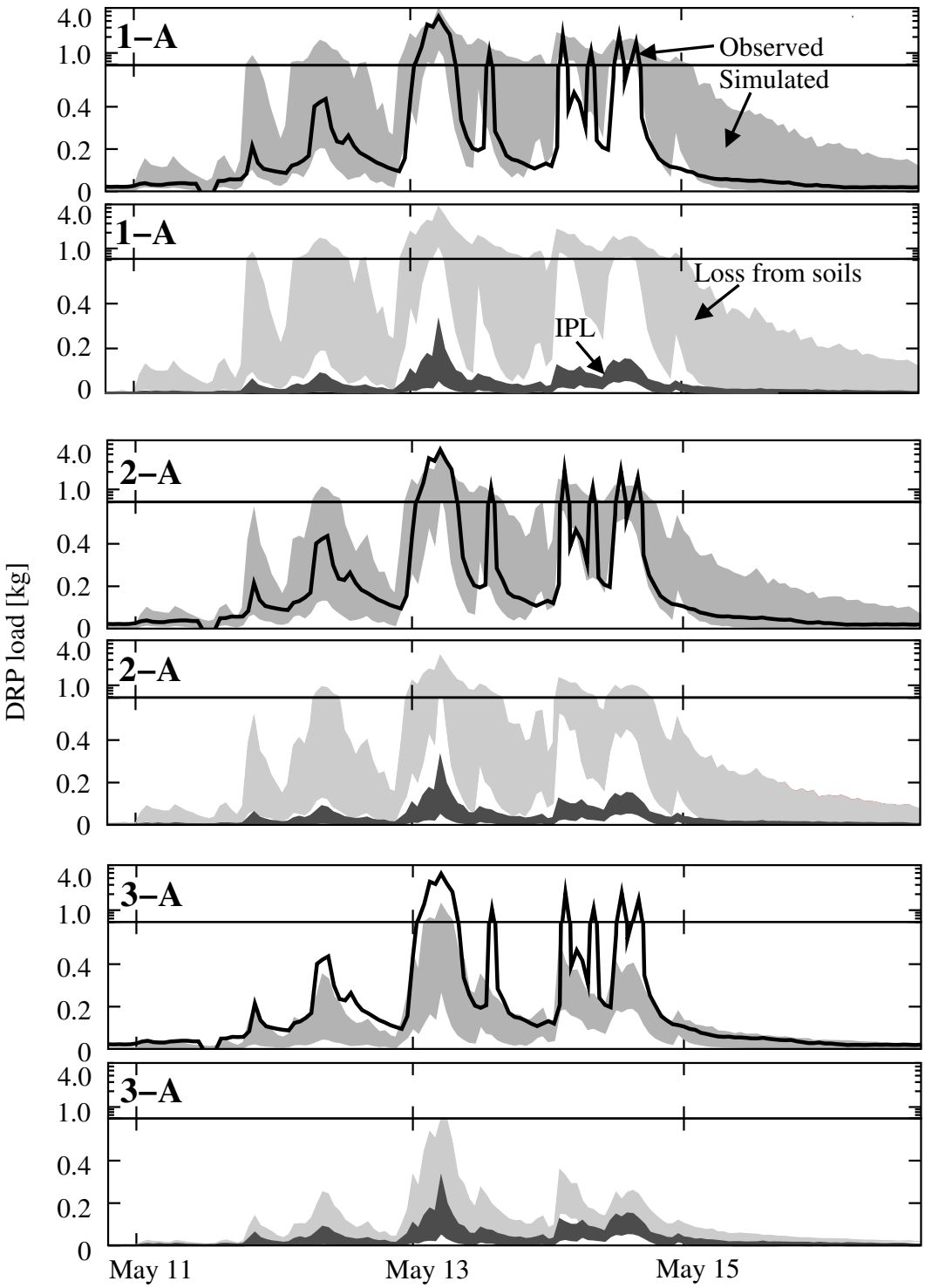

Figure 5.11: *Observed and simulated ranges of the DRP-loads (top figures) for the flood in May 1999 with three combined scenarios 1-A (top), 2-A (middle) and 3-A (bottom) which account for the mobilized P from soils. Black lines are the hourly observed DRP-loads and grey bands represent the ranges of the simulated total DRP-loads in the respective top figures. The simulated DRP-loss from soils (bright grey bands) and from IPL (dark grey bands) are in the bottom figures. All prediction bands exclude the minimum and maximum 10%-quantiles of the cumulated distribution of the hourly calculated DRP-loss. The vertical axis is first linear (0 to 0.6 kg) and the logarithmic (0.6 to 7 kg).*

Table 5.2: *Efficiency measure E_m and its 25%-, 50%- and 75%-quantiles distribution for 500 Monte-Carlo simulations for all combined scenarios based on the comparison between the total observed and simulated DRP-loss for five time periods in 1999.*

	May 5.-15			June 1.-17.			July 12.-24.			Aug. 8.-31.			Sept. 19.- Oct. 8.		
	25%	50%	75%	25%	50%	75%	25%	50%	75%	25%	50%	75%	25%	50%	75%
1-A	0.42	0.57	0.65	0.31	0.43	0.54	0.07	0.11	0.18	0.34	0.46	0.60	0.06	0.15	0.39
2-A	0.46	0.60	0.67	0.29	0.38	0.48	0.06	0.10	0.14	0.33	0.46	0.59	0.08	0.27	0.38
3-A	0.18	0.26	0.36	0.16	0.20	0.28	0.02	0.03	0.05	0.18	0.28	0.47	0.17	0.21	0.31
1-B	0.41	0.58	0.66	0.31	0.43	0.53	0.07	0.11	0.18	0.33	0.45	0.60	0.05	0.13	0.37
2-B	0.45	0.58	0.68	0.28	0.37	0.47	0.06	0.09	0.14	0.32	0.46	0.60	0.08	0.26	0.38
3-B	0.16	0.24	0.34	0.15	0.19	0.27	0.02	0.03	0.05	0.17	0.26	0.44	0.16	0.20	0.29

the calculated flow components. Clearly, the predicted DRP-loss from soils dominated over IPL, also when combining scenario 2 (logarithmic function) with scenario A. With the combined scenario 2-A the dynamic of the DRP-losses was matched too, but all high peaks were underrated. The smaller variation in the prediction bands for DRP-loss from the soil was due to the smaller variation of DRP_{Soil} in the logarithmic scenario and the resulting smaller maximum DRP_{Soil} at 25 mg l^{-1} while DRP_{Soil} could be even 3 times higher in scenario 1. This suggests that many soil-pixels contributing to fast flow had elevated WSP-levels during this flood. A poor agreement was found for the combined scenario 3-A where the observed peaks were strongly underestimated since the estimated DRP_{Soil} never exceeded 2.5 mg l^{-1}. Hence, IPL was dominated by the P-loss from soils irrespective of scenario 1 to 3.

This picture was also confirmed for other runoff events (Fig. 5.12) for scenario 2-B. The observed DRP-loads for the stormflows in June and August and for the first peak in September were mostly matched with the exception of the overrated DRP-loss at September 25 when the spatial extent of contributing areas to fast flow could be overestimated. This situation led to overrated flow production (0.6 mm h^{-1}) compared with the observed discharge (0.2 mm h^{-1}) and additional P-loss was calculated on fields that did not contribute to fast flow in reality.

In general, the estimated DRP-loss from IPL was smaller than the loss from soils but

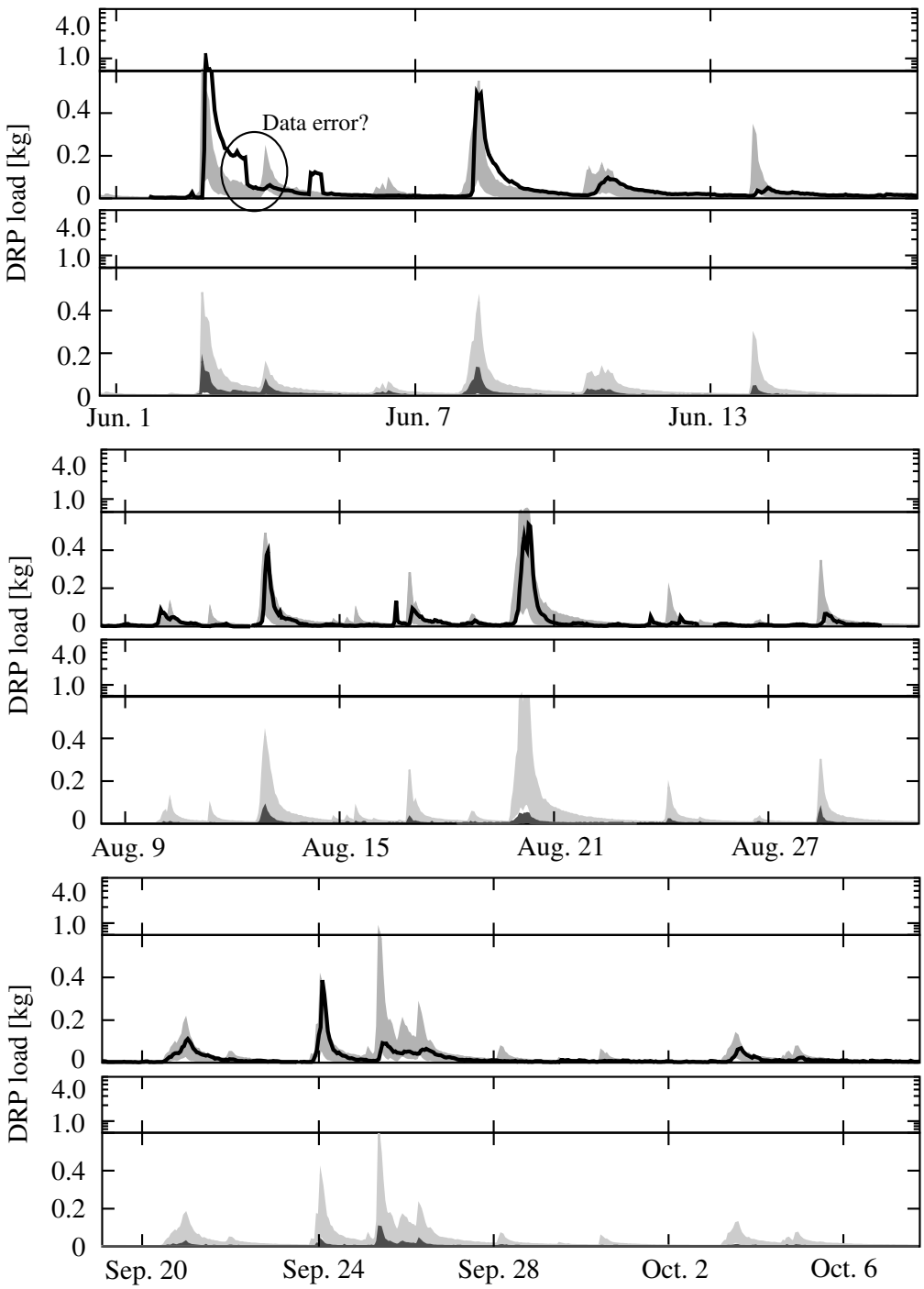

Figure 5.12: *Observed hourly DRP-loads and the simulated ranges of the total DRP-load and its contribution from IPL and from soils according to the scenario 2-B for June 1-17 (top), August 8-31 (middle) and September 19 until October 8 (bottom). The simulated DRP-loss from soils (bright grey bands) and from IPL (dark grey bands) are in the bottom figures. More explanations are given in the caption of Fig. 5.11*

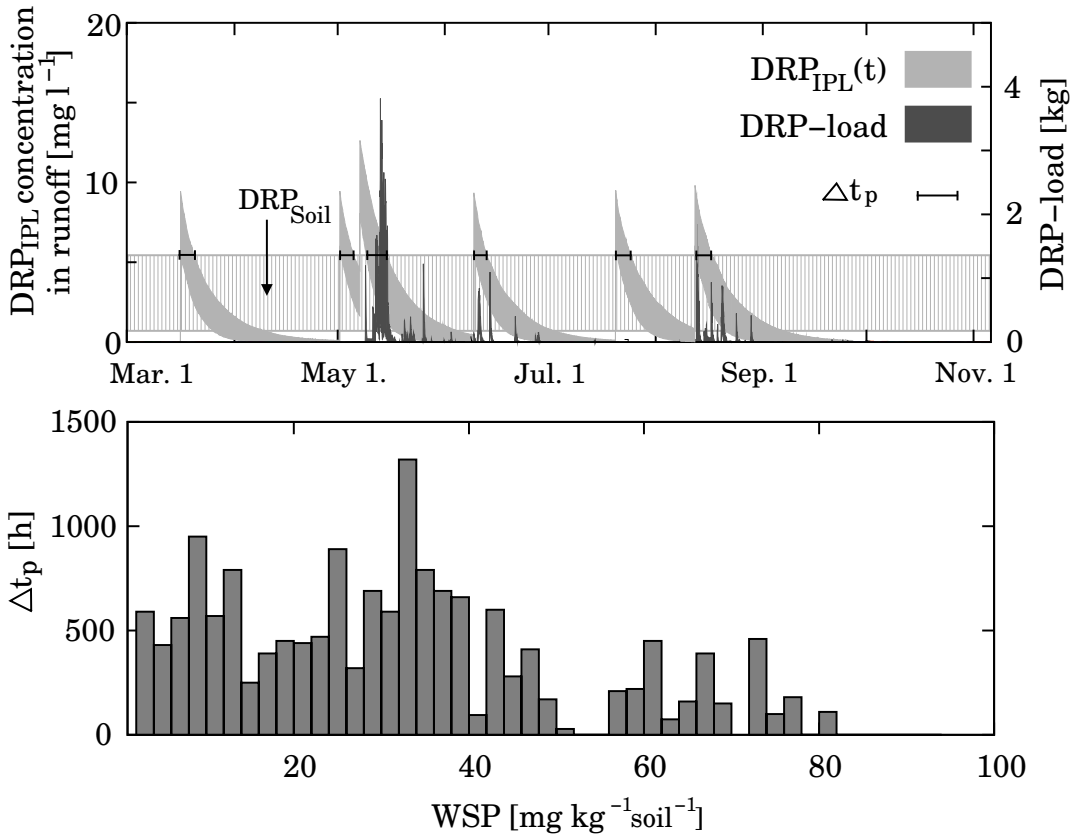

Figure 5.13: *Temporal evolution of $DRP_{\mathrm{IPL}}(t)$ potentially available for IPL (light grey bands), the produced IPL (dark grey bands) and the ranges for DRP_{Soil} (grey shaded box) for one contributing soil-pixel in the catchment (top). Distribution of the duration Δt_p for discrete classes of the soil-P status for all contributing soil-pixels in the catchment from March to November 1999 (bottom). Note that the bars represent the 90%-quantiles of each Δt_p-class.*

IPL varied from 5 to 10% of the total DRP-loss for the August and September events and made up to 30% during the June events. Over the growth period in 1999, IPL accounted for 5 to 7 kg DRP-loss only while the DRP-loss from soils dominated (23 to 110 kg DRP-loss depending on the scenarios, Tab. 5.1). Hence, the relevance of IPL in this catchment was relatively low with 5 to 23% of the total loss during the growth period in 1999.

Why dominates DRP-loss from soils over IPL?

It is helpful to compare the temporal evolution of $\mathrm{DRP_{IPL}(t)}$ as grey bands and $\mathrm{DRP_{Soil}}$ (grey shaded box) to explain why IPL was dominated by the loss from soils (Fig. 5.13 top). For the example of one soil-pixel in the catchment from March to November 1999 $\mathrm{DRP_{IPL}(t)}$ rarely exceeded $\mathrm{DRP_{Soil}}$ with the exception of a few short periods after manure application. Interestingly, no loss occured after the application in March while IPL (dark grey band)

amounted from 80 to 90 g during the flood in May since two applications two weeks prior to this flood caused high $\mathrm{DRP_{IPL}(t)}$ as this soil-pixel contributed to fast flow. The fact that $\mathrm{DRP_{Soil}}$ dominated over $\mathrm{DRP_{IPL}(t)}$ during most of the growth season showed that the duration Δt_{p}, when $\mathrm{DRP_{IPL}(t)}$ was above $\mathrm{DRP_{Soil}}$, strongly depends on the soil-P status. Therefore, we plot the duration Δt_{p} against the WSP-values of all contributing soil-pixels (Fig. 5.13 bottom). Obviously, the duration Δt_{p} declined on contributing soil-pixels with increasing WSP. This suggested that the mobilized $\mathrm{DRP_{IPL}(t)}$ dominated on soil-pixels with low WSP-levels but only during a few weeks. On soil-pixels with high WSP-values $\mathrm{DRP_{Soil}}$ was often higher than $\mathrm{DRP_{IPL}(t)}$. This indicates that the duration Δt_{p} was even shorter (only a few days) and IPL was generally less relevant compared with the DRP-loss from soils on those soil-pixels. This is the reason for the dominance of DRP-loss from soils over IPL since a large number of soils had an elevated soil-P status in this catchment.

5.5 Discussion

Although we calibrated the rainfall-runoff model against discharge only in four catchments and derived the relevant P-parameters exclusively from field-data a relatively close match was reached between the simulated and observed DRP-loss for some stormflow periods. However, the prediction bands largely varied despite that we used very detailed data of manure and soil-P status. This allowed only to distinguish coarse patterns such as the dominance of P-loss from soils over IPL. More detailed analysis such as to quantify the effect of different P-treatments from single fields on the P-loss would be overriden by the uncertainty, even with this data-set.

Despite the encouraging model performance limitations exhibited for some stormflow events. In that case, either the flow rates, the location of contributing areas to fast flow or the mobilized DRP-concentrations from those areas could be miscalculated. One reason refers to the concept of the topographic index which was combined with the soil moisture status of each soil-type to spatially predict the contributing areas and the flow components. This concept worked for wet periods when surface and subsurface flow dominated and adjusted soil moisture to topography, thereby improving the hydrological connectivity between fields. Under longer drained conditions with high evapotranspiration, however, this connectivity was reduced and the conceptual soil water storage declined too fast. As a result, the flow components could be underrated and compared with reality, too little fields could be classified as contributing to fast flow for a subsequent runoff event after

dry periods. This indicates that contributing areas could not be correctly identified for some runoff events. It seems that mismatches in the predicted DRP-loss for some periods is the result of limitations related to the hydrological simulations and to the simulations of the P-mobililzation processes in space and time as well. This seemed the case for the July events. Since it was often uncertain whether single soil-pixels were contributing or not (Chapter 4) misclassified contributing soil-pixels could strongly impact the predicted diffuse P-loss by generating excessive loss compared with reality.

We treated the soil-P status as time-invariant compared with a declining P-pool for IPL. In fact, this assumption does not hold in a strict sense since this pool was influenced by manure, P-loss, erosion, microbial activity, sorption processes, etc. However, we doubt that considering these processes at the catchment scale could really improve the model performance or lead to substantial gain in knowledge due to the large number of additional parameters that would be needed. Another limitation was to neglect soil compaction and the sealing of soil pores by manure, thereby decreasing the infiltration capacity and increasing surface runoff for P-transport. This effect could be partly responsible for the underestimation of the large DRP-peaks during stormflows and the small contribution from IPL.

Irrespective of the scenarios the DRP-loss from soils dominated over IPL although numerous studies at the plot-scale considered IPL as the main source for P-loss. However, at larger scales IPL may be less important (*Withers et al.*, 2003) since the relevance of IPL in a catchment depends on the soil-P status, the P-amount in manure and the frequency of manure application of all fields. Therefore, $\mathrm{DRP_{IPL}(t)}$ exceeded $\mathrm{DRP_{Soil}}$ only during a short duration Δt_{p} of a few weeks after recent application. This suggested that IPL was important only on soil-pixels having a relatively low soil-P status. Substantial IPL would have occurred if many fields received manure during wet periods when contributing areas had developed and the soil-P status was low. Obviously, this was hardly the case even during prolonged wet periods or in March when >2000 kg P were applied. Hence, IPL accounted for 5 to 23% of the total DRP-loss during the growth period in 1999 and its contribution varied up to 30% during single runoff events.

One possible explanation for the minor importance of IPL in the growth period in 1999 could be that farmers applied manure mostly during favourable weather conditions. Although we lack of adequate data for manure management and P-loss to prove this hypothesis it could also be hypothesized that the contributions from IPL were substantially

larger in the past, say 10 or 20 years ago when less storage capacity for manure was available and the issue of applying manure under optimal soil- and weather conditions was not well known. Although IPL may be smaller nowadays due to increased storage capacities and due to the education of the farmers a possible reduction in IPL over time might be counterbalanced by increased P-accumulation in the soils and the subsequent P-loss from soils nowadays. Hence, to keep IPL at that relatively low level as observed in 1999, measures to limit IPL are relevant as IPL amount up to 30% of the total DRP-loss during runoff events.

The DRP mobilized from soils, however, was a more permanent P-source and exceeded those concentrations from manure during most of the growth period. The reason is that the soil-P status was exceptionally high in this catchment due to excessive P-fertilization during decades as the high P-saturation index of 48% in the top 5 cm and 36% from 5 to 20 cm soil depth indicated. Hence, measures should primarily focus on reducing the soil-P status. However, the degradation of the soil-P status is a long-term issue as data from *Vollmer et al.* (in prep.) showed: After two years of zero-P fertilization DRP in surface runoff from grassland plots was still high. This theory is also supported by trend analysis based on flow-normalized annual P-loss: Small but non-significant declines ($\approx$3% y^{-1}) in the annual DRP-loss of this catchment were calculated implying that significant reductions cannot be expected before 6 to 10 years (*Moosmann et al.*, 2005). If IPL was dominating immediate reductions in the P-loss should have exhibited. With regard to measures farmers should reduce the soil-P status by adjusting the P-fertilization rate to the soil-P status of single fields or by ploughing the topsoils of fields with a very high soil-P status and subsequent grass-sowing.

5.6 Conclusions

The model reproduced well the DRP-loss for some stormflow periods but there were also periods when the model performed poorly. However, the overall mismatch between observed and simulated DRP-loss was surprisingly small given that we applied a parsimonious model focusing on the dominant processes for hydrology and P-transport and derived all P-parameters exclusively from available field data. This study showed that even this temporally and spatially high-resolution data-set for manure and soil-P could not reduce the large uncertainty in model predictions. This highlights the need for further field experiments especially on critical sites with a high soil-P status. Additional DRP_{Soil}-WSP data

could partly replace those scenarios and further reduce uncertainty in the predicted DRP-loss. This uncerainty, however, will substantially increase in larger catchments with less detailed P-data, so we question the postulated ability of many models to predict diffuse P-loss at the catchment scale.

Since the major part of the P-loss originated from P-mobilization from topsoils measures were primarily needed to reduce the high soil-P status. However, the natural decrease of the soil-P status takes >10 years to reach acceptable soil-P levels. This could be achieved in practice, among others, by adjusting the P-fertilization to the soil-P status.

Acknowledgments This paper is part of the project C00.0104 "Modeling P runoff at the catchment level" and was financially supported by the COST 832 action within the scope of "Agricultural contribution to eutrophication" and by the Soil Physics group at the Institute of Terrestrial Ecology, ETH Zürich. This study would have been impossible without the support of E. Butscher, C. Crespi and P. Herzog (Environmental Protection Agency of Kt. Luzern), A. Weidmann for calculating the P-amounts in manure, the farmers in the Lippenrütibach catchment being involved in this project and O. Barmettler, B. Koch and J. Blum from the Central Office for Ecology of Kt. Luzern (FÖK).

Chapter 6

Concluding remarks

This study aimed to test the efficiency of ecological measures to reduce diffuse P-loss from agricultural catchments. For this reason we developped the model concept based on the main principles how agricultural management and the mechanisms for water flow and P-transport interact and how these processes can be feasibly described at the catchment scale based on available field data. The extensive data-set for the soil-P status, manure application, discharge and DRP-concentrations allowed to quantify the DRP-loss from manure and from soils at the event-based time-scale. This data-set, in terms of P-data, is unique in Switzerland.

Since the P-loss is event-driven and variable in time a high-temporal resolution monitoring set-up was required to sample the P-export dynamic. The strong change in the P-export dynamic from the typical (high DRP-concentrations during flow events and low concentrations during baseflow) to the new pattern (weak increase of DRP or almost constant DRP with increasing flow rate and high concentrations at baseflow) during the growth period could not be properly explained by direct manure-input and diffuse P-loss during events commonly considered relevant for P-loss in agricultural catchments. Since leaks from manure-tanks could be mostly ruled out it seems possible that bio-geochemical processes in the saturated zone or in the brook sediments were responsible for this change. Despite an excellent monitoring of nutrients additional parameters of the water quality, such as dissolved oxygen or other parameters influencing P-sorption and desorption at the sediment-water-interface in the brook, should be further sampled to explain the new pattern. Areas in the catchment substantially contributing to P-loss could also be separated by additionally sampling the P-export dynamic of the drainage effluents of such subcatchments. In any case, long-term monitoring with high temporal resolution is required for all

flow conditions to better understand the P-export dynamic from this catchment. Unfortunately, such a change in the pattern of the P-export dynamic makes it difficult to assess the efficiency of ecological measures since possible effects of the measures might have been counterbalanced by increased P-loss during baseflow.

The hydrological results from different catchments indicate that well and poorly drained pedological units are representative units when assigning a slow and a fast flow component to each unit and weighting these flow rates with their respective areal fractions in catchments. The joint calibration of parameters by simultaneously comparing the hydrological response of catchments in four catchments yielded robust parameter sets to reproduce the catchment response for intermediate and high flow events. This hydrological model could also be applied to predict discharge in ungauged catchments in the Lake Sempach region, and possibly in catchments in the neighbouring Lake Baldegg or Hallwil if the calibrated model parameters are transferable into these regions.

One serious aspect in hydrological modeling is related to the quality of discharge data, especially to the relationships between water levels and discharge. Such relationships must be examined for plausibility since rainfall-runoff models are commonly calibrated against observed discharge only. In our case, large differences at high discharge rates between the original and the recalculated relationships occurred in one catchment. This caused substantial differences in the estimated parameters and led to different spatial predictions of hydrological risk areas in catchments.

It has been commonly assumed that the hydrological risk areas are the poorly drained soils with high water-tables and a smaller water storage capacity compared to well drained soils. However, our results suggest that during large stormflows the well drained soils substantially contributed to fast flow as soon as they were wet enough. This result should be accounted for when implementing measures.

Based on the classification of hydrological risk areas for distinct runoff events in the Lippenrütibach the major part of this catchment had a low risk during small and large runoff events. Even during flood events less than 20% of the catchment area had a very high risk. This suggests that the hydrological risk areas and associated diffuse P-loss may arise from a small part within the catchment. Such areas - hot spots - could be target areas for measures.

The combination of the rainfall-runoff model with the P-model reproduced well the observed DRP-loss for some stormflows in hourly time steps. One advantage of this par-

simonious model is that all relevant P-parameters could be derived from available field data. However, the prediction bands largely varied despite detailed data of manure and soil-P status. This allowed only to distinguish coarse patterns such as the dominance of P-loss from soils over IPL. Any more detailed analysis such as to quantify the effect of P-treatments from single fields on the P-loss would be overriden by the uncertainty, even with this data-set. This uncerainty, however, will substantially increase in larger catchments with less detailed P-data, so we question the postulated ability of many models to predict diffuse P-loss at the catchment scale.

The model results indicated that most of the DRP-loss originated from soils while IPL was of minor importance irrespective of the scenarios being used during the growth season in 1999. For single runoff events, however, IPL amounted up to 30% compared with the total DRP-loss, even during a flood period. The reason for the relatively small IPL contribution was the exceptionally high average soil-P status in this catchment due to the excessive P-fertilization over decades. As a result, the DRP-concentrations released from soils were mostly higher than those from manure during most of the growth season. On soils having a low soil-P status IPL was in general the main responsible for diffuse P-loss while the importance of IPL was generally overriden on soils with a high soil-P status.

For this reason, measures should primarily focus on the reduction of the high soil-P status in this catchment as being proposed by *Prasuhn and Lazzarotto* (in press). A noticeable reduction in the DRP-load could be expected only after many years since the natural degradation of the soil-P status to acceptable levels takes >10 years. This requires, of course, no further P-accumulation in soils. One step into this direction was already done as the average P-balances declined from 150% in 1992 to 93% in 2003 in the Lippenrütibach. However, P-accumulation in topsoils was still possible on single fields. One target must be to limit the P-balance to less than 100% instead of tolerating 110% as is the case nowadays. Another option is that farmers account for the soil-P status of fields by adjusting the P-fertilization rate. Alternatively, drastic measures could be applied on fields with a high soil-P status: To plough the topsoils with subsequent grass-sowing although this may cause erosion and nitrate leaching or to apply P-binding amendments which should be carefully assessed first.

One possible explanation for the minor importance of IPL in the growth period in 1999 could be that farmers applied manure mostly during favourable weather conditions. Although adequate data for manure management and P-loss is missing to prove this hy-

pothesis it could be hypothesized that the contributions from IPL were markedly larger in the past, say 10 or 20 years ago when less storage capacity for manure was available and the issue of applying manure under optimal soil- and weather conditions was not well known. Although IPL may be smaller nowadays due to increased storage capacities and due to further education of the farmers a possible reduction in IPL might be counterbalanced by increased P-accumulation in the soils and the subsequent P-loss from soils nowadays. Hence, to keep IPL at that relatively low level as observed in 1999, measures to limit IPL are still relevant as IPL amount up to 30% of the total DRP-loss during runoff events.

It is worth to mention that the Lippenrütibach is not a representative agricultural catchment in Switzerland since its average stock density, soil-P status and P-loss is high. The major problem still remains the high stock densities whose reduction is the only sustainable but economically painful way to prevent excessive diffuse P-inputs into surface waters in the long-term.

Appendix A

Appendix

A.1 Manure management and soil-P data

A.1.1 Calculation of the P-amounts in manure applications

The collected manure data of 30 farmers for each field in the catchment include information for each application such as the time and date of application, the applied volume in m^3 and intensity in m^3 ha^{-1}, the type of manure (pig or cattle) and the ratio ϵ of manure being diluted by water. This spatial and temporal information is required to simulate IPL and is used to calculate the farm-specific P-amounts for each application.

For each farm, the total P-amounts produced by the number of cattle (n_{cattle}) and pigs (n_{pig}) was derived from detailed farm-specific nutrient balances which account for the P-amounts arising from the age of cows and their associated milk quota, for the amounts of P-deficient fodder or for the amount of manure being exported from the farm among other things. For each farm we calculated annual P-concentrations P_{manure} in manure based on the dilution ratio ϵ, the annual manure volume V_{manure} and the animal-specific P-amounts m_{cattle} and m_{pig} per number of pigs n_{pig} and per cattle n_{cattle} assuming that the dilution ratio ϵ is time-invariant.

$$P_{\text{manure}} = \frac{\epsilon}{V_{\text{manure}}} \Big[m_{\text{cattle}} \cdot n_{\text{cattle}} + m_{\text{pig}} \cdot n_{\text{pig}} \Big] \tag{A.1}$$

This calculations were carried out in the scope of a diploma thesis by *Weidmann* (2004).

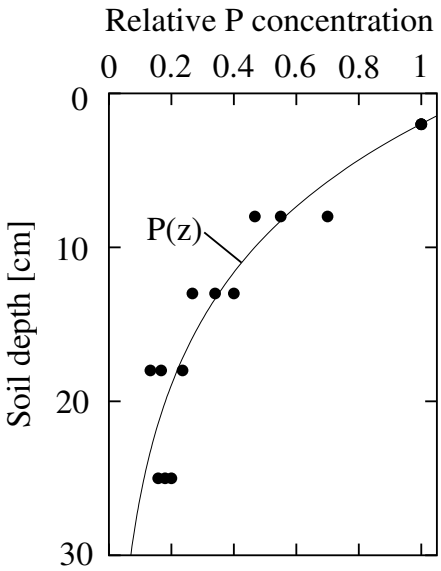

Figure A.1: *Fitted, P(z), and observed vertical distribution of the normalized P_{CaCl_2}-concentrations sampled from three pasture sites in the Lippenrütibach catchment. Data from Keller and van der Zee (2004)*

A.1.2 Comparison between the soil-P status in the Lippenrütibach and the region of Lake Greifen

Vollmer et al. (in prep.) analyzed the soils in the region of Lake Greifen for water-soluble P (WSP) and the CO_2-saturated water extractable P (P_{CO_2}) from the top 4 cm depth. To apply their found linear relationship between WSP and the DRP-concentrations in surface runoff from their plots (scenario 1 in Chapter 5) we transformed the P_{CO_2}-values measured in the Lippenrütibach (0 to 10 cm) into WSP-values for the top 4 cm depth.

First, to adjust P_{CO_2} from the top 10 cm to the top 4 cm we used data from *Keller and van der Zee* (2004) collected on three pasture sites in the Lippenrütibach. They sampled the soils from 0 to 30 cm depth in 5 cm intervals to determine the vertical distribution of P_{CaCl_2}. These concentrations were normalized within their minimum and maximum values and plotted against soil depth (Fig. A.1). This allowed to calculate the relative differences in P_{CaCl_2} between the soil depth 0 to 4 cm and 0 to 10 cm assuming that the normalized vertical distributions of P_{CaCl_2} were comparable with the vertical P_{CO_2}-distribution for all fields in the Lippenrütibach. An exponential function $P(z)$ was fitted to these normalized concentrations (R^2=0.98). The ratio f of the average P_{CaCl_2}-concentrations in the top 4 cm and those from the top 10 cm was derived by integrating $P(z)$ over both sampling depths.

According to Eq. A.2 P_{CaCl_2} was about 1.3 to 1.4 times larger in the top 4 cm compared to the top 10 cm which agrees to the findings of *Keller and van der Zee* (2004). Therefore,

all P_{CO_2}-values in the soil samples in the Lippenrütibach were multiplied by this correction factor $1.3 < f < 1.4$.

$$f = \frac{1}{4cm} \int_{z=4\text{cm}}^{0\text{cm}} P(z)dz \Big[\frac{1}{10cm} \int_{z=10\text{cm}}^{0\text{cm}} P(z)dz \Big]^{-1} \tag{A.2}$$

Finally, we transformed these depth-corrected P_{CO_2}-values from the soils in the Lippenrütibach into WSP-values based on correlations between WSP-values and P_{CO_2}-values found on plots in the region of Lake Greifen for 0 to 4 cm soil depth. Thus, the resulting WSP-values in the Lippenrütibach are comparable with the WSP-values in the region of Lake Greifen.

A.2 List of Symbols

a_i	[-]	Fast flow decline rate for the well and poorly drained HRU_i
b_i	[-]	Proportion of rainfall converted into fast flow on contributing areas of well and poorly drained HRU_i
c_i	[mm h^{-1}]	Factor relating the scaled soil water storage to the slow flow component of well and poorly drained HRU_i
$et^k(t)$	[mm h^{-1}]	Evapotranspiration rate in catchment k
f_d	[-]	Dimensionless Darcy friction coefficent
g	[m s^{-2}]	Gravity constant
h	[h^{-1}]	Decline rate of the DRP-concentration in runoff from manure due to P-sorption and P-uptake by plants
i		Index of the type of hydrological response units
k		Index of the catchment number
m		Index of the global parameter set
m_{cattle}	[kg P]	Farm-specific average P-amounts per cattle unit
m_{pig}	[kg P]	Farm-specific average P-amounts per pig unit
n_i	[-]	Exponent controlling the spatial expansion of areas contributing to fast flow for a given average soil moisture Θ_i for well and poorly drained HRU_i
n_{cattle}	[-]	Number of cattle per farm
n_{pig}	[-]	Number of pigs per farm
$q^k_{3,fast}(t)$	[mm h^{-1}]	Urban flow component in catchment k at time t
$q^k_{i,fast}(t)$	[mm h^{-1}]	Fast flow component from well and poorly drained HRU^k_i, in catchment k at time t
$q^k_{i,slow}(t)$	[mm h^{-1}]	Slow flow component from well and poorly drained HRU^k_i, in catchment k at time t
$r^k(t\text{-}\tau^k_{i,d})$	[mm h^{-1}]	Rainfall rate delayed by soil-type specific time-lags $\tau^k_{i,d}$
p	[-]	Probability for soil-pixels contributing to fast flow
t	[h]	Time of simulation
t_0	[h]	Begin of the simulation period
t_a	[h]	Time of manure application
t_e	[h]	End of the simulation period

$A_{profile}$	[m^2]	Area of the water-filled cross-section of a weir
$A_{upstream}$	[m^2]	Upstream area draining through a pixel at location [x,y] according to the digital elevation model
A_3^k	[-]	Lumped areal fraction of the urban areas in catchment k
A_i^k	[-]	Lumped areal fraction of the HRU_i^k in catchment k
$A_{i,fast}^k(t)$	[-]	Time-variant areal fraction of the well and poorly drained HRU_i^k contributing to fast flow in catchment k
DRP_{IPL}^0	[mg l^{-1}]	Initial DRP-concentration from manure in surface runoff
$DRP_{IPL}(t)$	[mg l^{-1}]	Calculated DRP-concentration from manure in runoff
DRP_{Soil}	[mg l^{-1}]	Calculated DRP-concentration in runoff due to P mobilized from soils
E_m	[-]	Modified Nash-and-Sutcliffe efficiency measure for the m-th global parameter set
$F(\lambda_i^k)$	[-]	Cumulative distribution function of the topographic index λ_i^k for well and poorly drained HRU_i^k in catchment k
K	[-]	Fit parameter used to recalculate the level-discharge curves
K_i	[mm h^{-1}]	Hydraulic conductivity of HRU_i
$\mathbf{P}_i$	[-]	Global parameter vector for the type HRU_i^k in all catchments k
L(t)	[kg h^{-1}]	Simulated total DRP-load at time t
$L_{obs}(t)$	[kg h^{-1}]	Observed DRP-load at time t
$\overline{L}$	[kg h^{-1}]	Average DRP-load over a considered period
P(z)	[-]	Fitted normalized P-concentration with depth z
P_{manure}	[kg m^{-3}]	Mean farm-specific P-concentration in manure
$\overline{Q}^k$	[mm h^{-1}]	Average discharge in catchment k over a certain period
$Q_{obs}^k(t)$	[mm h^{-1}]	Total observed discharge in catchment k at time t
$Q_{obs,recalc}^k(t)$	[mm h^{-1}]	Total observed discharge in catchment k at time t based on the recalculated level-discharge curves
$Q_{obs,orig}^k(t)$	[mm h^{-1}]	Total observed discharge in catchment k at time t based on the original level-discharge curves
$Q^k(t)$	[mm h^{-1}]	Total simulated discharge at time t in catchment k
R_h	[m]	Hydraulic radius of the through-flown cross-section
$S_{i,max}$	[mm]	Maximum water storage capacity for well and poorly drained HRU_i^k

$S_i^k(t)$	[mm]	Absolute soil water storage of well and poorly drained HRU_i^k in catchment k at time t
$\mathbf{V}_i^k(t)$	[-]	Vector of the time-variant local variables of HRU_i^k in the catchments k
V_{manure}	[m^3]	Farm-specific volume of manure
w_i	[m]	Area of the HRU i
β	[-]	Average slope of a pixel
Δt	[h]	Simulation time step
Δt^*	[h]	Duration between the manure application and the time of runoff onset
Δt_p	[h]	Duration when $DRP_{IPL}(t)$ was larger than DRP_{Soil} on a soil-pixel
γ	[-]	Channel slope
ϵ	[-]	Dilution ratio between water and manure
η	[-]	Fraction of new water in total discharge
λ_i^k	[-]	Topographic index of well and poorly drained HRU_i^k in catchment k
λ_{well}^k	[-]	Topographic index of well drained soils in catchment k
λ_{poor}^k	[-]	Topographic index of poorly drained soils in catchment k
$\lambda_{0,i}^k(t)$	[-]	Time-variant threshold of the topographic index for well and poorly drained HRU_i^k in catchment k at time t
∇h_i	[-]	Hydraulic gradient of HRU_i
$\Theta_i^k(t)$	[-]	Scaled soil water storage of the well and poorly drained HRU_i^k in catchment k at time t
$\Theta_{d,i}$	[-]	Drainable porosity of HRU_i
$\Theta_{well}(t)$	[-]	Scaled soil water storage for the well drained HRU
$\Theta_{poor}(t)$	[-]	Scaled soil water storage for the poorly drained HRU
$\tau_{i,d}^k$	[h]	Soil-type specific delay constant for fast flow responding to rainfall on the HRU_i^k in catchment k

A.3 List of Abbreviations

h	hours
Al	Aluminium
Ca	Calcium
cdf	Cumulative distribution function
DCE	Dairy-cow equivalents
DEM	Digital elevation model
DP	Dissolved phosphorus
DRP	Dissolved reactive phosphorus
Fe	Iron
HOST	Hydrology of Soil Types
HRU	Hydrological response units
IPL	Incidental phosphorus losses
LDC	Level-discharge curve
NH_4	Ammonia
NO_3	Nitrate
P	Phosphorus
P_{CaCl_2}	P-concentration extracted with the $CaCl_2$-method
P_{CO_2}	CO_2-saturated water extractable P
PP	Particulate or sediment-bound P
R^2	Coefficient of determination
RSM	Routine sampling monitoring
Sn(II)	Stannous ion
SPS	Soil-P status
TDP	Total dissolved P
TP	Total phosphorus
WSP	Water-soluble phosphorus

Bibliography

Abbott, M. B., J. C. Bathurst, A. Cunge, P. E. O'Connell, and J. Rassmussen (1986): An introduction to the SHE 2: Structure of a physically-based, distributed modeling system: *Journal of Hydrology*: *87*, 61–77.

AGBA (1993): Einzugsgebiet des Sempachersees - Übersichtsbodenkarte: *Tech. rep.*: Arbeitsgemeinschaft Beratender Agronomen. Ebikon.

Ambroise, B., K. J. Beven, and J. Freer (1996): Towards a generalization of the TOPMODEL concepts: Topographic indices of hydrological similarity: *Water Resources Research*: *32*(7), 2135–2145.

Andréassian, V., A. Oddos, C. Michel, F. Anctil, C. Perrin, and C. Loumagne (2004): Impact of spatial aggregation of inputs and parameters on the efficiency of rainfall-runoff models: A theoretical study using chimera watersheds: *Water Resources Research*: *40*(5): W05209 doi:10.1029/2003WR002854.

Arnold, J. G., R. Srinivasan, R. S. Muttiah, and J. R. Williams (1998): Large area hydrologic modelling and assessment part I: Model development: *Journal of American Water Resources Association*: *34*(1), 73–89.

Barrow, N. J. (1992): A brief discussion on the effect of temperature on the reaction of inorganic ions with soil: *Journal of Soil Science*: *43*, 37–45.

Bathurst, J. C. (2002): At-a-site variation and minimum flow resistance for mountain rivers: *Journal of Hydrology*: *269*, 11–26.

Beauchemin, S., R. R. Simard, and D. Cluis (1998): Forms and concentration of phosphorus in drainage waters of 27 tile-drained soils: *Journal of Environmental Quality*: *27*, 721–728.

Beven, K. J. (1989): Changing ideas in hydrology - the case of physically-based models?: *Journal of Hydrology*: *89*, 157–171.

Beven, K. J. (1993): Prophecy, reality and uncertainty in distributed hydrological modelling: *Advances in Water Resources*: *16*, 41–51.

Beven, K. J. (1996): A discussion of distributed modelling: in *Distributed Hydrological Modelling*, edited by J. C. Refsgaard and M. B. Abbott: pp. 255–278: Kluwer Acad., Norwell, Mass.

Beven, K. J. (1997): TOPMODEL: A critique: *Hydrological Processes*: *11*, 1069–1085.

Beven, K. J., and J. Freer (2001a): Equifinality, data assimilation, and uncertainty estimation in mechanistic modelling of complex environmental systems using the GLUE methodology: *Journal of Hydrology*: *249*, 11–29.

Beven, K. J., and J. Freer (2001b): A dynamic TOPMODEL: *Hydrological Processes*: *15*, 1993–2011.

Beven, K. J., and M. J. Kirkby (1979): A physically based, variable contributing area model of basin hydrology: *Hydrological Sciences-Bulletin-des Sciences Hydrologiques*: *24*(1), 43–69.

Blöschl, G., and M. Sivapalan (1995): Scale issues in hydrological modelling: A review: *Hydrological Processes*: *9*, 251–290.

Boorman, D. B., J. M. Hollis, and A. Lilly (1995): Hydrology of soil types: A hydrologically-based classification of the soils of the United Kingdom: *Tech. rep.*: Institute of Hydrology Report No. 126. Wallingford: Institute of Hydrology.

Bosch, J. M., and J. D. Hewlett (1982): A review of catchment experiments to determine the effect of vegetation changes on water yield and evapotranspiration: *Journal of Hydrology*: *55*, 3–23.

Braun, M., P. Hurni, and N. von Albertini (1993): Abschwemmung von Phosphor auf Grasland an zwei verschiedenen Standorten im Einzugsgebiet des Sempachersees: *Landwirtschaft Schweiz*: *6*(10), 615–620.

Braun, M., N. Aschwanden, and C. Wüthrich-Steiner (2001): Evaluation Ökomassnahmen: Abschwemmung von Phosphor: *Agrarforschung*: *8*(1), 36–41.

Bundesamt für Landwirtschaft (2001): Evaluation der Ökomassnahmen und Tierhaltungsprogrammen - Bereich Stickstoff und Phosphor, 4. Zwischenbericht.

Bundesversammlung der Schweizerischen Eidgenossenschaft (1991): Bundesgesetz über den Schutz der Gewässer vom 24. Januar 1991.

Burch, G. J., I. D. Moore, and J. Burns (1989): Soil hydrophobic effects on infiltration and catchment runoff: *Hydrological Processes*: *3*, 211–222.

Burkhardt, M., C. Stamm, C. Waul, H. Singer, and S. Müller (accepted): Surface Runoff and Transport of Sulfonamide Antibiotics and Tracers on Manured Grassland: *Journal of Environmental Quality.*

Burns, D. A., and J. J. McDonnell (1990): Effects of a beaver pond on runoff processes: comparison of two headwater catchments: *Journal of Hydrology*: *205*(3-4), 248–264.

Burns, D. A., J. J. McDonnell, R. P. Hooper, N. E. Peters, J. E. Freer, C. Kendall, and K. Beven (2001): Quantifying contributions to storm runoff through end-member mixing analysis and hydrologic measurements at the Panola Mountain Research Watershed (Georgia, USA): *Hydrological Processes*: *15*, 1903–1924.

Chardon, W. J., O. Oenema, P. Del Castilho, R. Vriesema, J. Japenga, and D. Blaauw (1997): Organic phosphorus in solutions and leachates from soils treated with animal slurries: *Journal of Environmental Quality*: *26*, 372–378.

Dils, R. M., and A. L. Heathwaite (1999): Phosphorus transport from diffuse agricultural sources: shallow subsurface pathways in grassland soils: in *Impact of land-use change on nutrient loads from diffuse sources*, vol. 257: pp. 57–64: IAHS.

Donigian, A. S., B. R. Bicknell, and J. C. Imhoff (1995): Hydrological Simulation Program Fortran (HSPF): in *Computer Models of Watershed Hydrology*, edited by V. P. Singh: pp. 395–442: Water Resources Publications, Highlands Ranch, Colorado.

Dunn, S. M., E. McAlister, and R. C. Ferrier (1998): Development and application of a distributed catchment-scale hydrological model for the River Ythan, NE Scotland: *Hydrological Processes*: *12*, 401–416.

Edwards, D. R., and T. C. Daniel (1993a): Effects of poultry litter application rate and rainfall intensity on quality of runoff from fescue grass plots: *Journal of Environmental Quality*: *22*, 361–365.

Edwards, D. R., and T. C. Daniel (1993b): Drying interval effects on runoff from fescue plots receiving swine manure: *Transactions of the American Society of Agricultural Engineers*: *36*, 1673–1678.

FAL and FAW and RAC (1995): Referenzmethoden: P-Bestimmung im CO_2-gesättigten Wasserextrakt: *Tech. rep.*: Eidg. landwirtschaftlichen Forschungsanstalten.

Flury, M., H. Flühler, W. A. Jury, and J. Leuenberger (1994): Susceptibility of soils to preferential flow of water: A field study: *Water Resources Research*: *30*, 1945–1954.

FÖK (2002): Entwicklung der Tierbestände und des Nährstoffeinsatzes im Einzugsgebiet des Sempachersees 1996-2001: *Tech. rep.*: Fachstelle für Ökologie, Sursee.

Forni, D., H. U. Gujer, L. Nyffenegger, S. Vogel, and U. Gantner (1999): Evaluation der Ökomassnahmen und Tierhaltungsprogramme: *Agrarforschung*: *6*(3), 107–110.

Foy, R. H., and P. J. A. Withers (1995): The contribution of agricultural phosphorus to eutrophication: *Proceedings of the Fertilizer Society*: *365*, 32pp.

Freer, J., and K. J. Beven (1996): Bayesian estimation of uncertainty in runoff prediction and the value of data: An application of the GLUE approach: *Water Resources Research*: *32*(7), 2161–2173.

Frossard, E., M. Brossard, M. J. Hedley, and A. Metherell (1995): Reactions controlling the cycling of P in soils: in *Phosphorus in the Global Environment*, edited by H. Tiessen: pp. 107–137: John Wiley and Sons.

Frossard, E., P. Julien, J.-A. Neyroud, and S. Sinaj (2004): Phosphor in Böden, Düngern, Kulturen und Umwelt - Situation in der Schweiz: in *Schriftenreihe Umwelt Nr. 368, Bern*: p. 183: Bundesamt für Umwelt, Wald und Landschaft BUWAL.

Fuller, C. C., and J. A. Davis (1989): Influence of coupling of sorption and photosynthetic processes on trace element cycles in natural waters: *Nature*: *340*, 52–54.

Gächter, R., and P. Stadelmann (1993): Gewässerschutz und Seenforschung: in *Sempachersee, Band 33*, edited by E. Rouss and C. Marti: pp. 343–377: Mitteilungen der Naturforschenden Gesellschaft Luzern.

Gächter, R., A. Mares, C. Stamm, U. Kunze, and J. Blum (1996): Dünger düngt Sempachersee: *Agrarforschung*: *3*(7), 329–332.

Gächter, R., J. M. Ngatiah, and C. Stamm (1998): Transport of phosphate from soil to surface waters by preferential flow: *Environmental Science and Technology*: *32*(13), 1865–1869.

Gaston, L. A., C. M. Drapcho, S. Tapadar, and J. L. Kovar (2003): Phosphorus runoff relationships for Louisiana Coastal Plain soils amended with poultry litter: *Journal of Environmental Quality*: *32*, 1422–1429.

Gburek, W., A. Sharpley, and H. Pionke (1996): Identification of critical source areas for phosphorus export from agricultural catchments: in *Advances in Hillslope Processes*, vol. 1, edited by M. G. Anderson and S. M. Brooks: pp. 263–282: John Wiley and Sons.

Gburek, W. J., and A. N. Sharpley (1998): Hydrologic controls on phosphorus loss from upland agricultural watersheds: *Journal of Environmental Quality*: *27*, 267–277.

Gburek, W. J., A. N. Sharpley, L. Heathwaite, and G. J. Folmar (2000): Phosphorus management at the watershed scale: A modification of the Phosphorus Index: *Journal of Environmental Quality*: *29*, 130–144.

Gerke, J. (1992): Phosphate, aluminium and iron in the soil solution of three different soils in relation to varying concentrations of citric acid: *Z. Pflanzenernähr. Bodenkd.*: *155*, 339–343.

Grayson, R. B., and G. Blöschl (2001a): Summary of pattern comparison and concluding remarks: in *Spatial patterns in catchment hydrology - Observations and modelling*, edited by R. B. Grayson and G. Blöschl: pp. 355–367: Cambridge University Press, New York.

Grayson, R. B., and G. Blöschl (2001b): Spatial processes, organisation and patterns: in *Spatial patterns in catchment hydrology - Observations and modelling*, edited by R. B. Grayson and G. Blöschl: pp. 3–16: Cambridge University Press, New York.

Grayson, R. B., I. D. Moore, and T. A. McMahon (1992): Physically based hydrologic modeling - 2. Is the concept realistic?: *Water Resources Research*: *28*(10), 2659–2666.

Groenendijk, P., and J. G. Kroes (1999): Modelling the nitrogen and phosphorus leaching to groundwater and surface water with ANIMO 3.5. Report 144: *Tech. rep.*: DLO Winand Staring Centre, Wageningen, Netherlands.

Gupta, V. K., and S. Sorooshian (1985b): The relationship between data and the precision of parameter estimates of hydrologic models: *Journal of Hydrology*: *81*, 57–77.

Harrison, A. F. (1987): Soil organic phosphorus: in *A review of world literature*: p. 256: CAB International, Wallingford UK.

Hartikainen, H., and M. Yli-Halla (1996): Solubility of soil phosphorus as influenced by urea: *Z. Pflanzenernähr. Bodenkd.*: *159*, 327–332.

Haygarth, P. M., and S. C. Jarvis (1999): Transfer of phosphorus from agricultural soils: *Advances in Agronomy*: *66*, 195–249.

Haygarth, P. M., and S. C. Jarvis (Eds.) (2002): *Agriculture, hydrology and water quality*: chap. 9 Hydrological source management of pollutants at the soil profile scale, pp. 197–223: CAB International.

Haygarth, P. M., L. Hepworth, and S. C. Jarvis (1998): Forms of phosphorus transfer in hydrological pathways from soil under grazed grassland: *European Journal of Soil Science*: *49*(1), 65–72.

Heathwaite, A. L. (1997): Sources and pathways of phosphorus loss from agriculture: in *Phosphorus loss from soil to water*, edited by H. Tunney, O. T. Carton, P. C. Brookes, and A. E. Johnston: chap. 9, pp. 205–223: CAB International, Wallingford.

Heathwaite, A. L., and R. M. Dils (2000): Characterising phosphorus loss in surface runoff and subsurface hydrological pathways: *Science of the Total Environment*: *251/252*, 523–538.

Heathwaite, A. L., and P. J. Johnes (1996): The contribution of nitrogen species and phosphorus fractions to stream water quality in agricultural catchments: *Hydrological Processes*: *10*, 971–983.

Heathwaite, A. L., P. Griffiths, and R. J. Parkinson (1998): Nitrogen and phosphorus in runoff from grassland with buffer strips following application of fertilisers and manures: *Soil Use Manage*: *14*, 142–148.

Heathwaite, A. L., A. I. Fraser, P. J. Johnes, M. Hutchins, E. Lord, and D. Butterfield (2003): The Phosphorus Indicators Tool: A simple model of diffuse P loss from agricultural land to water: *Soil Use and Management*: *19*(1-11).

Heckrath, G., P. C. Brookes, P. R. Poulton, and K. W. T. Goulding (1995): Phosphorus leaching from soils containing different phosphorus concentrations in the broadbalk experiment: *Journal of Environmental Quality*: *24*, 904–910.

Hesketh, N., and P. C. Brookes (2000): Development of an indicator for risk of phosphorus leaching: *Journal of Environmental Quality*: *29*, 105–110.

Hillel, D. (1986): Modeling in soil physics: A critical review: in *Future Developments in Soil Science Research*: pp. 35–42: Soil Science Society of America, Madison, Wisconsin.

Hoffmann-Riem, H. (2003): *Die Sanierung des Sempachersees. Eine Fallstudie über ökologische Lernprozesse*: Ökom Verlag, München, 250 Seiten.

Horton, R. E. (1933): The role of infiltration in the hydrologic circle: *Trans. Amer. Geophys. Union*: *14*, 446–460.

Johnes, P. J. (1996): Evaluation and management of the impact of land use change on the nitrogen and phosphorus load delivered to surface waters: The export coefficient modelling approach: *Journal of Hydrology*: *183*, 323–349.

Johnes, P. J., and L. Heathwaite (1997): Modelling the impact of land-use change on water quality in agricultural catchments: *Hydrological Processes*: *11*, 269–286.

Keller, A., and S. van der Zee (2004): Phosphorverfügbarkeit in intensiv genutzten Graslandböden: *Agrarforschung*: *11*(9), 396–401.

Kim, S., and J. W. Delleur (1997): Sensitivity analysis of extended TOPMODEL for agricultural watershed equipped with tile drains: *Hydrological Processes*: *11*, 1243–1261.

Kirchner, J. (2003): A double paradox in catchment hydrology and geochemistry: *Hydrological Processes*: *17*, 871–874.

Kirkby, M. (1975): Hydrograph modelling strategies: in *Processes in Physical and Human Geography*, edited by R. Peel, M. Chisholm, and P. Haggett: pp. 69–90: Heinemann, London.

Kleinmann, J. A., and A. N. Sharpley (2003): Effect of manure on runoff phosphorus concentrations over successive rainfall events: *Journal of Environmental Quality*: *32*, 1072–1081.

Knisel, W. G. (1980): CREAMS: A field-scale model for chemicals run-off and erosion from agricultural management systems. Conservation Report 26: *Tech. rep.*: US Department of Agriculture, Washington, D. C., USA.

Kronvang, B. (1990): Sediment associated phosphorus transport from two intensively farmed catchment areas: in *Soil erosion on agricultural land*, edited by J. Boardman, L. D. L. Foster, and J. A. Dearing: pp. 131–330: John Wiley and Sons, Chichester, New York, Brisbane, Toronto, Singapore.

Lazzarotto, P., V. Prasuhn, E. Butscher, C. Crespi, H. Flühler, and C. Stamm (2005): Phosphorus export dynamics from two Swiss grassland catchments: *Journal of Hydrology*: *304*, 139–150.

Leavesley, G. H., and L. G. Stannard (1995): The precipitation-runoff modelling system - PRMS: in *Computer Models of Watershed Hydrology*, edited by V. P. Singh: pp. 281–310: Water Resources Publications, Highlands Ranch, Colorado.

Lek, S., I. Dimopoulos, and A. Fabre (1996): Predicting phosphorus concentration and phosphorus load from watershed characteristics using backpropagation neural networks: *Acta Oecologica*: *17*(1), 43–53.

Leonard, R. A., W. G. Knisel, and D. A. Still (1987): Gleams: Groundwater loading effects of agricultural management systems: *Am. Soc. Agric. Eng. Trans.*: *30*, 1403–1418.

Leu, C., H. Singer, C. Stamm, S. R. Müller, and R. P. Schwarzenbach (2004): Variability of herbicide losses from 13 fields to surface water within a small catchment after a controlled herbicide application: *Environmental Science and Technology*: *38*, 3835–3841.

Lilly, A., D. B. Boorman, and J. M. Hollis (1998): The development of a hydrological classification of UK soils and the inherent scale changes: *Nutrient Cycling in Agroecosystems*: *50*, 299–302.

Lindström, G., B. Johansson, M. Persson, M. Gardelin, and S. Bergström (1997): Development and test of the distributed HBV-96 model: *Journal of Hydrology*: *201*, 272–288.

McDowell, R. W., and A. N. Sharpley (2001): Approximating phosphorus release from soils to surface runoff and subsurface drainage: *Journal of Environmental Quality*: *30*, 508–520.

McDowell, R. W., and S. T. Trudgill (2000): Variation in phosphorus loss from a small catchment in South Devon, UK: *Agriculture Ecosystems and Environment*: *79*, 143–157.

McGlynn, B., J. J. McDonnell, J. B. Shanley, and C. Kendall (1999): Riparian zone flowpath dynamics during snowmelt in a small headwater catchment: *Journal of Hydrology*: *222*, 75–92.

McIsaac, G. F., M. C. Hirschi, and J. K. Mitchell (1991): Nitrogen and phosphorus in eroded sediment from corn and soybean tillage systems: *Journal of Environmental Quality*: *20*, 663–670.

Metropolis, N., A. W. Rosenbluth, M. N. Rosenbluth, A. H. Teller, and E. Teller (1953): Equation of state calculations for fast computing machines: *Journal of Chemical Physics*: *21*, 1087–1092.

Moosmann, L., B. Müller, R. Gächter, E. Butscher, P. Herzog, and A. Wüest (2005): Trend-oriented sampling strategy and estimation of soluble reactive phosphorus loads in streams: *Water Resources Research*: *41*: W01020,doi:10.1029/2004WR003539.

Mosley, M. P. (1979): Streamflow generation in a forested watershed, New Zealand: *Water Resources Research*: *15*(4), 795–806.

Müller, B., M. Reinhardt, and R. Gächter (2003): High temporal resolution monitoring of inorganic nitrogen load in drainage waters: *Journal of Environmental Monitoring*: (5), 1–7.

Murphy, J., and J. P. Riley (1962): A modified single solution method for the determination of phosphate in natural waters: *Analytica Chemica Acta*: *229*, 115–120.

Nash, J. E., and J. V. Sutcliffe (1970): River flow forecasting through conceptual models, part 1 - A discussion of principles: *Journal of Hydrology*: *10*, 282–290.

Nimick, D. A., C. H. Gammons, T. E. Cleasby, J. P. Madison, D. Skaar, and C. M. Brick (2003): Diel cycles in dissolved metal concentrations in streams: Occurrence and possible causes: *Water Resources Research*: *39*(9), 1247–1264.

O'Loughlin, E. M. (1981): Saturation regions in catchments and their relations to soil and topographic properties: *Journal of Hydrology*: *53*, 229–246.

O'Loughlin, E. M. (1986): Prediction of surface saturation zones in natural catchments by topographic analysis: *Water Resources Research*: *22*(5), 794–804.

Pacini, N., and R. Gächter (1999): Speciation of riverine particulate phosphorus during rain events: *Biogeochemistry*: *47*, 87–109.

Pionke, H. B., W. J. Gburek, R. R. Schnable, A. N. Sharpley, and G. F. Elwinger (1999): Seasonal flow, nutrient concentrations and loading patterns in stream flow draining an agricultural hill-land watershed: *Journal of Hydrology*: *220*, 62–73.

Pote, D. H., T. C. Daniel, A. N. Sharpley, P. A. Moore, Jr., D. R. Edwards, and D. J. Nichols (1996): Relating extractable soil phosphorus to phosphorus losses in runoff: *Soil Science Society of America Journal*: *60*, 855–859.

Prasuhn, V., and P. Lazzarotto (in press): Phosphorabschwemmung von Grasland im Einzugsgebiet des Sempachersees: *Schriftenreihe der FAL: Wirkung des ökologischen Leistungsnachweises auf Stickstoff- und Phosphorflüsse in der Schweizerischen Landwirtschaft, Zürich.*

Preedy, N., K. McTiernan, R. Matthews, L. Heathwaite, and P. Haygarth (2001): Rapid incidental phosphorus transfer from grassland: *Journal of Environmental Quality*: *30*, 2105–2112.

Quinn, P. F., K. Beven, P. Chevallier, and O. Planchon (1991): The prediction of hillslope flow paths for distributed hydrological modelling using digital terrain models: *Hydrological Processes*: *5*, 59–79.

Quinton, J. N., J. A. Catt, and T. M. Hess (2001): The selective removal of phosphorus from soil: Is event size important?: *Journal of Environmental Quality*: *30*, 538–545.

Quinton, J. N., P. Strauss, N. Miller, E. Azazoglu, M. Yli-Halla, and R. Uusitalo (2003): The potential for soil phosphorus test to predict phosphorus losses in overland flow: *Journal of Plant Nutrition and Soil Science*: *166*, 432–437.

Refsgaard, J. C. (1997): Parameterisation, calibration and validation of distributed hydrological models: *Journal of Hydrology*: *198*, 69–97.

Reichert, P., and M. Omlin (1997): On the usefulness of overparameterized ecological models: *Ecological Modelling*: *95*, 289–299.

Richards, L. A. (1931): Capillary conduction of liquids through porous mediums: *Physics*: *1*, 318–333.

Ritsema, C. J., and L. W. Dekker (2000): Preferential flow in water repellent sandy soils: Principles and modeling implications: *Journal of Hydrology*: *231-232*, 308–319.

Russell, M. S., and H. Wheater (2004): Multiple objective evaluation of a simple phosphorus transfer model: *Hydrological Processes*: *18*, 1703–1720.

Ryden, J. C., J. K. Syers, and R. F. Harris (1973): Phosphorus in runoff and streams: *Advantages in Hygronomy*: *25*, 1–45.

Schärer, M. (2003): The influence of processes controlling phosphorus availability on phosphorus losses in grassland soils: Ph.D. thesis: Diss. Nr. 15312, Swiss Federal Institute of Technology, Zurich.

Schärer, M., T. Vollmer, C. Stamm, E. Frossard, H. Flühler, and S. Sinaj (2005): The influence of water quality on phosphorus concentration in runoff and phosphate exchangeability in two grassland soils: *Submitted to European Journal of Soil Science*.

Scherrer, S., and F. Naef (2003): A decision scheme to indicate dominant hydrological flow processes on temperate grassland: *Hydrological Processes*: *17*(2), 391–401.

Schmocker-Fackel, P. (2004): A method to delineate runoff processes in a catchment and its implications for runoff simulations: Ph.D. thesis: Diss. Nr. 15638, Swiss Federal Institute of Technology, Zürich.

Schoumans, O. F., and P. Groenendijk (2000): Modeling soil phosphorus levels and phosphorus leaching from agricultural land in the Netherlands: *Journal of Environmental Quality*: *29*, 111–116.

Seibert, J., and J. J. McDonnell (2002): On the dialog between experimentalist and modeler in catchment hydrology: Use of soft data for multicriterial model calibration: *Water Resources Research*: *38*(11), 23.1–23.14.

Sharpley, A., and S. Rekolainen (1997): Phosphorus in agriculture and its environmental implications: in *Phosphorus loss from soil to water*, edited by H. Tunney, O. T. Carton, P. C. Brooks, and A. E. Johnston: pp. 1–53: CAB International, Wallingford.

Sharpley, A. N. (1997): Rainfall frequency and nitrogen and phosphorus in runoff from soil amended with poultry litter: *Journal of Environmental Quality*: *26*, 1127–1132.

Sharpley, A. N., and J. R. Williams (1990): EPIC - Erosion/productivity Impact Calculator: 1. Model documentation: *Tech. rep.*: U.S. Department of Agriculture, Agricultural Research Service, Technical Bulletin No. 1785.

Sharpley, A. N., S. J. Smith, O. R. Jones, W. A. Berg, and G. A. Coleman (1992): The transport of bioavailable phosphorus in agricultural runoff: *Journal of Environmental Quality*: *21*, 30–35.

Sharpley, A. N., B. Foy, and P. Withers (2000): Practical and innovative measures for the control of agricultural phosphorus losses to water: An overview: *Journal of Environmental Quality*: *29*, 1–10.

Sibbesen, E., and A. N. Sharpley (1997): Setting and justifying upper critical limits for phosphorus in soils: in *Phosphorus loss to water from agriculture.*, edited by H. Tunney, O. T. Carton, P. C. Brooks, and A. E. Johnston: pp. 151–176: CAB International, Wallingford.

Simard, R. R., S. Beauchemin, and P. M. Haygarth (2000): Potential for preferential pathways of phosphorus transport: *Journal of Environmental Quality*: *29*, 97–105.

Sims, J. T., R. R. Simard, and B. C. Joern (1998): Phosphorus loss in agricultural drainage: Historical perspective and current research: *Journal of Environmental Quality*: *27*, 277–293.

Singh, V. P. (1995): *Computer models of watershed hydrology*: chap. Watershed modelling., pp. 1–22: Water Resources Publications, Highlands Ranch, Colorado.

Slash, M. G., M. K. Stewart, and A. J. Pearce (1986): Storm runoff generation in humid headwater catchments 2. A case study of hillslope and low-order stream response: *Water Resources Research*: *22*(8), 1273–1282.

Smith, K. A., D. R. Jackson, and P. J. A. Withers (2001): Nutrient losses by surface run-off following the application of organic manures to arable lands. 2. Phosphorus: *Environmental Pollution*: *112*(1), 53–60.

Stadelmann, P. (1988): Zustand des Sempachersees: *Wasser, Energie, Luft*: *3*(4), 81–96.

Stamm, C., H. Flühler, R. Gächter, J. Leuenberger, and H. Wunderli (1998): Preferential transport of phosphorus in drained grassland soils: *Journal of Environmental Quality*: *27*(3), 515–522.

Stamm, C., R. Sermet, J. Leuenberger, H. Wunderli, H. Wydler, H. Flühler, and M. Gehre (2002): Multiple tracing of fast transport in a drained grassland soil: *Geoderma*: *109*, 245–268.

Tabbara, H. (2004): Phosphorus loss to runoff water twenty-four hours after application of liquid swine manure or fertilizer: *Journal of Environmental Quality*: *32*, 1044–1052.

Tattari, S., I. Bärlund, S. Rekkolainen, M. Posch, K. Siimes, H.-R. Tuhkanen, and M. Yli-Halla (2001): Modeling sediment yield and phosphorus transport in Finnish clayey soils: *American Society of Agricultural Engineers*: *44*(2), 297–307.

Torbert, H., T. Daniel, J. Lemunyon, and R. Jones (2002): Relationship of soil test phosphorus and sampling depth to runoff phosphorus in calcareous and noncalcareous soils: *Journal of Environmental Quality*: *31*(4), 1380–1387.

Turner, B. L., and P. M. Haygarth (1999): Phosphorus leaching under cut grassland: *Water Science and Technology*: *39*(12), 63–67.

Turner, B. L., and P. M. Haygarth (2001): Phosphorus solubilization in rewetted soils: *Nature*: *411*(6835), 258.

Van der Zee, S. E. A. T. M., and W. H. van Riemsdijk (1988): Model for long-term phosphate reaction kinetics in soil: *Journal of Environmental Quality*: *17*, 35–41.

Viney, N. R., M. Sivapalan, and D. Deeley (2000): A conceptual model of nutrient mobilisation and transport applicable at large catchment scales: *Journal of Hydrology*: *240*, 23–44.

Vollenweider, R., and J. Kerekes (1980): The loading concept as a basis for controlling eutrophication: Philosophy and preliminary results of the OECD program on eutrophication: *Progr. Water Technol.*: *12*, 5–38.

Vollmer, T., M. Schärer, C. Stamm, S. Sinaj, H. Flühler, and E. Frossard (in prep.): Remediation treatments to reduce Phosphorus losses (P) from P-enriched grassland soils: II. P losses in surface runoff.

von Albertini, N., M. Braun, and P. Hurni (1993): Oberflächenabfluss und Phosphorabschwemmung von Grasland: *Landwirtschaft Schweiz*: *6*(10), 575–582.

Weidmann, A. (2004): Phosphoreinsatz durch Hofdünger im Einzugsgebiet Lippenrütibach: Master's thesis: Technikerschule Strickhof, Lindau.

Western, A. W., R. B. Grayson, and G. T. R. (1999): The Tarrawarra project: High resolution spatial measurement, modelling and analysis of soil moisture and hydrological response: *Hydrological Processes*: *13*, 633–652.

Western, A. W., G. Blöschl, and R. B. Grayson (2001): Toward capturing hydrologically significant connectivity in spatial patterns: *Water Resources Research*: *37*(1), 83–97.

Withers, P. J. A., I. A. Davidson, and R. H. Foy (2000): Prospects for controlling phosphorus loss to water: A UK perspective: *Journal of Environmental Quality*: *29*, 167–175.

Withers, P. J. A., S. D. Clay, and V. G. Breeze (2001): Phosphorus transfer in runoff following application of fertilizer, manure and sewage sludge: *Journal of Environmental Quality*: *30*, 180–188.

Withers, P. J. A., B. Ulen, C. Stamm, and M. Bechmann (2003): Incidental phosphorus losses - are they significant and can they be predicted?: *Journal of Plant Nutrition and Soil Science*: *166*, 459–468.

Wood, E. F., M. Sivapalan, K. J. Beven, and L. Band (1988): Effects of spatial variability and scale with implications to hydrologic modeling: *Journal of Hydrology*: *109*, 29–47.

Yapo, P. O., H. V. Gupta, and S. Sorooshian (1996): Automatic calibration of conceptual rainfall-runoff models: Sensitivity to calibration data: *Journal of Hydrology*: *181*, 23–48.

Young, R. A., C. A. Onstad, and D. D. Bosch (1995): AGNPS: an agricultural nonpoint source model: in *Computer Models of Watershed Hydrology*, edited by V. P. Singh: pp. 1001–1020: Water Resources Publications, Highlands Ranch, Colorado.

A.4 Curriculum vitae

Surname	Lazzarotto	
First name	Patrick	
Date of birth	21 January 1974	
Citizen of	Oberriet (SG), Switzerland	
School education	1981 - 1987	Primary school in Wil
	1987 - 1990	Secondary school in Wil
	1990 - 1995	High School graduation (Matura type E)
Higher education	1995 - 2000	Studies in Earth Sciences, Swiss Federal Institute of Technology, ETH Zurich Diploma in Earth Sciences
	2000 - 2004	Scientific collaborator at the Institute of Terrestrial Ecology of ETH Zurich, group of Soil Physics and Agroscope FAL Reckenholz, Zurich